1085-9195/04/40/1–80/$25.00

ORIGINAL ARTICLE

Adult Reserve Stem Cells and Their Potential for Tissue Engineering

Henry E. Young,[*,1,2] *Cecile Duplaa,*[5] *Marina Romero-Ramos,*[6] *Marie-Francoise Chesselet,*[6] *Patrick Vourc'h,*[6] *Michael J. Yost,*[7] *Kurt Ericson,*[7] *Louis Terracio,*[8] *Takayuki Asahara,*[9,10] *Haruchika Masuda,*[9,10] *Sayaka Tamura-Ninomiya,*[9,10] *Kristina Detmer,*[1] *Robert A. Bray,*[11] *Timothy A. Steele,*[12] *Douglas Hixson,*[13] *Mohammad el-Kalay,*[14] *Brian W. Tobin,*[1,2] *Roy D. Russ,*[1] *Michael N. Horst,*[1] *Julie A. Floyd,*[1] *Nicholas L. Henson,*[1] *Kristina C. Hawkins,*[1] *Jaime Groom,*[1] *Amar Parikh,*[1] *Lisa Blake,*[1] *Laura J. Bland,*[1] *Angela J. Thompson,*[1] *Amy Kirincich,*[7] *Catherine Moreau,*[5] *John Hudson,*[4] *Frank P. Bowyer III,*[2] *T. J. Lin,*[3] *and Asa C. Black Jr.*[1,3]

[1]Division of Basic Medical Sciences, [2]Department of Pediatrics, [3]Department of Obstetrics and Gynecology, and [4]Department of Internal Medicine, Mercer University School of Medicine, Macon, GA; [5]INSERM U441, Avenue du Haut Leveque,France; [6]Department of Neurology, UCLA School of Medicine, Reed Neurological Research Center, Los Angeles, CA; [7]Department of Surgery, University of South Carolina School of Medicine, Columbia, SC; [8]New York University College of Dentistry, New York, NY; [9]Cardiovascular Research and Medicine, Tufts University School of Medicine,Elizabeth's Medical Center, Boston, MA; [10]Kobe Institute of Biomedical Research and Innovation/RIKEN Center of Developmental Biology, Chuo, Kobe, Japan; [11]Department of Pathology and Laboratory Medicine, Emory University Hospital, Atlanta, GA; [12]Des Moines University–Osteopathic Medical Center, Des Moines, IA; [13]Department of Medicine, Brown University, Providence, RI; [14]MorphoGen Pharmaceuticals, Inc., San Diego, CA

Abstract

Tissue restoration is the process whereby multiple damaged cell types are replaced to restore the histoarchitecture and function to the tissue. Several theories have been proposed to explain the phenomenon of tissue restoration in amphibians and in animals belonging to higher orders. These

[*]Author to whom all correspondence and reprint requests should be addressed: Henry E. Young, Division of Basic Medical Sciences, Mercer University School of Medicine, 1550 College Street, Macon, GA. E-mail: young_he@mercer.edu

theories include dedifferentiation of damaged tissues, transdifferentiation of lineage-committed progenitor cells, and activation of reserve precursor cells. Studies by Young et al. and others demonstrated that connective tissue compartments throughout postnatal individuals contain reserve precursor cells. Subsequent repetitive single cell-cloning and cell-sorting studies revealed that these reserve precursor cells consisted of multiple populations of cells, including tissue-specific progenitor cells, germ-layer lineage stem cells, and pluripotent stem cells. Tissue-specific progenitor cells display various capacities for differentiation, ranging from unipotency (forming a single cell type) to multipotency (forming multiple cell types). However, all progenitor cells demonstrate a finite life span of 50 to 70 population doublings before programmed cell senescence and cell death occurs. Germ-layer lineage stem cells can form a wider range of cell types than a progenitor cell. An individual germ-layer lineage stem cell can form all cells types within its respective germ-layer lineage (i.e., ectoderm, mesoderm, or endoderm). Pluripotent stem cells can form a wider range of cell types than a single germ-layer lineage stem cell. A single pluripotent stem cell can form cells belonging to all three germ layer lineages. Both germ-layer lineage stem cells and pluripotent stem cells exhibit extended capabilities for self-renewal, far surpassing the limited life span of progenitor cells (50–70 population doublings). The authors propose that the activation of quiescent tissue-specific progenitor cells, germ-layer lineage stem cells, and/or pluripotent stem cells may be a potential explanation, along with dedifferentiation and transdifferentiation, for the process of tissue restoration. Several model systems are currently being investigated to determine the possibilities of using these adult quiescent reserve precursor cells for tissue engineering.

Index Entries: Adult; pluripotent; stem cells; mammals; humans; embyonic; mesenchymal; neurodegenerative; diabetes; infarction.

DEFINITIONS

Precursor cells are the three general categories of reserve cells present within the connective tissue compartments of organs and tissues throughout the adult (postnatal) body. These three general categories of precursor cells are tissue-specific progenitor cells, lineage-committed (ectodermal, mesodermal, and endodermal) germ-layer lineage stem cells, and lineage-uncommitted pluripotent epiblastic-like stem cells.

Progenitor cells are precursor cells that have a finite life span of less than or equal to Hayflick's limit of 50–70 population doublings before programmed cell senescence and cell death. In addition, particular progenitor cells are committed to form particular tissue types. For example, a myogenic progenitor cell has the potential to only form myogenic tissues (i.e., skeletal muscle, smooth muscle, and/or cardiac muscle). A chondrogenic progenitor cell has the potential to only form chondrogenic tissues (i.e., hyaline cartilage, articular cartilage, elastic cartilage, growth plate cartilage, and/or fibrocartilage). In addition, an adipogenic progenitor cell has the potential to only form adipogenic cell types (i.e., unilocular fat cells and/or multilocular fat cells). Also, progenitor cells may be unipotent, forming a single cell type; bipotent, forming two cell types; tripotent, forming three cell types; or multipotent, forming multiple cell types.

Stem cells are precursor cells that have extended capabilities for self-renewal, far exceeding Hayflick's limit of 50–70 population doublings, and are telomerase-positive. There are two subgroups, with one subgroup of stem cells committed to the primary germ-layer lineages of ectoderm, mesoderm, and endoderm. But these particular (ectodermal, mesodermal, or endodermal) germ-layer lineage stem cells will not form a select few cells within that lineage but rather will form *all* cell types within their respective embryonic germ-layer lineage.

Mesodermal germ-layer lineage stem cells will form skeletal muscle, smooth muscle, cardiac muscle, unilocular adipocytes, multilocular adipocytes, fibrous connective tissues, dermis, tendons, ligaments, dura mater, arachnoid mater, pia mater, organ capsules, organ stroma, tunica adventitia, tunica serosa, fibrous scar tissue, hyaline cartilage, articular cartilage, elastic cartilage, growth plate cartilage, fibrocartilage, endochondral bone, intramembranous bone, arterial endothelial cells, venous endothelial cells, capillary endothelial cells, lymphoidal endothelial cells, sinusoidal endothelial cells, endothelial cells, erythrocytes, monocytes, macrophages, T-lymphocytes, B-lymphocytes, plasma cells, eosinophils, basophils, Langerhan cells, dendritic cells, natural killer (NK) cells, bone marrow stroma, adrenal cortex zona fasciculata, adrenal cortex zona glomerulosa, adrenal cortex zona reticularis, the proximal convoluted tubule, the distal convoluted tubule, the loop of Henle, podocytes, juxtaglomerular cells, mesangial cells, the transitional epithelium, seminiferous tubules, tubuli recti, the rete testis, Sertoli cells, interstitial cells of Leydig, efferent ductules, the ductus epididymis, the ductus deferens, the seminal vesicle, ejaculatory ducts, ovarian stroma, follicular cells/granulosa cells, fallopian tube tissues, the uterine endometrium, uterine glands, the upper two-thirds of the vagina, and so forth. Thus far, we have tentatively identified 40 of the above cell types and developed assay procedures to objectively verify 25 of them within induced clonal rodent mesodermal germ-layer lineage stem cell lines, cell-sorted human mesodermal germ-layer lineage stem cell lines, and induced human and rodent pluripotent epiblastic-like stem cell lines.

Ectodermal germ-layer lineage stem cells will form epidermis, hair, nails, sweat glands, sebaceous glands, Apocrine glands, salivary gland mucous cells, salivary gland serous cells, gonadotrophs, somatotrophs, thyrotrophs, corticotrophs, mammanotrophs, the lens, the corneal epithelium, enamel, neurons, astrocytes, oligodendrocytes, dorsal root ganglion cells, sympathetic ganglion cells, parasympathetic ganglion cells, ependyma, the olfactory epithelium, retina, the iris, smooth muscle (sphincter and dilator pupillae), the ciliary body, pituicytes, the hypothalamus, the thalamus, pinealocytes, spinal nerves, Schwann cells, motor nerve endings, Meissner's touch corpuscles, Merkel's disks, Krause end bulbs, free nerve endings, Pacinian touch corpuscles, melanocytes, odontocytes, cementocytes, amine precursor uptake decarboxylase (APUD) cells, chromaffin cells, enterochromaffin cells, adrenal medulla, pheochromocytes, parafollicular C-cells, heart valves, the cardiac skeleton, the pulmonary trunk, chorda tendinae, the ascending aorta, cardiac cushions, the membranous atrial septum, the membranous ventricular septum, and the corneal endothelium. Thus far, we have tentatively identified 20 of the above cell types and developed assay procedures to objectively verify 10 of them within induced clonal rodent ectodermal germ-layer lineage stem cell lines and induced human and rodent pluripotent epiblastic-like stem cell lines.

Endodermal germ-layer lineage stem cells will form thyroid follicular cells, brush cells, goblet cells, Clara cells, type I alveolar cells, type II alveolar cells, the epithelium of the esophagus, gastric mucous cells, gastric parietal cells, gastric chief cells, cardiac glands, gastric glands, pyloric glands, Brunner's glands, the epithelium of the small intestine, the epithelium of the large intestine, the epithelium of the appendix, the epithelium of the rectum, the epithelium of the gallbladder, goblet cells, hepatocytes, biliary cells, canalicular cells, oval cells, acinar cells, α-cells, β-cells, δ-cells, polypeptide P-cells, the epithelium lining of pharyngeal pouches, the lining of the middle ear, pharyngeal tonsils, the thymus, parathyroid oxyphil cells, and parathyroid chief cells. Thus far, we have tentatively identified 18 of the above cell types and developed assay procedures to objectively verify 11 of them within induced clonal rodent endodermal germ-layer lineage stem cell lines and induced human and rodent pluripotent epiblastic-like stem cell lines.

Pluripotent epiblastic-like stem cells will form any somatic cell of the body, crossing all

three primary germ-layer lineages (ectoderm, mesoderm, and endoderm). Thus far, we have tentatively identified almost 80 cell types and developed assay procedures to objectively verify 46 of them within induced clonal rodent cell lines and induced cell-sorted human pluripotent epiblastic-like stem cell lines.

THEORIES CONCERNING TISSUE RESTORATION

Restoration of tissue histoarchitecture and function is the Holy Grail for tissue engineering. Limb regeneration in amphibians is a classic example of tissue engineering that occurs naturally. Transection of the amphibian limb initiates reepithelialization of the distal tip to form an epidermal cap/ridge and formation of the blastema, a mass of undifferentiated cells that underlie the epidermal cap/ridge. Signals emanating from the epidermal cap/ridge direct the subsequent proliferation, outgrowth, and differentiation of the blastema into the missing tissues of the limb, forming a fully functional appendage (Figs. 1A–N).

Dedifferentiation is one of several theories that have been proposed to explain the phenomenon of tissue restoration. Toole and Gross *(1)* reported that blastema formation in the juvenile aquatic salamander occurred by the process of dedifferentiation of the transected tissues. The dedifferentiation theory is predicated on the assumption that stem cells either do not exist within the tissues or do not function in the process of tissue restoration. The theory of dedifferentiation proposes that differentiated cells damaged during the initial trauma revert to a more primitive undifferentiated state to form the blastema, prior to their proliferation and subsequent redifferentiation to restore the missing tissues *(2,3)*.

The theory of transdifferentiation of tissue-specific progenitor cells offers an alternate explanation of the events leading to tissue restoration. This theory proposes that each tissue within the postnatal individual contains only its own unique contingent of tissue-specific progenitor cells. The theory further proposes that the normal function of these progenitor cells is limited to the maintenance and repair of the tissue in which they reside *(4)*. Transdifferentiation is proposed to occur during tissue restoration when tissue-specific progenitor cells derived from one organ are "reprogrammed" to form tissues of another organ *(5,6)*. For example, cells derived from bone marrow have been reported to form neurons and neural supportive tissues *(7–9)*, as well as hepatic oval cells *(10–12)* and muscle cells *(13,14)*. Cells derived from neuronal tissues have been reported to form blood elements *(15,16)* and muscle cells *(17–19)*. In addition, cells derived from skeletal muscle have been reported to form blood *(20)*. These investigators proposed that the tissue-specific progenitor cells they isolated from one organ were reprogrammed or transdifferentiated to form cells and tissues of another organ.

The activation of quiescent reserve precursor cells offers another theory to explain the phenomenon of tissue restoration in postnatal individuals. This hypothesis proposes that connective tissue compartments in postnatal individuals contain multiple populations of reserve precursor cells and that these precursor cells consist of tissue-specific progenitor cells, germ-layer lineage stem cells, and lineage-uncommitted pluripotent stem cells. Tissue-specific progenitor cells residing in the tissues of the body are postulated to be involved in the routine maintenance of those tissues. Examples of tissue-specific progenitor cells demonstrating this function include the basal epithelial cells of gastrointestinal mucosa *(21)* and the myosatellite cells of skeletal muscle *(22,23)*. Heretofore unrecognized populations of germ-layer lineage stem cells and pluripotent stem cells *(24–60)* are postulated to undergo activation, proliferation, and differentiation to assist the progenitor cells in the replacement or restoration of the damaged and/or missing tissues. We will now examine this third proposed hypothesis in more detail.

RESERVE PRECURSOR CELLS

Limb Regeneration in Adult Terrestrial Salamanders

Urodeles in the aquatic phase, such as the juvenile and adult newt, juvenile and adult axolotl, and the juvenile larval salamander, have the capacity to regenerate completely a functional appendage after traumatic or surgical amputation *(61–64)*. In these species, complete restoration of the missing tissues was observed during a relatively short period of time: 40 d for the newt *(65)*, 30+ d for the axolotl *(66,67)*, and 44 d for the juvenile larval salamander *(68)*. In salamanders, metamorphosis appeared to be critical for the process of regeneration. In metamorphosis, the juvenile aquatic salamander is transformed into the adult terrestrial salamander. Complete absence of limb regeneration or the formation of only heteromorphic regenerates was reported to follow limb transection in adult terrestrial salamanders *(69)*. Thus, it was generally accepted that the adult terrestrial form had lost its intrinsic ability to regenerate any appendage. The mechanism for the loss of regenerative ability in the adult urodele salamander was unknown *(70,71)*.

Young et al. reported that adverse laboratory conditions and length of time examined accounted for the apparent loss of regenerative ability in adult terrestrial salamanders *(24–27,31)*. When the laboratory environment was adjusted for terrestrial conditions, adult salamanders (i.e., *Ambystoma annulatum*, *Ambystoma maculatum*, *Ambystoma texanum*, and *Ambystoma tigranum*) completely regenerated functional limbs within 155 to 370 d after amputation (Figs. 1A–N) *(32–35)*. Because of the increased time for complete regeneration to occur (i.e., 155–370 d for terrestrial salamanders vs 30–44 d for aquatic species) and the increased number of time-points examined (i.e., 62–148 for terrestrial salamanders vs 12–18 for aquatic species), additional studies *(36,72)* noted that the transected tissues of the limb did not undergo dedifferentiation into more primitive cells *(73)*. Rather, the damaged tissues were completely removed by a debridement/inflammatory response by neutrophils and macrophages (Fig. 2A,B). The cells forming the blastema were present in the adult salamanders as quiescent stem cells. The reserve stem cells were located in the proximal connective tissues of the skeletal muscle, dermis, fat, cartilage, bone, and loose fibrous connective tissues of the limb (Fig. 2C–E). Upon activation, these putative stem cells released themselves from the supporting connective tissues and migrated to the apical epidermal ridge to form the blastema. The spatial and temporal scenario for posttraumatic blastema formation and subsequent outgrowth of the limb is as follows. Before amputation, no morphological or histochemical differences were detected between the quiescent stem cells and the other differentiated cells of the connective tissues. Immediately following amputation, a select population of cells began synthesizing heparan sulfate proteoglycan (HS-PG). These cells demonstrated a transient shift from intracellular to pericellular HS-PG. Glycoproteins (GP) emanating from the forming epidermal cap (Fig. 2F) bound to the pericellular HS-PG. The select population of cells exhibiting pericellular HS-PG bound to the GP then migrated along a concentration gradient (Fig. 2G) of glycoproteins and hyaluronic acid emanating from the apical epidermal cap (Fig. 2H,I). This select population of cells formed the subepidermal ridge blastema (SERB) and blastema (BL) (Fig. 2I,J). Once formed, the two blastemal populations proliferated to increase the length of the limb. During this process, the proximal blastemal cells located near the differentiated tissues acquired cell surface coats consisting of HS-PG and acidic, neutral, and basic glycoproteins. The proteoglycans of the extracellular matrix then developed tissue-specific compositions indicative of skeletal muscle, fat, cartilage, bone, connective tissues, and dermis *(35,36,72,74)*. In the process of forming the missing tissues, alterations in proteoglycan profiles of the extracellular matrix preceded

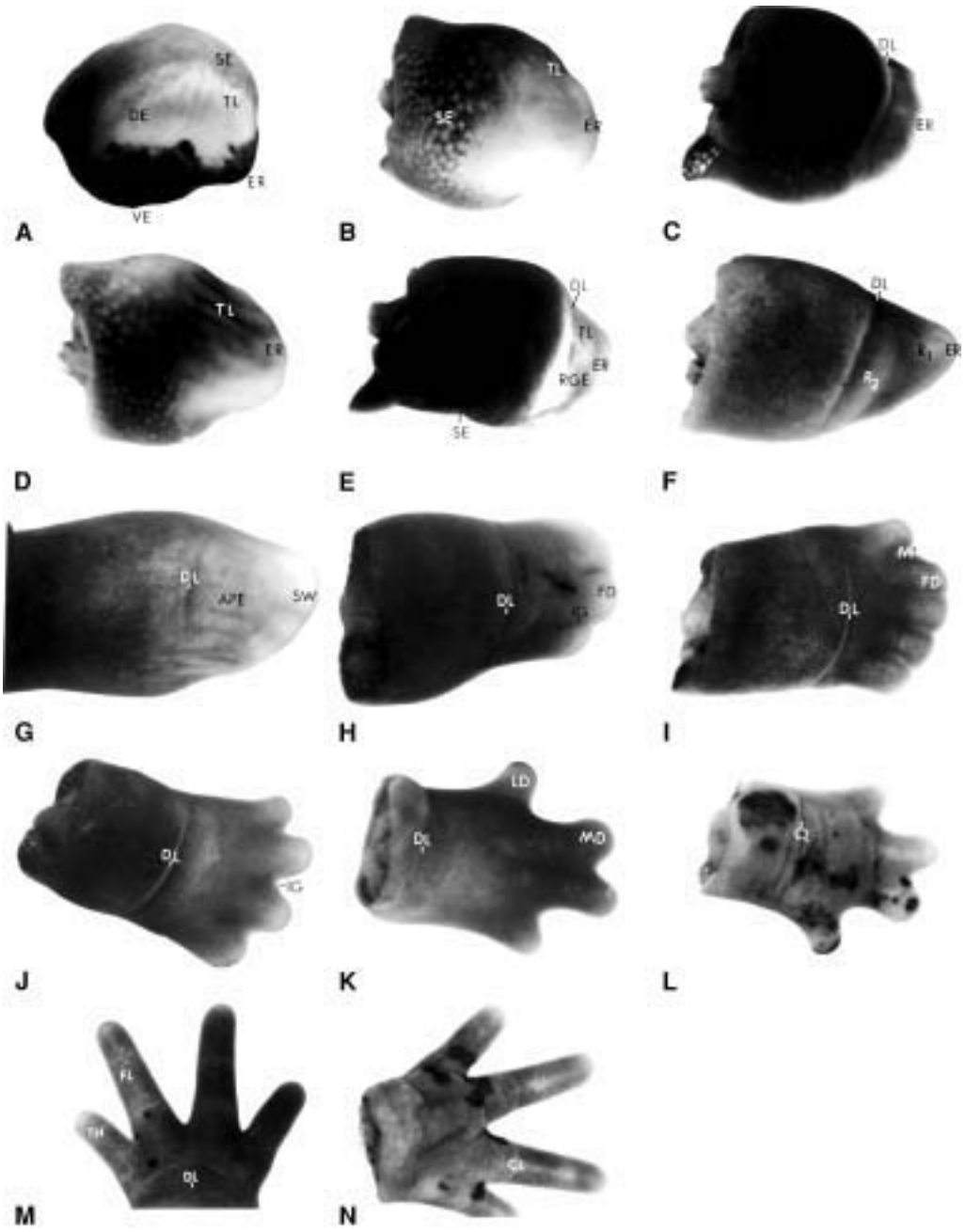
A
SE
TL
DE
ER
VE
B
TL
SE
ER
C
DL
ER
D
TL
ER
E
DL
TL
ER
PGE
SE
F
DL
ER
G
DL
APE
SW
H
DL
FD
I
DL
FD
J
DL
K
LD
DL
MD
L
M
FL
TH
DL
N

Fig. 1. **(A)** Wound healing stage, dorsal oblique view, shows a slight swelling in the regenerate epidermis at the distal tip and the first evidence for the bud outgrowth, *Ambystoma annulatum*, ×100. **(B)** Early bud stage, ventral view, shows the rounded outgrowth of the blastema with the epidermal ridge at its distal tip, *A. annulatum*, ×70. **(C)** Middle bud stage, dorsal view, shows a demarcation line separating the stump tissues from a symmetrical cone-shaped blastemal outgrowth, *A annulatum*, ×94. **(D)** Middle bud stage, ventral view of the same bud as in **C**. Tension lines are visible from the epidermal ridge to the stump tissues, *A. annulatum*, ×90.

(E) Late bud stage, dorsal view of a flattened cone-shaped outgrowth. The demarcation line continues to separate the blastemal outgrowth from the remaining portion of the limb, *A. annulatum*, ×60.**(F)** Early palette stage, dorsal view of a paddle-shaped outgrowth that can be segregated into two regions: region 1 comprises the area of the future digits; region 2 comprises the area of the future "hand," *A. annulatum*, ×70.

(G) Middle palette stage, dorsal view of an elongated palette-shaped outgrowth. The apical palette epidermis covers the outgrowth, and a demarcation line separates the stump tissues from regenerate outgrowth tissues. Along the distal ridge of the outgrowth, slight swellings begin to replace the epidermal ridge, *A. annulatum*, ×70. **(H)** Late palette stage, dorsal view of an elongated palette-shaped outgrowth. A demarcation line separates proximal stump tissues from the distal regenerate tissues. Distinct swellings are visible along the distal border and are indicative of forming digits, *A. annulatum*, ×90. **(I)**: Early digit stage, dorsal view of the regenerate structure that has the distinct appearance of a forming "hand" containing digits. The forming digits are beginning to separate from each other, *A. annulatum*, ×60. **(J)** Middle digit stage, dorsal view of a definitive "hand"-like regenerate structure consisting of separated digital regions, *A. annulatum*, ×70. **(K)** Late digit stage, a dorsal view showing continued separation of the digits, *A. annulatum*, ×70. **(L)** Late digit stage, a ventral view of the same regenerate as seen in **K**. Patches of chromatophores (melanocytes) are appearing along this surface. Transverse crease lines overlie future joint areas, such as those for the interphalangeal joints, *A. annulatum*, ×70. **(M)** Complete limb regenerate stage, a dorsal view of all digits separated from each other, with the regenerate forelimb indistinguishable from either the original or sham-operated control limbs. Within the regenerated limb, the demarcation line remains and marks the spot of the original amputation site, *A. annulatum*, ×60. **(N)** Complete regenerate stage, a ventral view of **M**. At the beginning of this stage, patches of chromatophores appear along the ventral surface, but by the end of this stage, the pigmentation pattern assumes that of its respective species (i.e., annular rings for *A. annulatum*, spots for *A. maculatum*, a mottled appearance for *A. texanum*, and stripes for *A. tigranum*), *A. annulatum*, ×60. APE, apical palette epidermis; C, chromatophores; CL, crease lines; DE, dorsal regenerative epidermis; DL, demarcation line; ER, epidermal ridge; FD, forming digits; FL, finger-like digits; IG, interdigital grooves; IW, interdigital wedge; LD, lateral digits; MD, middle digits; R1, distal one-third of outgrowth, region 1; R2, proximal two-thirds of outgrowth, region 2; RGE, regenerate epidermis; SE, stump epidermis; SW, swellings; TH, thumb-like digit; TL, tension lines; VE, ventral regenerate epidermis. (Reproduced with permission from Young, H. E., Bailey, C. F., and Dalley, B. K. [1983] Gross morphological analysis of limb regeneration in postmetamorphic adult Ambystoma. *Anat. Rec.* **206,** 295–306. Copyright 1983, Alan R. Liss, Inc.)

overt changes in cellular morphology. These results suggested that the blastema in adult terrestrial salamanders originated from quiescent stem cells located within the more proximal connective tissues of the limb. During subsequent differentiation, the blastemal cells formed an intermediate tissue-specific (lineage-committed) phenotype prior to overt differentiation into the adult form. The inductive agents for these events were endogenous

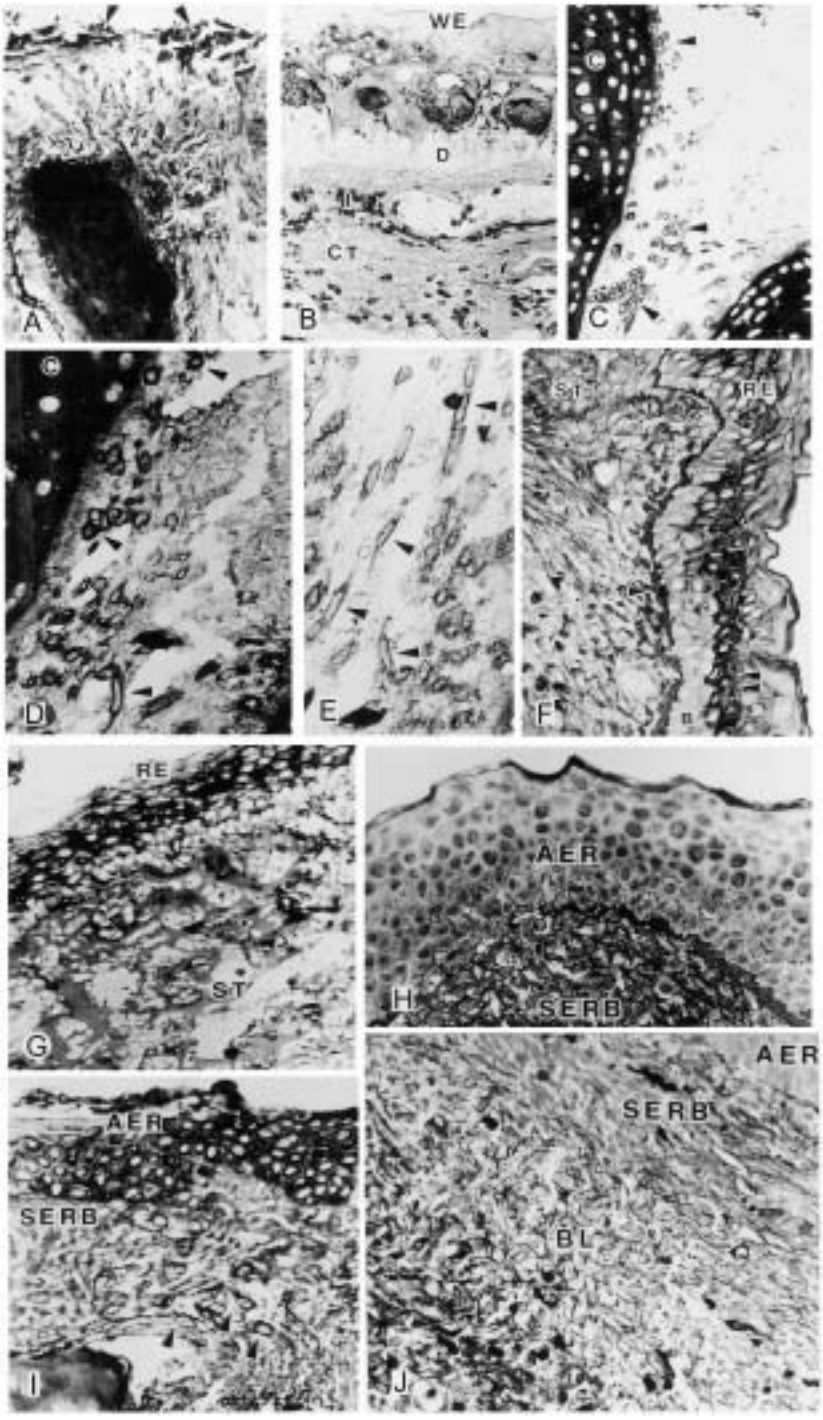
A
WE
D
CT
B
C
D
E
S-T
RE
F
RE
S-T
G
AER
SERB
H
AER
SERB
I
AER
SERB
BL
J

Fig. 2. **(A)** Limb tissues transected by amputation 18 to 20 h after amputation. Arrowheads denote degenerating tissues along amputation surface, ×450. **(B)** Postaxial border of stump tissue area just proximal to amputation site, 18 to 20 h after amputation. Stump epidermis adjacent to amputation site demonstrates intracellular staining for hyaluronic acid and glycoproteins. Dermis consists of dense fibrous connective tissue. Inflammatory cells (macrophages and neutrophils) located within and around blood vessel periphery and interspersed within connective tissues, ×900. **(C)** Proximal area of stump tissues between two cartilage masses 5 d after amputation. Arrowheads demonstrate cells with intracellular heparan sulfate glycosaminoglycans, pericellular heparan sulfate glycosaminoglycans and glycoproteins, and extracellular hyaluronic acid. This figure reveals putative (mesenchymal-like) blastemal cells associated with the perichondrial sheath covering the cartilage and within the connective tissues between the cartilage masses, ×600. **(D)** Area of the stump tissues proximal to the amputation site 6 d after amputation. Arrowheads denote cells with intracellular heparan sulfate glycosaminoglycans, pericellular heparan sulfate glycosaminoglycans and glycoproteins, and extracellular hyaluronic acid. These cells are the putative (mesenchymal-like) blastemal cells that are associated with the perichondrium and associated connective tissues adjacent to the cartilage mass, ×1200. **(E)** Area of the connective tissues located between skeletal muscle and adjacent cartilage 6 d after amputation. This area is within the tissues proximal to the amputation site. Putative (mesenchymal-like) blastemal cells containing intracellular heparan sulfate glycosaminoglycans, pericellular heparan sulfate glycosaminoglycans and glycoproteins, and extracellular hyaluronic acid (arrowheads) interspersed within the connective tissue, ×1200. **(F)** Histological view of wound closure by regenerate epidermal cuff across surface of stump tissues 10 d after amputation. Intracellular staining for hyaluronic acid and glycoproteins occurs within middle layers of regenerate epidermis (double arrowheads), absent in basal layers of regenerate epidermis (**B**) and present extracellularly within adjacent underlying wound tissues (single arrowhead), ×1200. **(G)** Regenerate epidermis overlying wound surface 22 d after amputation. An increase in intracellular staining for both hyaluronic acid and glycoproteins occurs in all layers of the regenerate epidermis. Increased extracellular staining for both hyaluronic acid and glycoproteins is located within underlying stump tissue matrices, ×550. **(H)** Distal regenerate portion of the stump-regenerate complex, sectioned perpendicular to the preaxial/postaxial axis 25 d after amputation. Regenerate epidermis begins to thicken, forming a "cap" of epidermis covering the wound site. This structure is designated as the apical epidermal cap. The "pioneering" cells and the "trailing" cells become the cell population beneath the forming apical epidermal cap. This region is designated as the *subregenerate epidermal blastema*. Hyaluronic acid is present intracellularly within all layers of the apical epidermal cap and extracellularly within the subregenerate epidermal blastema, ×600. **(I)** Stump-regenerate complex 30 d after amputation. All layers of the apical epidermal cap stain intracellularly for hyaluronic acid and glycoproteins, whereas the subregenerate blastema stains extracellularly for the same material. Future blastemal cells (arrowheads) are visible near the subregenerate epidermal blastema. These blastemal cells stain intracellularly for heparan sulfate glycosaminoglycans, pericellularly for heparan sulfate glycosaminoglycans and glycoproteins, and extracellularly for hyaluronic acid, ×550. **(J)** Regenerate portion of stump-regenerate complex 35 d after amputation. The individual mesenchymal-like cells have congregated into a large mass of cells, designated the *core blastema*, which lies deep (internal) to the subregenerate epidermal blastema, and the apical epidermal cap, ×600. AEC, apical epidermal cap; B, basal layers of regenerate epidermis; C, cartilage; CB, core blastema; CT, loose connective tissues; D, dermis; E, epithelial-like cells; F, free cell population; FM, fine filamentous material; G/GM, granulated wound surface matrix; I, inflammatory cells (macrophages and neutrophils); N, nerve; RE, regenerate epidermis; SREB, subregenerate epidermal blastema; ST, stump tissues; TP, trailing cells; WE, wound epidermis. (Reproduced with permission from Young, H. E., Dalley, B. K., and Markwald, R. R. [1989] Glycoconjugates in normal wound tissue matrices during the initiation phase of limb regeneration in adult Ambystoma. *Anat. Rec.* **223,** 231–241. Copyright 1989, Alan R. Liss, Inc.)

bioactive factors (glycosylated compounds) emanating from the regenerating epidermis.

Reserve Precursor Cells in Higher Order Animals

Previous studies demonstrated the existence of tissue-specific unipotent, bipotent, tripotent, and multipotent progenitor cells in differentiated tissues. For example, unipotent myosatellite myoblasts were reported for skeletal muscle *(22,75,76)*; unipotent adipoblasts for adipose tissue *(77)*; unipotent chondrogenic cells and osteogenic cells for the perichondrium and periosteum, respectively *(78)*; bipotent adipofibroblasts for adipose tissue *(79)*; bipotent chondrogenic/osteogenic cells for marrow *(80–83)*; tripotent chondrogenic, osteogenic, and adipogenic cells for marrow *(84)*; and multipotent hematopoietic cells for marrow *(85–87)*.

On the basis of previous studies in adult terrestrial salamanders *(32–35)*, Young et al. *(36,72)* postulated the existence of reserve stem cells among the connective tissues of animals belonging to higher orders. They postulated that quiescent stem cells (i.e., lineage-restricted germ-layer lineage stem cells and lineage-uncommitted pluripotent stem cells) having the capacity to form multiple cell types also resided within the connective tissue compartments of postnatal individuals. Three years of empirical experiments led to the determination of the optimal conditions for the isolation, cultivation, and cryopreservation of these putative stem cells *(38,39)*. A quantitative bioassay, consisting of histochemical, immunochemical, and biochemical procedures, was developed to measure and quantify biological activity *(40)*. This assay, coupled with morphological, pharmacological, physiological/functional, and molecular assays, was used to assess phenotypic expression markers characteristic of differentiated and undifferentiated cells *(41–47)*.

Verification for the existence of these reserve precursor cells required isolating clonal populations, in which the cells under study were all derived from a single cell. Clones generated were derived by repetitive single-cell clonogenic analysis *(41,42,44,46)*. The precursor cells used for cloning were isolated from the connective tissue compartments of dermis, skeletal muscle, and heart, and 1158 clones of cells were generated in the initial cloning experiments *(41)*. All clones displayed contact inhibition at confluence. Approximately 70% of the clones demonstrated the ability to generate multiple cell types within the mesodermal germ-layer lineage. These clones formed skeletal muscle, smooth muscle, unilocular (white) fat, multilocular (brown) fat, hyaline cartilage, articular cartilage, elastic cartilage, growth plate cartilage, fibrocartilage, endochondral bone, and intramembranous bone *(41)*. The remaining 30% of the clones demonstrated the ability to form cells belonging to one or more cell types. Some clones were tripotent, forming chondrogenic, osteogenic, and adipogenic cells. Others were bipotent, forming cells belonging to two lineages. Some of these cells belonged to the myo-fibrogenic lineage (forming cells of the myogenic and fibrogenic lineages). Others formed cells of the adipo-fibrogenic lineage (forming cells of the adipogenic and fibrogenic lineages). Still others formed cells of the chondro-osteogenic lineage (forming cells of the chondrogenic and osteogenic lineages). Other clones were unipotent, forming cells limited to a single cell lineage, such as the adipogenic, myogenic, fibrogenic, chondrogenic, and osteogenic lineages *(41)*.

Other differences were noted between the populations of precursor cells. Clones displaying tripotency, bipotency, or unipotency would proliferate through 30 to 50 population doublings and then senesce and die. In other words, they conformed to Hayflick's limit of 50–70 population doublings, the characteristic life-span for lineage-committed progenitor cells *(88)*. Furthermore, these clones were unresponsive to a general inductive agent, such as dexamethasone. They also failed to respond to specific inductive agents whose actions were directed at a different cell type. For example, clones that would only form skeletal muscle were unresponsive to bone morphogenetic protein–2 (BMP-2), which induces the formation of cartilage and bone *(43,44)*. However, progenitor cell clones were responsive to progression agents, which accelerated the time frame for

Table 1
Distribution and Age of Donor Tissue

									Human	
Age	Avian	Mouse	Rat	Rabbit	Dog	Goat	Sheep	Pig	Male	Female
Fetal	+	+	+						24 wk	25 wk
Newborn		+	+						+	
Adolescent		+	+							+
Adult		+	+	+	+	+	+	+	37 yr	17 yr
									48 yr	25 yr
										36 yr
										40 yr
Geriatric		30 mo							67 yr	77 yr

expression of their particular cell type. For example, clones that would only form cartilage demonstrated the chondrogenic phenotype in 2–3 wk in the presence of a progression agent (insulin, insulin-like growth factor–1, or insulin-like growth factor–2), whereas 4 or more wk were required to express the cartilage phenotype in the absence of a progression agent *(28,43)*.

Mesodermal germ-layer lineage stem cell clones displayed the ability to form skeletal muscle, smooth muscle, unilocular fat, multilocular fat, hyaline cartilage, articular cartilage, elastic cartilage, growth plate cartilage, fibrocartilage, endochondral bone, and intramembranous bone from a single cell. These clones proliferated well past 200 population doublings without any apparent effect on their differentiation potential. They were responsive to both a general nonselective inductive agent (such as dexamethasone) that would induce their full range of mesodermal cell types, as well as specific inductive agents, such as BMP-2. However, these same clones were unresponsive to progression agents, which had no effect on the clones as long as they remained tissue/cell uncommitted. Once these multifunctional clones committed to a particular tissue or cell type, they assumed all the characteristics of progenitor clones for that respective tissue. Their life span before senescence and death was 50–70 population doublings. They were unresponsive to induction agents outside their lineage but were responsive to progression agents. Clones having extended capabilities for self-renewal and the capacity to form multiple (more than four) distinct mesodermal cell types from a single cell were originally designated (ca. 1992) as "pluripotent mesodermal stem cells" *(39)*. Because of current definitions for stem cells, they will be designated herein as mesodermal germ-layer lineage (GLL) stem cells. They received this designation because of their extended capabilities for self-renewal and their ability to form multiple tissues and cells originating from the embryonic mesodermal germ-layer lineage. The repetitive single-cell clonogenic studies were repeated with putative mesodermal GLL stem cells derived from mice and rats, and similar results were noted *(44,46,57)*.

Phylogenetic Distribution

We postulated that if mesodermal GLL stem cells were involved in tissue restoration, they should be present throughout phylogeny, even in higher order mammals, such as humans. We have addressed this hypothesis by isolating and examining putative stem cell populations from various species. Putative quiescent stem cells with characteristics identical to the original mesodermal GLL stem cell clones have been

Table 2
Source Tissue for Reserve Stem Cells

Source tissue	Avian	Mouse	Rat	Rabbit	Dog	Goat	Sheep	Pig	Human
Skeletal muscle CT	+	+	+	+	+	+	+	+	+
Dermis	+	+	+						
Heart CT	+	+	+						
Granulation tissue			+						+
Other sites[a]	+		+						+

[a]Associated connective tissues of periosteum, perichondrium, fat, ligaments, tendons, nerve sheaths, meninges, blood vessels, blood, bone marrow, trachea, esophagus, stomach, duodenum, jejunum, ileum, large intestine, liver, pancreas, spleen, kidney, and urinary bladder.

isolated from mice, rats, rabbits, dogs, sheep, goats, pigs, and humans (Table 1) *(29,43,45–47, 53,56,57,59,* unpublished observations*)*.

Age of Donor

We postulated that if mesodermal GLL stem cells were involved in tissue restoration, they should be present at all stages of life. This hypothesis was examined in mice using the National Institute of Health (NIH) mouse aging model CBF-1 *(89)* through 30 mo of age and in humans through 77 yr of age (Table 1). In both mice and humans, no differences were detected with respect to age or the differentiation potentials of these cells. The differentiation potentials examined were the ability to induce phenotypic expression markers for skeletal muscle, smooth muscle, cardiac muscle, unilocular (white) fat, multilocular (brown) fat, hyaline cartilage, articular cartilage, elastic cartilage, growth plate cartilage, fibrocartilage, endochondral bone, intramembranous bone, tendon, ligament, dermis, scar tissue, endothelial cells, and hematopoietic cells using dexamethasone as a general nonselective inductive agent (Table 1) *(28,29,45,47)*.

Location of Reserve Stem Cells

We further postulated that if mesodermal GLL stem cells were involved in tissue restoration, they should be present throughout all body organs and tissues. Using the same protocols for isolation, propagation, and testing as above, precursor cells from 26 different tissues and organs were isolated and examined. Cells with the same characteristics as mesodermal GLL stem cells were located in all tissues or organs examined possessing connective tissue compartment(s) (Table 2) *(28–30,38,42,45–47,53,56,57,59,* unpublished observations*)*.

Novel Bioactive Activities

In recent years, considerable attention has focused on the isolation and characterization of endogenous bioactive factors and their importance in influencing aspects of tissue development, maturation, aging, replacement, and repair. Demineralized bone matrix has been shown to contain a number of factors that influence proliferation, chemotaxis, angiogenesis, chondrogenesis, and osteogenesis *(90–93)*. Of particular interest has been the family of bone morphogenetic proteins (BMP) in the transforming growth factor–beta (TGF-β) superfamily *(94–96)*, cartilage morphogenetic protein *(97)*, TGF-β, basic fibroblast growth factor (b-FGF), insulin, insulin-like growth factor–1 (IGF-1), and insulin-like growth factor–2 (IGF-2) *(91,98)*. On the basis of the presence of these compounds in bone matrix, we fractionated a water-soluble extract from a demineralized bone matrix (Fig. 3A,B) and assayed for additional bioactive activities. We discovered activ-

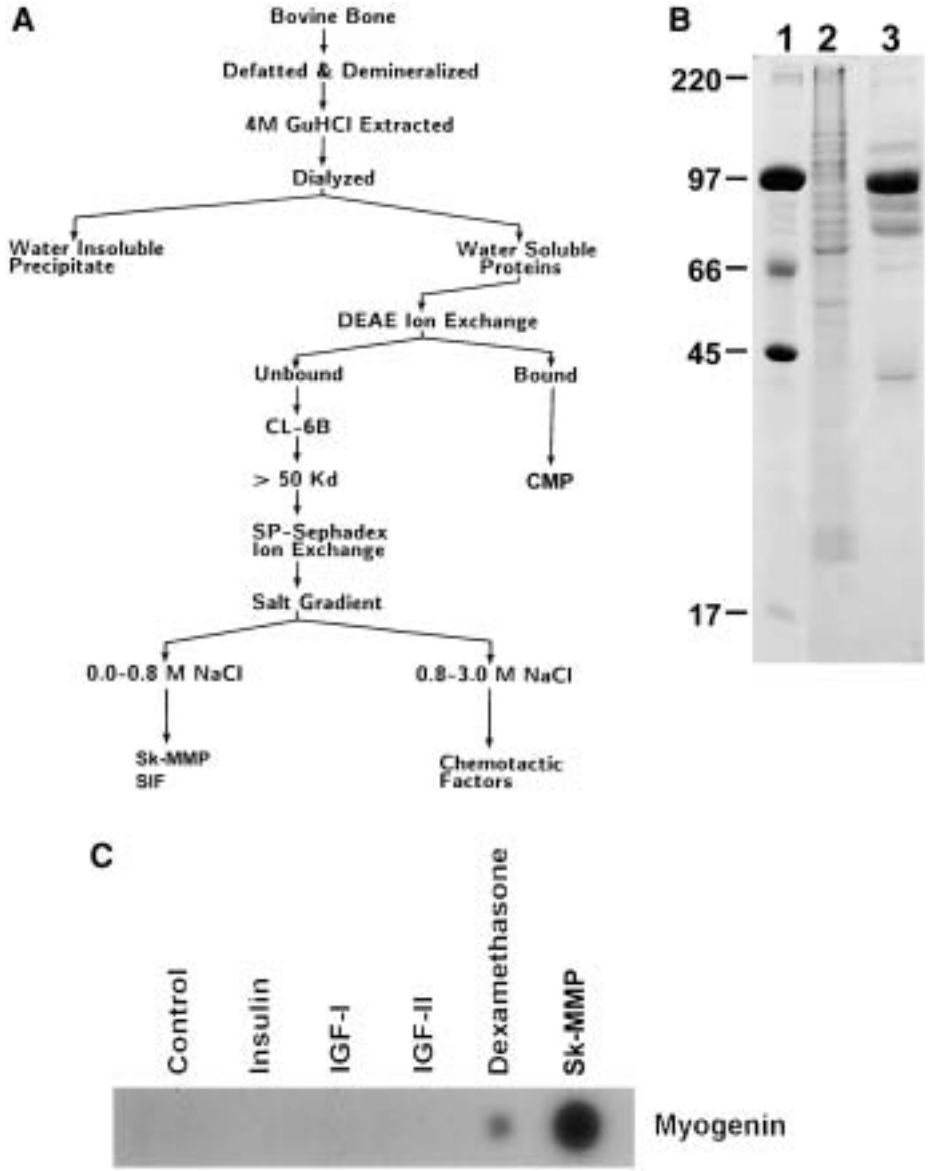

Fig. 3. **(A)** Protocol for the isolation of skeletal muscle morphogenetic protein (Sk-MMP) and scar inhibitory factor (SIF) from a water-soluble extract of demineralized bovine bone. **(B)** Coomassie Blue stained sodium dodecyl sulfate–polyacrylamide gel electrophoresis (SDS-PAGE) of water-soluble extracts derived from demineralized bovine bone. Lane 1, molecular weight standards; lane 2, water-soluble proteins containing Sk-MMP and SIF activities postdialysis to remove 4 *M* guanidine hydrochloride (4 *M* HCl); and lane 3, 0.0 to 0.8 *M* NaCl salt gradient fractions, containing Sk-MMP and SIF activities, from SP-Sephadex ion-exchange chromatography column. **(C)** Northern dot-blot hybridization analysis of induced myogenin expression in a mesodermal GLL stem cell clone *(44)*. The following bioactive factors were examined: control (10% SS10), 2 µg/mL insulin (insulin), 200 ng/mL insulin-like growth factor–1 (IGF-1), 200 ng/mL insulin-like growth factor–2 (IGF-2), 10^{-8} *M* dexamethasone (dex), and 200 ng/mL dry weight Sk-MMP.

ity corresponding to two factors within the water-soluble fractions *(29,30,43,51)*. These activities were designated as skeletal muscle morphogenetic protein (Sk-MMP) and scar inhibitory factor (SIF). These designations were made based on their ability to stimulate myogenic gene expression (Sk-MMP) (Fig. 3C) and inhibit fibrogenesis (SIF) (Table 3), as well as their combined activity in vivo in a model system for skeletal muscle repair in the adult mouse (Sk-MMP and SIF) (*see* Skeletal Muscle Repair section). We postulated that the bioactive factors isolated from demineralized bone matrix—that is, BMPs, TGF-β, IGF-1, IGF-2, insulin, Sk-MMP, SIF, and so forth—were produced by cells not belonging to the osteogenic lineage. The cells producing these factors would presumably secrete the compounds into the blood. We therefore began analyzing various lots of commercially available serum to determine if these serum lots contained other inductive activities. On the basis of their respective interaction with mesodermal GLL stem cells in vitro, we identified the following activities from serum and designated the compounds responsible for their activity as platelet-derived growth factor (PDGF)-like (proliferative) activity, Sk-MMP (Fig. 4A), smooth muscle morphogenetic protein (Sm-MMP) (Fig. 4B), adipocyte morphogenetic protein (AMP) (Fig. 4C), fibroblast morphogenetic protein (FMP) (Fig. 4D), SIF, leukemia inhibitory factor (LIF)-like (inhibitory) activity, and antidifferentiation factor (ADF)-like (inhibitory) activity (Tables 3 and 4) *(29,43)*.

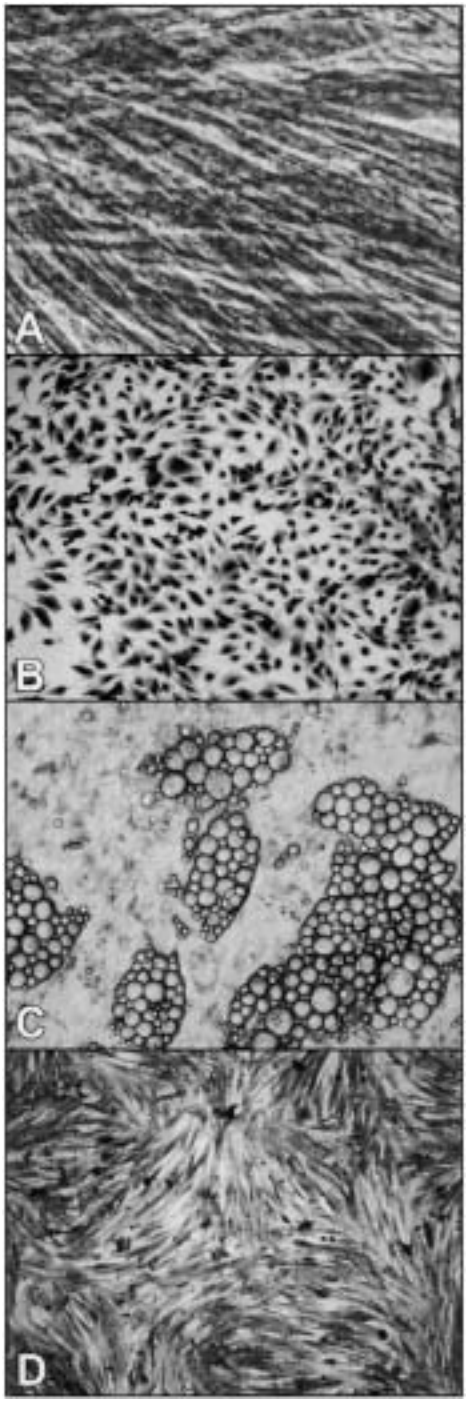

Effects of Bioactive Factors

We compared the effects of various combinations of bioactive factors on clones of tissue-specific progenitor cells and tissue-uncommitted mesodermal GLL stem cells (Table 4). We mixed equal quantities (20%) of five progenitor cell clones, each expressing a unipotent capability for the myogenic, adipogenic, chondrogenic, osteogenic, or fibrogenic lineage *(41)*. This mixed population of unipotent progenitor cell clones was then compared to a single clone of mesodermal GLL stem cells. The clone of mesodermal

Fig. 4. Reserve stem cell clones induced with novel inductive compounds. **(A)** A mixed culture containing equal quantities of a mesodermal GLL stem cell clone (St), a unipotent myoblast progenitor cell clone (Bp), and a unipotent fibroblast progenitor cell clone (Sp) *(41)* was used. Cells were plated in medium containing PDGF-like (proliferative) and ADF-like (inhibitory) activities *(28,29)*. After an initial 48 h, cultures were switched to basal medium containing FMP, Sk-MMP, and SIF *(28,43)* and incubated for an additional 12 d. Cultures were halted, processed, and stained with toluidine blue. The nuclei in ten ×40 fields were counted. Approximately 95% of the nuclei resided in multinucleated structures (MT). Parallel immunostained cultures demonstrated positive staining for sarcomeric myosin, skeletal muscle fast myosin, myosin heavy chain, and myosin fast chain, all indicative of a multinucleated skeletal muscle phenotype. **(B)** A Lac-Z-transfected adult rat pluripotent epiblastic-like stem cell clone *(29,49)* was plated in medium containing PDGF-like (proliferative) and ADF-like (inhibitory) activities *(28,29)*. After 48 h, the cultures were switched to medium containing smooth muscle morphogenetic protein activity (Sm-MMP) *(28)* and incubated for 14 d. Cultures were halted, processed for ELICA using an antibody to β-galactosidase, and costained with an antibody to smooth muscle α-actin (IA4) *(40)*. The nuclei in ten ×40 fields were counted. Approximately 90% of the nuclei residing in cells demonstrated intracellular staining for the IA4 antibody. **(C)** A Lac-Z-transfected adult rat pluripotent epiblastic-like stem cell clone *(29,49)* was plated in medium containing PDGF-like (proliferative) and ADF-like (inhibitory) activities *(28,29)*. After 48 h, the cultures were switched to medium containing AMP *(28)* and incubated for an additional 14 d. Cultures were halted, fixed *(46)*, and photographed. Approximately 60% of cells contained intracellular refractile vesicles. Parallel experiments generated similar structures demonstrating intracellular staining for saturated neutral lipids using Oil Red-O and Sudan Black-B histochemistry *(46,47)*. **(D)** A mixed culture containing equal quantities of a mesodermal GLL stem cell clone (St), a unipotent myoblast progenitor cell clone (Bp), and a unipotent fibroblast progenitor cell clone (Sp) *(41)* was used. Cells were plated in medium containing PDGF-like (proliferative) and ADF-like (inhibitory) activities *(28,29)*. After 48 h, the cultures were switched to medium containing fibroblast morphogenetic protein activity (FMP) *(28,43)* and incubated for an additional 12 d. Cultures were halted, fixed, and stained with toluidine blue. The nuclei in ten ×40 fields were counted. Approximately 98% of the nuclei resided in mononucleated spindle-shaped cells (Sp). Parallel experiments using human pluripotent mesodermal stem cell lines ($CD10^+$, $CD13^+$, $CD34^+$, $CD56^+$, $CD90^+$, MHC-I^+) *(47)* generated similar-appearing spindle-shaped structures demonstrating staining for fibroblast-specific protein.

GLL stem cells contained the capacity to generate phenotypic markers for the same five mesodermal tissue lineages (i.e., the myogenic, adipogenic, chondrogenic, osteogenic, and fibrogenic lineages) *(41)*. We used the enzyme-linked immunoculture (ELICA) bioassay *(40)* to quantify phenotypic expression in the treated cultures. The bioactive factors examined, both individually and in combination, included recombinant human platelet-derived growth factor–AA (rh-PDGF-AA), platelet-derived growth factor–BB (rh-PDGF-BB), platelet-derived growth factor–AB (rh-PDGF-AB), platelet-derived endothelial cell growth factor (rh-PD-ECGF), basic fibroblast growth factor (rh-b-FGF), transforming growth factor–beta (rh-TGF-β), dexamethasone (dex), Sk-MMP, bone morphogenetic protein–2 (BMP-2), cartilage morphogenetic protein (CMP), FMP, AMP, insulin, IGF-1, IGF-2, recombinant murine–ESGRO (rm-LIF), leukemia inhibitory factor (rh-LIF), SIF, and antidifferentiation factor (rh-ADF). Examples of single and combinatorial experiments performed are given in Table 4. Those studies demonstrated four basic types of biological activity expressed by the

Table 3
Inhibitors of Induction and/or Differentiation

	SIF	ESGRO	h-LIF	ADF
Species	All	Murine	Human and rat	All
Affect postconfluent cells	Yes	Yes	Yes	Yes
Affect postconfluent cells	Yes	No	No	Yes
Titration	Quantity per inductive factor	Quantity per cell number	Quantity per cell number	Quantity per inductive factor
Amount	2 ng/mL (FMP)	2000 U/mL (10^6 cells)	2000 U/mL (10^6 cells)	2 U/mL (MMP)
Inhibition of inductive factors[a]	FMP (only)	All	All	All
Inhibition of progression factors[b]	None	None	None	All

[a]Inductive factors examined: dexamethasone, bone morphogenetic protein-2, skeletal muscle morphogenetic protein, smooth muscle morphogenetic protein, adipocyte morphogenetic protein, fibroblast morphogenetic protein.

[b]Progression factors examined: insulin, insulin-like growth factor–1, insulin-like growth factor–2.

SIF, scar inhibitory factor (not purified); ESGRO, murine-leukemia inhibitory factor (recombinant murine protein); h-LIF, human-leukemia inhibitory factor (recombinant human protein); ADF, antidifferentiation factor (recombinant human protein).

bioactive factors examined on both the mixed population of progenitor cell clones and the single mesodermal GLL stem cell clone. The four activities were proliferative (initiating and/or accelerating proliferation), progressive (accelerating differentiative phenotypic expression), inductive (committing cells to one or more tissue lineages or cell types), and/or inhibitory (preventing induction and/or progression [acceleration of phenotypic marker expression for differentiated cell types]) *(28,30,43,51,54,55,58)*.

Windows of Inductive Activity

Our previous studies examining the differentiative capabilities of mesodermal GLL stem cell clones *(41,43,44,57)* demonstrated that myogenesis and adipogenesis would occur within 2 wk after incubation with dexamethasone, chondrogenesis would occur after 4 wk of incubation, and osteogenesis would occur after 6 wk of incubation. These time periods for phenotypic expression could be sharply reduced by the addition of a progression factor (such as insulin) to the culture medium. These results suggested that the process of induction (gene activation) might occur earlier within the incubation time period necessary for the complete expression of the phenotype. Using novel (Sk-MMP) and recombinant (BMP-2) factors, Lucas et al. *(50–53,99,* unpublished observations*)* determined that myogenesis, chondrogenesis, and osteogenesis could be induced during the first week of incubation. The remaining time period was necessary for the progression and expression of differentiative phenotypic markers. Next, Lucas et al. initiated a series of studies to determine whether the entire 7-d time period was necessary for induction or whether there might be discrete win-

Table 4
Percentage of Phenotypic Expression in Mixed Progenitor Cell Clones and a Mesodermal Germ-Layer Lineage Stem Cell (MGLLSC) Clone

Bioactive factors	Myogenic	Adipogenic	Chondrogenic	Osteogenic	Fibrogenic	MGLLSC clone
INS	20	20	20	20	20	0
MMP	20	0	0	0	0	80 (Myo)
FMP	0	0	0	0	20	95 (Fibro)
SIF	0	0	0	0	0	0
MMP + INS	20	20	20	20	20	95 (Myo)
MMP + FMP	0	0	0	0	95	95 (Fibro)
MMP + SIF	20	0	0	0	0	80 (Myo)
FMP + INS	0	0	0	0	20	95 (Fibro)
FMP + SIF	0	0	0	0	0	0
SIF + INS	20	20	20	20	0	0
MMP + INS + FMP	0	0	0	0	20	95 (Fibro)
MMP + INS + SIF	20	0	0	0	0	95 (Myo)
MMP + FMP + SIF	20	0	0	0	0	80 (Myo)
MMP + INS + FMP + SIF	20	0	0	0	0	95 (Myo)
MMP fb INS	0	0	0	0	0	0
INS fb MMP	20	20	20	20	20	95 (Myo)
MMP fb FMP	0	0	0	0	0	0
FMP fb MMP	20	0	0	0	20	95 (Fibro)
MMP fb SIF	0	0	0	0	0	0
SIF fb MMP	20	0	0	0	0	80 (Myo)
FMP fb INS	0	0	0	0	20	95 (Fibro)
INS fb FMP	0	0	0	0	0	0
FMP fb SIF	0	0	0	0	20	95 (Fibro)
SIF fb FMP	0	0	0	0	0	0
SIF fb INS	0	0	0	0	0	0
INS fb SIF	20	20	20	20	20	0
MMP + INS fb FMP	0	0	0	0	0	0
MMP + SIF fb FMP	0	0	0	0	0	0
MMP + INS + SIF fb FMP	0	0	0	0	0	0
FMP + INS fb MMP	20	0	0	0	20	95 (Fibro)
FMP + SIF fb MMP	20	0	0	0	0	80 (Myo)
FMP + INS + SIF fb MMP	20	0	0	0	0	80 (Myo)
FMP + SIF fb MMP + INS	20	0	0	0	0	95 (Myo)

INS, insulin. Sk-MMP, skeletal muscle morphogenetic protein: a novel compound that induces the expression of transcription factors MyoD and myogenin in vitro *(44)*, induces formation of multinucleated spontaneously contracting structures demonstrating cross-striations and staining with antibodies to skeletal muscle myosin in vitro *(28,44)*, and induces skeletal muscle regeneration in vivo. FMP, fibroblast morphogenetic protein: a novel compound that induces expression of fibrogenic phenotype in vitro *(28)* and stimulates scar tissue formation in vivo. SIF, scar inhibitory factor: a novel compound that inhibits fibrogenic induction and progression in vitro *(28)* and inhibits scar tissue formation in vivo. fb, followed by: initial experiments used a 3-d incubation for the first agent(s) *followed by* a 24-h incubation in control medium, *followed by* a 3-d incubation with the second agent(s). The combination/reciprocal experiments demonstrated overlapping windows of activity for FMP (1–3 d), AMP (2–4 d), BMP-2 (3–5 d), and Sk-MMP (4–6 d) bioactive factors.

dows of activity for the tissue-specific induction factors. The experimental design was a twofold reciprocal experiment. Both series of experiments consisted of seven sets of identical cultures. In the first series, seven sets of cultures were fed inductive factors on d 1, six sets on d 2, and so forth, ending with one set on d 7. The second series of inductive factor incubations was the reciprocal experiment. In this series, one set of cultures was incubated with inductive factors on d 1, a second set of cultures was started on inductive factors on d 2, and so forth, ending with a seventh set of cultures that was started on inductive factors on d 7. Their results showed that BMP-2 induced chondrogenic and osteogenic activity in the cultures during a 3- to 5-d window and that Sk-MMP induced myogenesis in the cultures during a 4- to 6-d window. We have repeated those experiments using BMP-2, Sk-MMP, FMP, and AMP with a clone of mesodermal GLL stem cells. We noted that, once activated, the mesodermal GLL stem cells exhibited overlapping windows of activity with respect to inductive compounds acting on the mesodermal lineage. In sequential order, the windows of inductive activity were fibrogenic (d 1–3), adipogenic (d 2–4), chondrogenic/osteogenic (d 3–5), and myogenic (d 4–6) *(28,43)*.

Unique Cell Surface Markers

We are involved in strategies designed to facilitate the immediate isolation of purified populations of reserve stem cells from the connective tissues of human subjects for potential use in transplantation therapies. We are analyzing cell surface cluster of differentiation (CD) markers *(100)* coupled with flow cytometric analysis to determine if we can identify unique marker combinations on these stem cells. The following 58 CD markers have been examined thus far: CD1a, CD2, CD3, CD4, CD5, CD7, CD8, CD9, CD10, CD11b, CD11c, CD13, CD14, CD15, CD16, CD18, CD19, CD20, CD22, CD23, CD24, CD25, CD31, CD33, CD34, CD36, CD38, CD41, CD42b, CD44, CD45, CD49d, CD55, CD56, CD57, CD59, CD61, CD62E, CD65, CD66e, CD68, CD69, CD71, CD79, CD83, CD90, CD95, CD105, CD117, CD123, FLT3 (CD135), CD166, Glycophorin-A, HLA Class-I, HLA-DRII, FMC-7, Annexin-V, and LIN antigens *(45,47,48)*. Six CD markers (i.e., CD10, CD13, CD34, CD56, CD90, and MHC-I) were identified as forming a unique "fingerprint" for mesodermal GLL stem cells using cell lines generated from human fetal, newborn, adult, and geriatric donors (Fig. 5A–F) *(29,45,47)*.

Reserve Stem Cells Residing in Tissues

Procedures designed specifically for the immediate harvest of mesodermal GLL stem cells from connective tissue compartments, coupled with CD cell surface marker analysis, were used to analyze stem cells within postnatal human connective tissue compartments. On the basis of our previous studies, we had hypothesized that a single population of mesodermal GLL stem cells would be present in adult connective tissues of mesodermal origin. Much to our surprise, we found five separate populations of putative stem cells, each with their own unique profile of CD markers. We are currently characterizing two of these five populations—the mesodermal GLL stem cells *(28,30,46,47)* and pluripotent epiblastic-like stem cells *(29,48,49)*.

Mesodermal Germ-Layer Lineage Stem Cells

The first population characterized expressed the $CD10^+$, $CD13^+$, $CD34^+$, $CD56^+$, $CD90^+$, MHC-I^+, $CD1a^-$, $CD2^-$, $CD3^-$, $CD4^-$, $CD5^-$, $CD7^-$, $CD8^-$, $CD9^-$, $CD11b^-$, $CD11c^-$, $CD14^-$, $CD15^-$, $CD16^-$, $CD18^-$, $CD19^-$, $CD20^-$, $CD22^-$, $CD23^-$, $CD24^-$, $CD25^-$, $CD31^-$, $CD33^-$, $CD36^-$, $CD38^-$, $CD41^-$, $CD42b^-$, $CD45^-$, $CD49d^-$, $CD55^-$, $CD57^-$, $CD59^-$, $CD61^-$, $CD62E^-$, $CD65^-$, $CD66e^-$, $CD68^-$, $CD69^-$, $CD71^-$, $CD79^-$, $CD83^-$, $CD95^-$, $CD105^-$, $CD117^-$, $CD123^-$, $CD135^-$, $CD166^-$, Glycophorin-A^-, HLA-$DRII^-$, FMC-7^-, Annexin-V^-, and LIN^- cell surface profile. This population displayed all the characteristics seen previously for mesodermal GLL stem cells isolated from both human cell

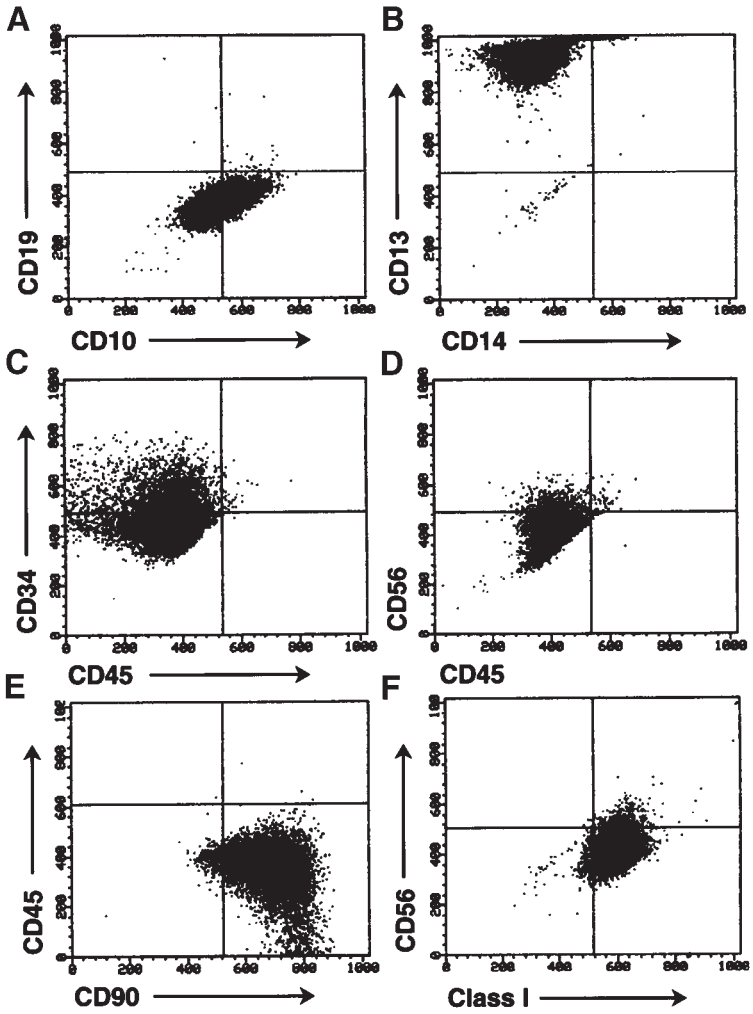

Fig. 5. Human pluripotent mesodermal stem cells analyzed by flow cytometry for cluster of differentiation markers. *X*-axis and *Y*-axis noted on figure. Cell line derived from 25-yr-old adult human female dermal biopsy specimen propagated to 30 cell doublings and analyzed with antibodies to cell surface cluster of differentiation markers. **(A)** CD19 and CD10. **(B)** CD13 and CD14. **(C)** CD34 and CD45. **(D)** CD56 and CD45. **(E)** CD45 and CD90. **(F)** CD56 and Class-I. (Reproduced with permission from Young, H. E., Steele, T. A., Bray, R. A., Detmer, K., Blake, L. W., Lucas, P. A., et al. [1999] Human pluripotent and progenitor cells display cell surface cluster differentiation markers CD10, CD13, CD56, and MHC Class-I. *Proc. Soc. Exp. Biol. Med.* **221,** 63–71. Copyright 1999, Society for Experimental Biology and Medicine, Blackwell Science; Young, H. E., Steele, T., Bray, R. A., Hudson, J., Floyd, J. A., Hawkins, K. C., et al. [2001] Human reserve pluripotent mesenchymal stem cells are present in the connective tissues of skeletal muscle and dermis derived from fetal, adult, and geriatric donors. *Anat. Rec.* **264,** 51–62. Copyright 2001, Wiley-Liss.)

lines and nonhuman clones. The stem cells were shown to be 10–20 μm in size by flow cytometric analysis of unfixed cells. The stem cells displayed extended capabilities for self-renewal well past Hayflick's limit, propagating past 200 population doublings without loss of differentiative potential *(28,46,47)*. These stem cells remained quiescent in serum-free defined medium lacking leukemia inhibitory factor or antidifferentiation factor (Fig. 6A). They did not express embryonic stem cell markers, such as stage-specific embryonic antigen–1, –3, –4; carcinoembryonic antigen; or carcinoembryonic antigen-cell adhesion molecule (Table 5) *(29)*. In serum-free defined medium without proliferation factors, inductive factors, or inhibitory factors (i.e., leukemia inhibitory factor or antidifferentiation factor), the stem cells existed in a quiescent state. They displayed no proliferation, no spontaneous differentiation, and no cell death. In the presence of proliferation factors, these stem cells displayed contact inhibition at confluence, ceasing cell proliferation once a single layer of cells covered the culture surface (Fig. 6B) *(46)*. This occurred even in the presence of known proliferation agents such as platelet-derived growth factors *(28,43)*. These stem cells were responsive to both general and specific inductive factors *(28,30,43)*, but only with respect to cells of the embryonic mesodermal germ-layer lineage, demonstrating the ability to form 18 or more exclusively mesodermal phenotypes *(29,46–49)* (Table 5, Figs. 6C–G, 7A–Z). These stem cells were unresponsive to specific inductive factors for ectodermal or endodermal lineage cells (Table 5). Mesodermal GLL stem cells were unresponsive to progression factors *(28,43)* in the undifferentiated tissue-uncommitted state. Mesodermal GLL stem cells formed progenitor stem cells limited to the embryonic mesodermal germ-layer lineage following induction of tissue/cell commitment (Tables 4 and 5). Once committed to a particular tissue or cell type, the new lineage-specific progenitor cells were unresponsive to inductive factors outside their respective tissue or cell type. Thus, newly formed progenitor cells committed to form myogenic tissues were unresponsive to BMP-2, and cells committed to form chondrogenic tissues were unresponsive to Sk-MMP *(28)*. However, these same newly formed progenitor cells responded to progression factors (such as insulin, IGF-1, or IGF-2) by accelerating the expression of their differentiated phenotype. They also assumed Hayflick's limit of 50 to 70 population doublings before programmed cell senescence and cell death occurred *(28–30, 43,45–47)*.

Pluripotent Epiblastic-Like Stem Cells

The second population of putative reserve stem cells derived from adult human connective tissues expressed a $CD10^+$, $CD66e^+$, $CD1a^-$, $CD2^-$, $CD3^-$, $CD4^-$, $CD5^-$, $CD7^-$, $CD8^-$, $CD9^-$, $CD11b^-$, $CD11c^-$, $CD13^-$, $CD14^-$, $CD15^-$, $CD16^-$, $CD18^-$, $CD19^-$, $CD20^-$, $CD22^-$, $CD23^-$, $CD24^-$, $CD25^-$, $CD31^-$, $CD33^-$, $CD34^-$, $CD36^-$, $CD38^-$, $CD41^-$, $CD42b^-$, $CD45^-$, $CD49d^-$, $CD55^-$, $CD56^-$, $CD57^-$, $CD59^-$, $CD61^-$, $CD62E^-$, $CD65^-$, $CD68^-$, $CD69^-$, $CD71^-$, $CD79^-$, $CD83^-$, $CD90^-$, $CD95^-$, $CD105^-$, $CD117^-$, $CD123^-$, $CD135^-$, $CD166^-$, Glycophorin-A^-, MHC-I^-, HLA-$DRII^-$, FMC-7^-, Annexin-V^-, and LIN^- cell surface profile. We also cloned putative stem cell populations with similar characteristics from postnatal rats. Both the sorted adult human cells and cloned postnatal rat cells show similarities and differences with respect to the mesodermal GLL stem cells. Similarities include extended capabilities for self-renewal, quiescence in serum-free defined media without inhibitory agents, responsiveness to inductive factors, unresponsiveness to progression factors, and assumption of progenitor cell status once committed to a particular tissue or cell type. The induced tissue-specific progenitor cells derived from $CD10^+$ and $CD66e^+$ cells exhibited contact inhibition at confluence, lack of responsiveness to induction factors outside their respective tissue or cell type, responsiveness to progression factors accelerating their phenotypic expression, and conformance to Hayflick's limit of 50–70 population doublings before programmed cell senescence and cell death occurred.

Table 5
Induction of Phenotypic Expression in Native and Induced Adult Precursor Stem Cell Lines

Phenotypic markers	ELSCs	EctoGLLSCs	MGLLSCs	EndoGLLSCs	PanPCs	3D-ILS
Embryonic						
Alkaline phosphatase	+	–	–	–	–	–
SSEA-1	+	–	–	–	–	–
SSEA-3	+	–	–	–	–	–
SSEA-4	+	–	–	–	–	–
CEA	+	–	–	–	–	–
HCEA	+	–	–	–	–	–
CD66e	+	–	–	–	–	–
CEA-CAM	+	–	–	–	–	–
Ectoderm						
Neuronal progen cells	+	+	–	–	–	–
Neurons	+	+	–	–	–	–
Ganglia	+	+	–	–	–	–
Oligodendrocytes	+	+	–	–	–	–
Astrocytes	+	+	–	–	–	–
Radial glial cells	+	+	–	–	–	–
Keratinocytes	+	+	–	–	–	–
Mesoderm						
Skeletal muscle	+	–	+	–	–	–
Smooth muscle	+	–	+	–	–	–
Cardiac muscle	+	–	+	–	–	–
White fat	+	–	+	–	–	–
Brown fat	+	–	+	–	–	–
Hyaline cartilage	+	–	+	–	–	–
Articular cartilage	+	–	+	–	–	–
Elastic cartilage	+	–	+	–	–	–
Growth plate cartilage	+	–	+	–	–	
Fibrocartilage	+	–	+	–	–	–
Endochondral bone	+	–	+	–	–	–
Intramembrane bone	+	–	+	–	–	–
Tendon/ligament	+	–	+	–	–	
Dermis	+	–	+	–	–	–
Scar tissue	+	–	+	–	–	–
Endothelial cells	+	–	+	–		
Hematopoietic cells	+	–	+	–	–	–
Endoderm						
Endodermal progenitor cells	+	–	–	+	–	–
Gastrointestinal epithelium	+	–	–	+	–	–
Liver oval cells	+	–	–	+	–	–
Liver hepatocytes	+	–	–	+	–	–
Liver biliary cells	+	–	–	+	–	–
Liver canalicular cells	+	–	–	+	–	–
Pancreas progenitor cells	+	–	–	+	+	–
Pancreas ductal cells	+	–	–	+	+	+
Pancreatic β-cells	+	–	–	+	+	+
Pancreatic α-cells	+	–	–	+	+	+
Pancreatic δ-cells	+	–	–	+	+	+

PPELSCs, pluripotent epiblastic-like stem cells (isolated and cloned). EctoGLLSCs, ectodermal germ-layer lineage stem cells (induced). MGLLSCs, mesodermal germ-layer lineage stem cells (isolated and cloned). EndoGLLSCs, endodermal germ-layer lineage stem cells (induced). PanPCs, pancreatic progenitor cells (induced). 3D-ILS, 3D-islet-like structures (induced). CEA, carcinoembryonic antigen. HCEA, human carcinoembryonic antigen. CD66e, carcinoembryonic antigen. CEA-CAM, carcinoembryonic antigen-cell adhesion molecule *(29,48,49)*.

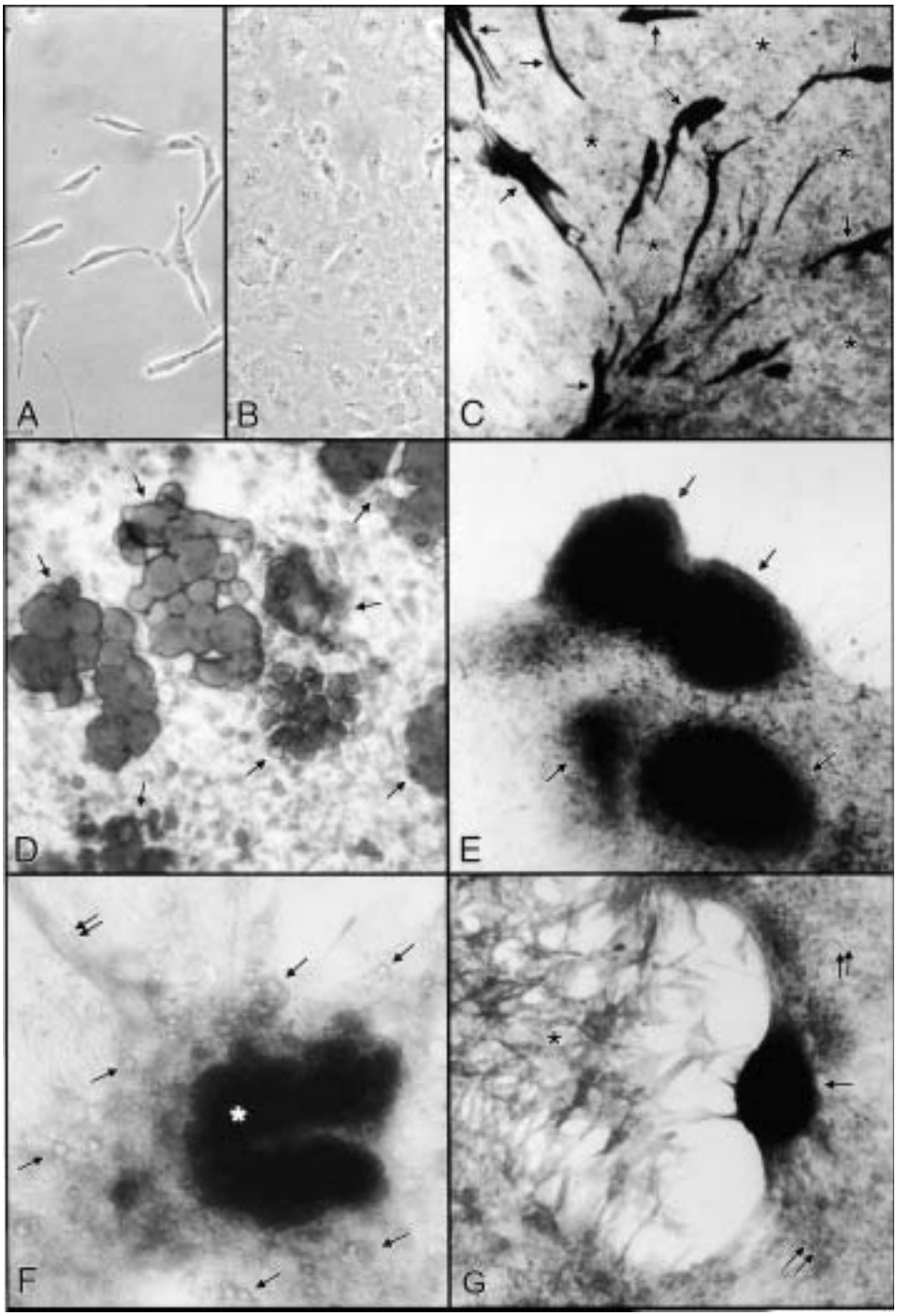
A
B
C
D
E
F
G

Fig. 6. Postnatal rat mesodermal GLL stem cell clone demonstrating mesodermal morphologies. Clone Rat-A2A2 incubated in stem cell medium (SCM), testing medium-6 (TM-6), or TM-6 with 10^{-6} *M* Dexamethasone (dex) for 1 to 42 d *(46)*. SCM contained PDGF-like (proliferative) and ADF-like (inhibitory) activities *(28,29)*. TM-6 contained Sk-MMP-like, AMP-like, and BMP-2-like inductive activities *(28)*. Cultures were grown in SCM (**A**), TM-6 only (**B**), or TM-6 with dex (**C–G**) for 24 h (**A**) or 6 wk (**B–G**). Morphologies and histochemical and immunochemical staining as noted. Photographed with phase contrast (**A**, **B**) and brightfield (**C–G**) microscopy; original magnifications ×200 (**A**, **B**) and ×100 (**C–G**). **(A)** Small mononucleated cells with large ratios of nucleus to cytoplasm. **(B)** Single layer of nondescript contact-inhibited cells. **C:** Dark structures stained with antibody to sarcomeric myosin (MF-20) (arrow). Most of the unstained cells in background are adipocytes (fat cells) (asterisks). **(D)** Cells with multiple Oil Red-O stained intracellular vesicles indicative of saturated neutral lipid-containing adipocytes (arrow). **(E)** Aggregating nodules of rounded cells with pericellular matrix halos staining with antibody to type II collagen (CIIC1) (arrow). **(F)** Aggregating nodule of cells overlaid with horseshoe-shaped extracellular matrix staining with antibody to bone sialoprotein (WV1D1) (white asterisk). Unstained refractile intercellular vesicles belong to adipocytes (single arrows). A diagonally oriented smooth muscle cell stained with an antibody to smooth muscle α-actin (1A4) (double arrows) is located in the upper left-hand corner of photograph. **(G)** Aggregating nodule of cells (single arrow) with pericellular matrix halos staining with antibody to type IX collagen (D1-9). Also note aggregation of unstained adipocytes (double arrows) and individual cells (asterisk) stained with antibody to smooth muscle α-actin (1A4). (Reproduced with permission from Young, H. E., Duplaa, C., Young, T. M., Floyd, J. A., Reeves, M. L., Davis, K. H., et al. [2001] Clonogenic analysis reveals reserve stem cells in postnatal mammals: I. Pluripotent mesenchymal stem cells. *Anat. Rec.* **263,** 350–360. Copyright 2001, Wiley-Liss.)

However, differences existed between the mesodermal GLL stem cells expressing the $CD10^+$, $CD13^+$, $CD34^+$, $CD56^+$, $CD90^+$, and MHC-I^+ cell surface markers and the putative stem cells expressing the $CD10^+$ and $CD66e^+$ cell surface markers. These differences strongly suggested the existence of a separate and unique category of stem cells. This second category of stem cells, expressing a $CD10^+$ and $CD66e^+$ CD marker cell surface profile and derived from adults, was shown to consist of small stellate cells (Figs. 8A, 9A) of 6–8 μm in size by flow cytometric analysis of unfixed cells. These stem cells did not exhibit contact inhibition at confluence but rather formed multiple confluent layers in vitro (Figs. 8B, 9B). These adult-derived cells expressed embryonic stem cell markers—that is, alkaline phosphatase; stage-specific embryonic antigen–1, –3, and –4; carcinoembryonic antigens; carcinoembryonic antigen-cell adhesion molecule (Table 5, Figs. 8C–H, 9C–D), and *Oct-4* gene expression (Fig. 10A,B) in a quiescent undifferentiated state. These stem cells, either sorted (using $CD10^+$ and $CD66e^+$) or cloned from single cells by repetitive single-cell clonogenic analysis, have formed more than 36 distinct cell types thus far from all three primary germ layers: 7 or more ectodermal cell types (i.e., neuronal progenitor cells, neurons, ganglia, astrocytes, oligodendrocytes, radial glial cells, keratinocytes) (Table 5, Figs. 11A–L, 12A–I), 18 or more mesodermal cell types (i.e., skeletal muscle, cardiac muscle, smooth muscle, white fat, brown fat, hyaline cartilage, elastic cartilage, growth plate cartilage, articular cartilage, fibrocartilage, cortical bone, trabecular bone, loose fibrous connective tissues, tendon, ligament, scar-connective tissue, endothelial cells, hematopoietic cells) (Table 5, Figs. 13A–DD, 14A–U), and 11 or more endodermal cell types (i.e., endodermal progenitor cells, gastroin-

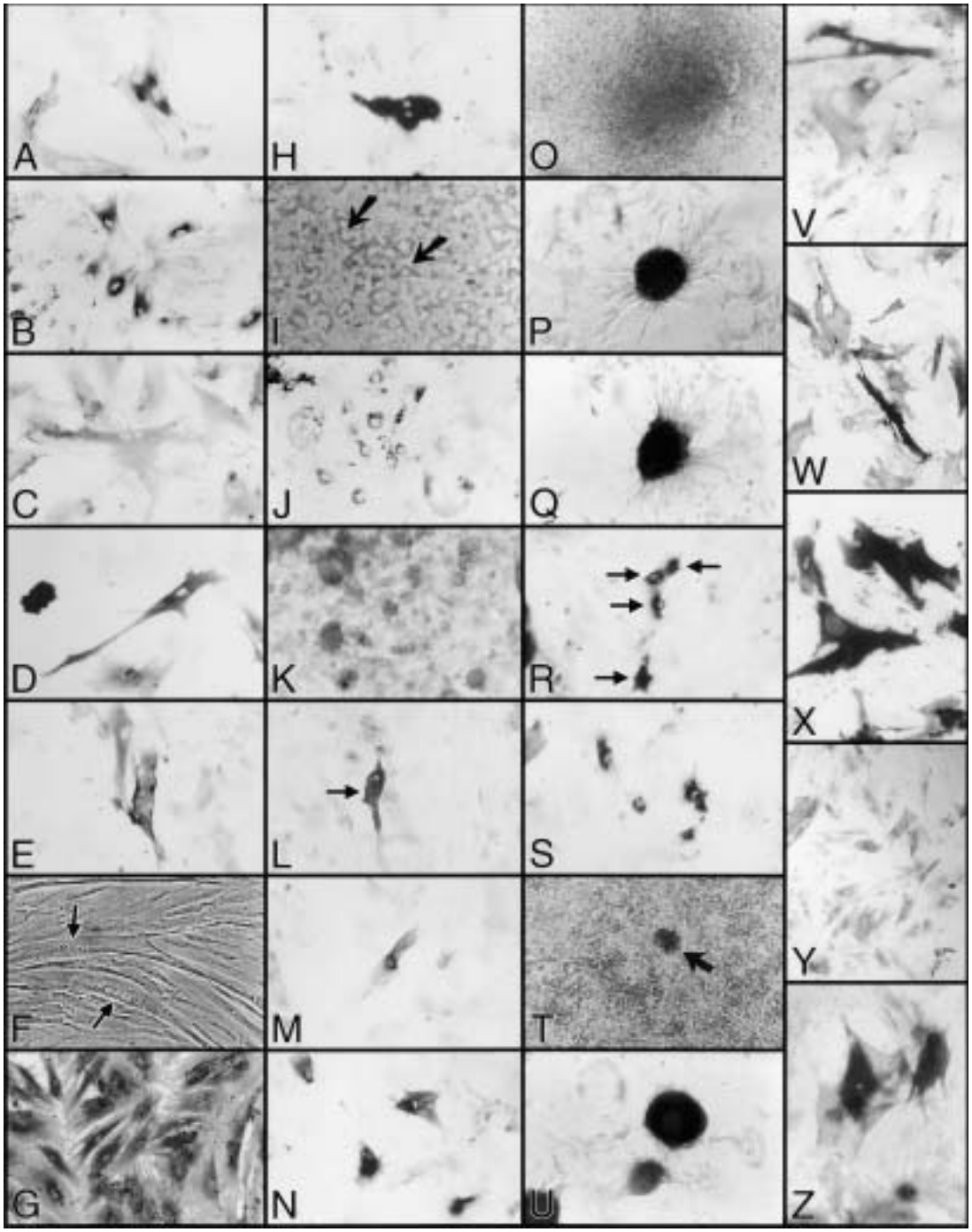
A
H
O
V
B
I
P
W
C
J
Q
D
K
R
X
E
L
S
Y
F
M
T
G
N
U
Z

Fig. 7. Human mesodermal GLL stem cell lines: NHDF2 cells, derived from 36-yr-old human female dermal biopsy specimen, at 80 cell doublings (**A–I**, **K–O**, **R–T**, **V–Z**) and PAL3 cells, derived from 67-yr-old human male skeletal muscle biopsy specimen, at 150 cell doublings (**J**, **P**, **Q**, **U**). Cells were grown for 14 (**B**, **G**, **I**), 28 (**O**), 42 (**J**, **P**, **Q**, **T**, **U**), or 56 (**A**, **C**, **D–F**, **H**, **K–N**, **R**, **S**, **V–Z**) d in testing medium (TM) containing Sk-MMP-like, AMP-like, and BMP-2-like endothelial inductive activities *(28)* (**A–I**, **K–P**, **R–T**, **V–Z**), Sm-MMP-like activity *(28)* (**J**, **Q**, **U**), and 10^{-6} *M* dex (**A–P**, **R–T**, **V–Z**) or 10^{-10} *M* dex (**Q**, **U**) *(47)*. Morphologies and histochemical and immunochemical staining as noted. Cells were photographed at ×25 (**O**), ×40 (**T**, **Y**), ×50 (**Q**, **U**), ×100 (**A–E**, **G**, **H**, **J–N**, **P–S**, **U–Z**), or ×125 (**I**) magnification in either brightfield (**A–E**, **G**, **H**, **J–N**, **P–S**, **U–Z**) or phase contrast (**F**, **I**, **O**, **T**) microscopy. **(A)** Mononucleated cells staining intracellularly for myogenin (F5D). **(B)** Mononucleated cells staining intracellularly for sarcomeric myosin (MF-20). **(C)** Trinucleated cells staining intracellularly for skeletal muscle fast myosin (MY-32). **(D)** Mononucleated cells staining intracellularly for myosin heavy chain (ALD58). **(E)** Mononucleated cells staining intracellularly for myosin fast chain (A4.74). **(F)** Two linear structures (arrows) containing multiple nuclei. **(G)** Mononucleated cells staining intracellularly for smooth muscle α-actin (IA4). **(H)** Binucleated cell costaining intracellularly for sarcomeric myosin (MF-20) and smooth muscle α-actin (IA4). **(I)** Mononucleated cells with intracellular refractile vesicles. **(J)** Mononucleated cells with intracellular vesicles stained for saturated neutral lipids (Sudan Black-B). **(K)** Mononucleated cells with intracellular vesicles stained for saturated neutral lipids (Oil Red-O). **(L)** Mononucleated cell staining intracellularly for type II collagen (CIIC1). **(M)** Mononucleated cells staining intracellularly for type II collagen (II-4CII). **(N)** Mononucleated cells staining intracellularly for type IX collagen (D1-9). **(O)** Aggregation of cells with pericellular matrix halos. **(P)** Nodule stained for chondroitin sulfate and keratan sulfate glycosaminoglycans (Alcian Blue, pH 1.0). **(Q)** Nodule stained for sulfated moieties (Perfix/Alcec Blue). **(R)** Mononucleated cells staining intracellularly for bone sialoprotein II (WV1D1). **(S)** Mononucleated cells staining intracellularly for osteopontine (MP111). **(T)** 3D matrix (arrow) overlying cell cluster. **(U)** Nodules stained for calcium phosphate (von Kossa). **(V)** Mononucleated cells stained for fibroblast-specific protein (1B10). **(W)** Mononucleated cells stained for human endothelial cell surface marker (P1H12). **(X)** Mononucleated cells stained for peripheral cell adhesion molecule (P2B1). **(Y)** Mononucleated cells stained for vascular cell adhesion molecule (P8B1). **(Z)** Mononucleated cells stained for E-selectin (P2H3). (Reproduced from Young, H. E., Steele, T., Bray, R. A., Hudson, J., Floyd, J. A., Hawkins, K. C., et al. [2001] Human reserve pluripotent mesenchymal stem cells are present in the connective tissues of skeletal muscle and dermis derived from fetal, adult, and geriatric donors. *Anat. Rec.* **264,** 51–62. Copyright 2001, Wiley-Liss.)

testinal epithelium, liver oval cells, liver hepatocytes, liver biliary cells, liver canalicular cells, pancreatic progenitor cells, pancreatic ductal cells, and glucagon-secreting α-cells, insulin-secreting β-cells, and somatostatin-secreting δ-cells of pancreatic islets) (Table 5, Figs. 15A–K, 16A–R). We propose that the second population of stem cells is a sequestered embryonic-like stem cell existing within an adult. We have designated this population as a *pluripotent epiblastic-like stem cell* because of its capacity for extended self-renewal and the ability to form cell types from all three primary germ-layer lineages *(29,48,49)*.

Capacity for Extended Self-Renewal

One of the hallmarks of embryonic stem cells is their capacity for extended self-renewal *(101,102)*, enabling them to proliferate well past Hayflick's limit of 50–70 population doublings *(88)*. We hypothesized that if the adult stem cells discussed herein were similar to embryonic stem cells in their ability to propa-

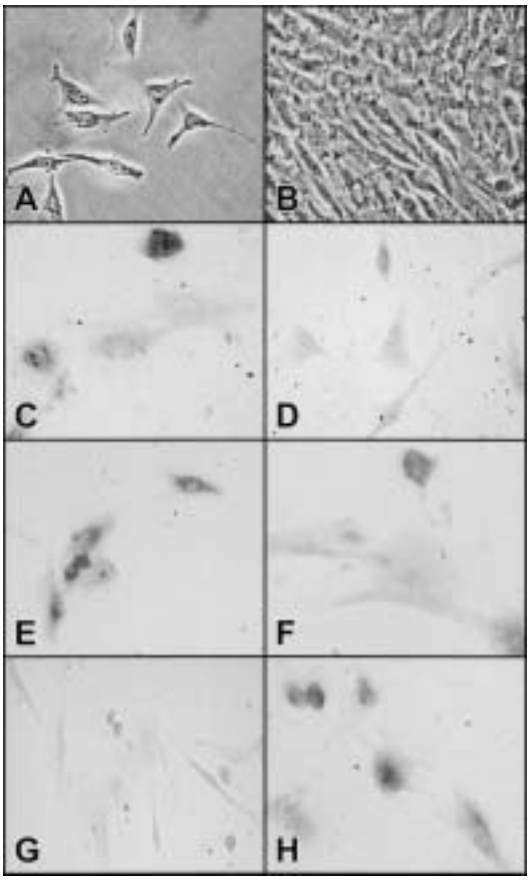

Fig. 8. Human ($CD10^+$, $CD66e^+$) postnatal pluripotent epiblastic-like stem cell line (PPELSC) demonstrating embryonic markers. Multiple PPELSC lines were grown for 24 h to 8 wk in serum-free testing medium (TM) only *(49)* (**A**), TM with PDGF-like (proliferative) and ADF-like (inhibitory) activities *(28,29)* (**B**), or TM with 2 μg/mL insulin (**C–H**) for 24 h (**A**) or 7 d (**B–H**). Morphologies and immunochemical staining as noted. Photographed with phase contrast (**A**, **B**) and brightfield microscopy (**C–H**). Original magnifications, ×200 (**A**, **B**, **G**) and ×250 (**C–F**, **H**). **(A)** Very small cells with high nuclear to cytoplasmic ratios. **(B)** Multilayered confluent cells maintaining stellate morphology. **(C)** Moderate to heavy staining for stage-specific embryonic antigen–1 (SSEA-1). **(D)** Moderate staining for stage-specific embryonic antigen–3 (SSEA-3). **(E)** Moderate to heavy staining for stage-specific embryonic antigen–4 (SSEA-4). **(F)** Moderate to heavy staining for human carcinoembryonic antigen (HCEA). **(G)** Moderate staining for carcinoembryonic antigen cell adhesion molecule–1 (CEA-CAM1). **(H)** Moderate to heavy staining for human carcinoembryonic antigen (CD66e).

gate past Hayflick's limit, then they should display telomerase activity. Thus far, we have examined clones of mesodermal GLL stem cells and pluripotent epiblastic-like stem cells derived from adult rats. Both sets of clones displayed telomerase activity (Fig. 10C) *(29,49)*. The presence of telomerase activity is therefore consistent with the capability for extended self-renewal, as demonstrated by embryonic stem cells *(101,102)*, mesodermal GLL stem cells, and pluripotent epiblastic-like stem cells *(29,46,49)*.

Paradigm Shift

Recently, there has been an apparent paradigm shift regarding stem cell biology and embryogenesis, particularly with respect to the source of the precursor cells derived from adult tissues. In the past few years, researchers have reported that tissue-specific progenitor cells derived from one organ are "reprogrammed" to form tissues of another organ. For example, cells derived from bone marrow have been reported to form neurons and neural supportive tissues *(7–9)*, hepatic oval cells *(10–12)*, and muscle cells *(13,14)*. Cells derived from neuronal tissues have been reported to form blood elements *(15,16)* and muscle cells *(17–19)*. In addition, cells derived from skeletal muscle have been reported to form blood *(20)*. These investigators proposed that the tissue-specific progenitor cells they isolated from one organ were reprogrammed or transdifferentiated to form cells and tissues of another organ.

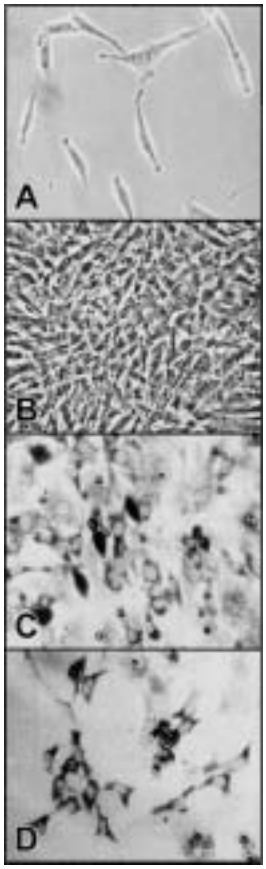

Fig. 9. Adult rat pluripotent epiblastic-like stem cell clone (PPELSC) demonstrating embryonic markers. Multiple PPELSC clonal lines were grown for 24 h to 8 wk in serum-free testing medium (TM) only *(49)* (**A**), TM with PDGF-like (proliferative) and ADF-like (inhibitory) activities *(28,29)* (**B**), or TM with 2 µg/mL insulin (**C**, **D**) for either 24 h (**A**) or 7 d (**B–D**). Morphologies and immunochemical staining as noted. Photographed with phase contrast (**A**, **B**) brightfield microscopy (**C**, **D**). Original magnifications, ×200. **(A)** Very small cells with high nuclear to cytoplasmic ratios. **(B)** Multiple confluent layers of cells maintaining stellate morphology. **(C)** Mononucleated cells demonstrating moderate to heavy staining for stage-specific embryonic antigen–4 (SSEA-4). **(D)** Mononucleated cells demonstrating moderate to heavy staining for carcinoembryonic antigen cell adhesion molecule–1 (CEA-CAM1).

However, none of these studies addressed either the identity or differentiative capabilities of their isolated "progenitor" cells prior to experimentation.

Our studies *(24–50, 53–59, see* Transdifferentiation vs Mixed Cell Populations section*)* and those of others *(103,104)* support another hypothesis to account for the previous results. We observed that the connective tissue compartments of many organs and tissues contain a variety of different categories of reserve precursor cells. This concept has been substantiated through the use of morphological, histochemical, immunocytochemical, molecular, clonogenic, pharmacological, and physiological-functional analyses; isolation studies; repetitive single cell clonogenic analyses; cell-sorting studies; and phenotypic expression studies across nine different species, including humans. These studies demonstrated that approx 50% of the resident precursor cells residing in a specific connective tissue compartment are tissue-specific progenitor cells specific for that particular cell type. Approximately 40% of the resident precursor cells are tissue-specific unipotent, bipotent, tripotent, and multipotent progenitor cells for other ectodermal, mesodermal, and endodermal cell types. Approximately 9% of the resident precursor cells are stem cells belonging to the ectodermal, mesodermal, and/or endodermal germ-layer lineages. Also, approx 1% of the resident precursor cells are pluripotent epiblastic-like stem cells, capable of forming any somatic cell of the body. Using the precursor cells derived from skeletal muscle connective tissue as an example, approx 50% consist of progenitor cells specifically are committed to the myogenic lineage (i.e., myoblasts, myosatellite cells, etc.). Approximately 40% are progenitor cells committed to other specific tissue lineages (i.e., adipoblasts, fibroblasts, osteoblasts, chondroblasts, endothelioblasts, hematoblasts, neuroblasts, glioblasts, hepatoblasts, etc.). Approximately 9% are germ-layer lineage stem cells (i.e., ectodermal GLL stem cells, mesodermal GLL stem cells, and endodermal GLL stem cells). In addition, approx 1% are pluripotent epiblastic-like stem cells. Precursor

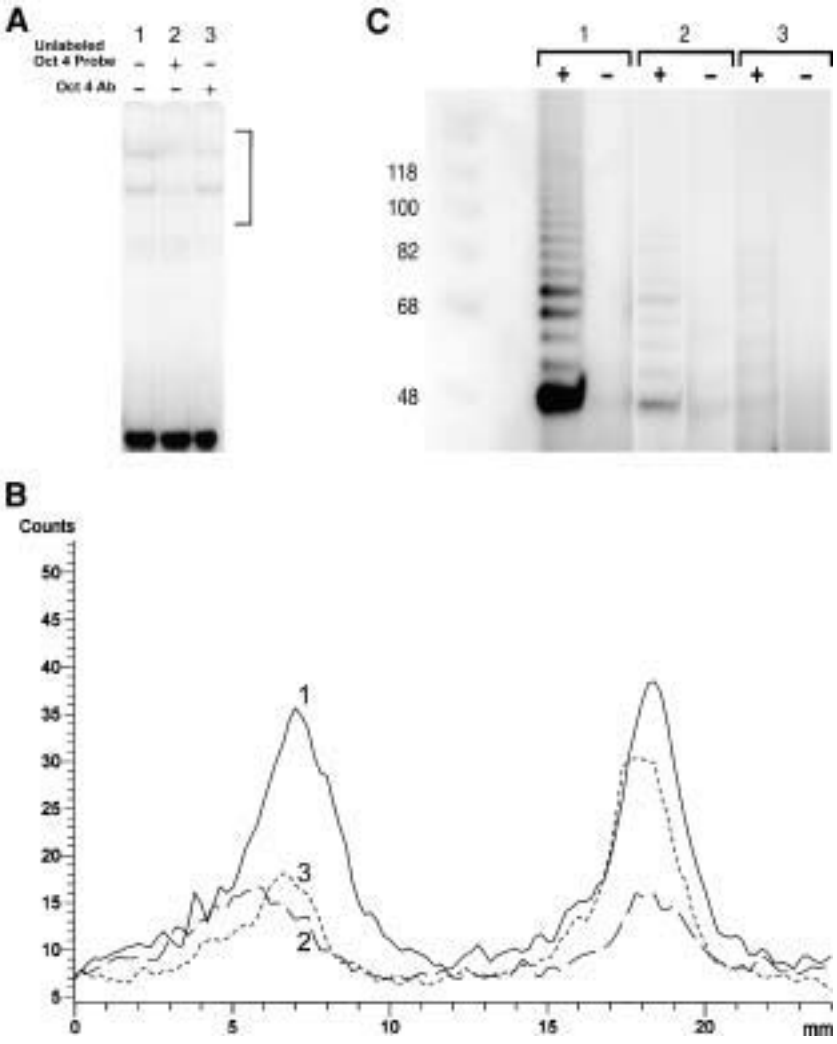

cells from the connective tissue compartments of such diverse tissues as dermis of the skin, fat, bone marrow, blood, brain, perichondrium, periosteum, and viscera appear to follow the same pattern of progenitor cell, germ-layer lineage stem cell, and pluripotent stem cell distribution *(28,29,41–43,46–49)*.

Our work suggests that the reports supporting cell reprogramming (i.e., transdifferentiation) might also be explained by the presence of unrecognized quiescent pluripotent stem cells, germ-layer lineage stem cells, and/or tissue-specific progenitor cells that are specific for other tissue lineages as resident cell populations within the differentiated tissues. For example, we propose that pluripotent stem cells, mesodermal GLL stem cells, and/or hematopoietic progenitor cells present in skeletal muscle could give rise to the blood cells reported by Jackson and Goodell *(20)*. Indeed, McKinney-Freeman et al. *(105)*, in an elegant study, demonstrated that $CD45^+$ (hematopoietic) stem cells residing in skeletal muscle gave rise to blood cells, whereas the $CD45^-$ (nonhematopoietic) stem cells resid-

Fig. 10. Molecular analysis of *Oct-4* expression and telomerase activity in Lac-Z-transfected adult rat pluripotent epiblastic-like stem cell clone *(29,49)* (β-PPELSC) and Lac-Z-transfected adult rat mesodermal GLL stem cell clone *(47,49)* (β-PPMSC). **(A)** Presence of *Oct-4*. *Oct-4* was detected by the electrophoretic mobility shift assay using the oligonucleotide 5′-TGTCGAATGCAAATCAC-TAGA-3′ containing the *Oct-1* consensus binding site. A β-PPELSC clone at 52 passages and 234 cell doublings was used. Cells were thawed, plated, and expanded in medium containing PDGF-like (proliferative) and ADF-like (inhibitory) activities *(28,29)*. Cells were harvested *(45)*, processed for whole-cell extracts *(244)*, and aliquoted to 5000 cell equivalents. Cell aliquots were incubated for 30 min at room temperature with lane 1, no competitor; lane 2, 100-fold excess of unlabeled *Oct-1* oligonucleotide; and lane 3, *Oct-4*-specific antibody in 20 m*M* Tris (pH 7.5), 4% glycerol 0.5 m*M* dithiothreitol, and 2 μg poly dIdC. ^{32}-P-labeled *Oct-1* oligonucleotide (1 ng) was added and the mixture incubated for 30 min at room temperature before electrophoresis through a 5% polyacrylamide gel. After drying, bands were visualized with a phosphorimager and quantified using the accompanying software. Two bands that represent binding by members of the Oct family of transcription factors were obtained, as shown by the competition for binding by unlabeled Oct oligonucleotide. **(B)** Densitometric analysis of the area contained in the sidebar of the electrophoretic mobility shift assay in **A**. Lane 1, solid line; lane 2, long dashes; and lane 3, short dashes. Incubation with *Oct-4*-specific antibody substantially decreased the formation of the upper band and slightly decreased the formation of the lower band, indicating the presence of *Oct-4*. **(C)** Polyacrylamide gel electrophoresis of telomerase activity in pluripotent stem cells. β-PPELSC clone, at 52 passages and 234 cell doublings, and β-PPMSC clone, at 31 passages and 151 cell doublings, were used. Cells were propagated as described in **A**, harvested *(45)*, and processed for telomerase activity as described (TRAPeze Assay, Intergen). Lane 1 +, extract of telomerase-positive cells (control), 1 –, extraction buffer; lane 2 +, test extract of β-PPELSC clone, 2 –, heat-inactivated extract of β-PPELSC clone; lane 3 +, test extract of β-PPMSC clone, 3 –, heat-inactivated extract of β-PPMSC clone. Note the presence of ladders of bands denoting the presence of telomerase activity; compare + lanes 1–3. (Reproduced with permission from Young, H. E., Duplaa, C., Yost, M. J., Henson, N. L., Floyd, J. A., Detmer, K., [2004] Clonogenic analysis reveals reserve stem cells in postnatal mammals: II. Pluripotent epiblastic-like stem cells. *Anat. Rec.* Manuscript accepted for publication. Copyright 2004, Wiley-Liss.)

ing in skeletal muscle formed muscle. Unfortunately, these investigators did not completely examine the CD45$^-$ stem cells isolated from skeletal muscle to determine their full differentiation potential (i.e., whether they would form other cell/tissue types in addition to skeletal muscle). Several possibilities exist. The CD45$^-$ stem cell could be a progenitor cell committed to the myogenic lineage. Alternatively, the CD45$^-$ stem cell could be a mesodermal GLL stem cell or a pluripotent epiblastic-like stem cell. The CD45$^-$ cells could also be a combination of all three types of precursor cells because all of these types of cells are CD45$^-$ by flow cytometric analysis *(28,29,47,48)*.

Similarly, we propose that pluripotent stem cells, ectodermal GLL stem cells, mesodermal GLL stem cells, endodermal GLL stem cells, and/or neuroblasts, glioblasts, hepatoblasts, or myogenic progenitor cells in bone marrow could give rise to neurons and neural supportive tissues *(7–9)*, hepatic oval cells *(10–12)*, and muscle cells *(13,14)*. Likewise, pluripotent stem cells, mesodermal GLL stem cells, and/or hematopoietic progenitor cells or myogenic progenitor cells in neuronal tissues could form blood elements *(15,16)* and muscle cells *(17–19)*. We believe that the experimental results that appear to require transdifferentiation or dedifferentiation of progenitor cells

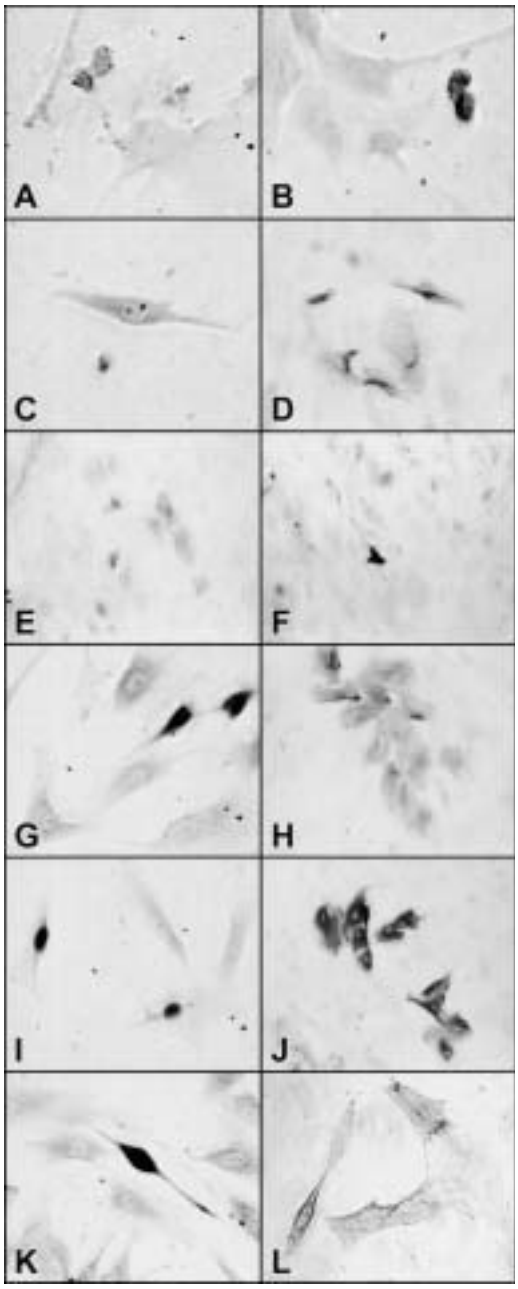

Fig. 11. Human ($CD10^+$, $CD66e^+$) postnatal pluripotent epiblastic-like stem cell (PPELSC) line induced to express neuroectodermal and surface ectodermal phenotypic expression markers. Multiple PPELSC lines were grown for 24 h to 8 wk in testing medium (TM) only, TM with dex, TM with ectodermal inductive activity, or TM with dex and 10 ectodermal inductive activity. In this particular series, PPELSC were grown for 7 d in TM with 10^{-6} *M* dex and ectodermal inductive activity. Morphologies and immunochemical staining as noted. Photographed with brightfield microscopy, original magnifications, ×200 (**A–D**, **G–L**), ×100 (**E**, **F**).

(A) Mononucleated cells moderately stained for neural precursor cell expression marker (FORSE-1). **(B)** Mononucleated cells showing moderate to heavy intracellular staining for neurofilaments (RT-97). **(C)** Mononucleated cells showing moderate intracellular staining for neurons (8A2). **(D)** Mononucleated cells showing moderate to heavy intracellular staining for neuronal nestin (Rat-401). **(E)** Mononucleated cells showing moderate intracellular staining for nestin (HNES). **(F)** Mononucleated cell showing heavy intracellular staining for nestin (MAB353). **(G)** Mononucleated cells showing moderate to heavy intracellular staining for b-tubulin III (T8660). **(H)** Mononucleated cells showing moderate intracellular staining for neuroglia (oligodendrocytes and astroglia) (CNPase). **(I)** Mononucleated cells showing moderate to heavy intracellular staining for oligodendrocytes (Rip). **(J)** Mononucleated cells showing heavy intracellular staining for neuronal expression marker (S-100). **(K)** Mononucleated cells showing moderate to heavy intracellular staining for neuronal vimentin for radial cells and radial glial cells (40E-C). **(L)** Mononucleated cells showing moderate staining for keratinocytes (VM-1).

may actually be caused by contamination of the tissue isolate by unrecognized progenitor cells, germ-layer lineage stem cells, and/or pluripotent stem cells that are stimulated to form new progenitor cells of a different tissue type. Based on the proposed theory of activation of quiescent precursor cells, no reprogramming of either differentiated cells or

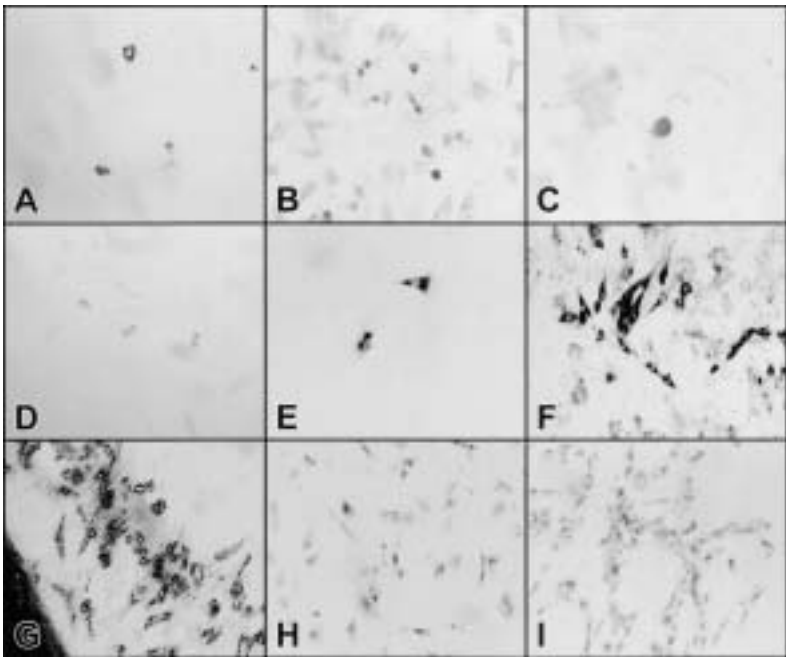

Fig. 12. Adult rat pluripotent epiblastic-like stem cell clone (PPELSC) clone *(49)* induced to express ectodermal lineage phenotypic expression markers. Multiple PPELSC clonal lines were grown for 24 h to 8 wk in testing medium (TM) only, TM with dex, TM with ectodermal inductive activity, or TM with dex and 10 ectodermal inductive activity. In this particular series, the clone was incubated for 7 d in TM with 10^{-6} *M* dex and ectodermal inductive activity. Morphologies and immunochemical staining as noted. Photographed with brightfield microscopy. Original magnifications, ×100 (**A**, **B**, **D**, **E**, **G–I**), ×200 (**C**, **F**). **(A)** Mononucleated cells staining for neural precursor cell expression marker (FORSE-1). **(B)** Mononucleated cells showing intracellular staining for neurofilaments (RT-97). **(C)** Mononucleated cells showing intracellular staining for neurons (8A2). **(D)** Mononucleated cells showing intracellular staining for neuronal nestin (Rat-401). **(E)** Mononucleated cells showing intracellular staining for b-tubulin III (T8660). **(F)** Mononucleated cells showing intracellular staining for oligodendrocytes (Rip). **(G)** Mononucleated cells showing intracellular staining for neuronal expression marker (S-100). **(H)** Mononucleated cells showing intracellular staining for neuronal vimentin for radial cells and radial glial cells (40E-C). **(I)** Mononucleated cells showing intracellular staining for ganglion cells (TuAg1).

lineage-committed stem cells would thus be required to explain the results obtained by these investigators.

Transdifferentiation vs Mixed Cell Populations

In an ongoing series of studies *(28,29,41–44,* unpublished data*)*, we have attempted to verify transdifferentiation as the hypothesis of choice to explain tissue restoration. These experiments were performed using fully characterized tissue-specific progenitor cell clones, mesodermal GLL stem cell clones, and pluripotent epiblastic-like stem cell clones, all derived by repetitive single-cell clonogenic analysis. We postulated that if transdifferentiation were a reality, then we could induce a unipotent tis-

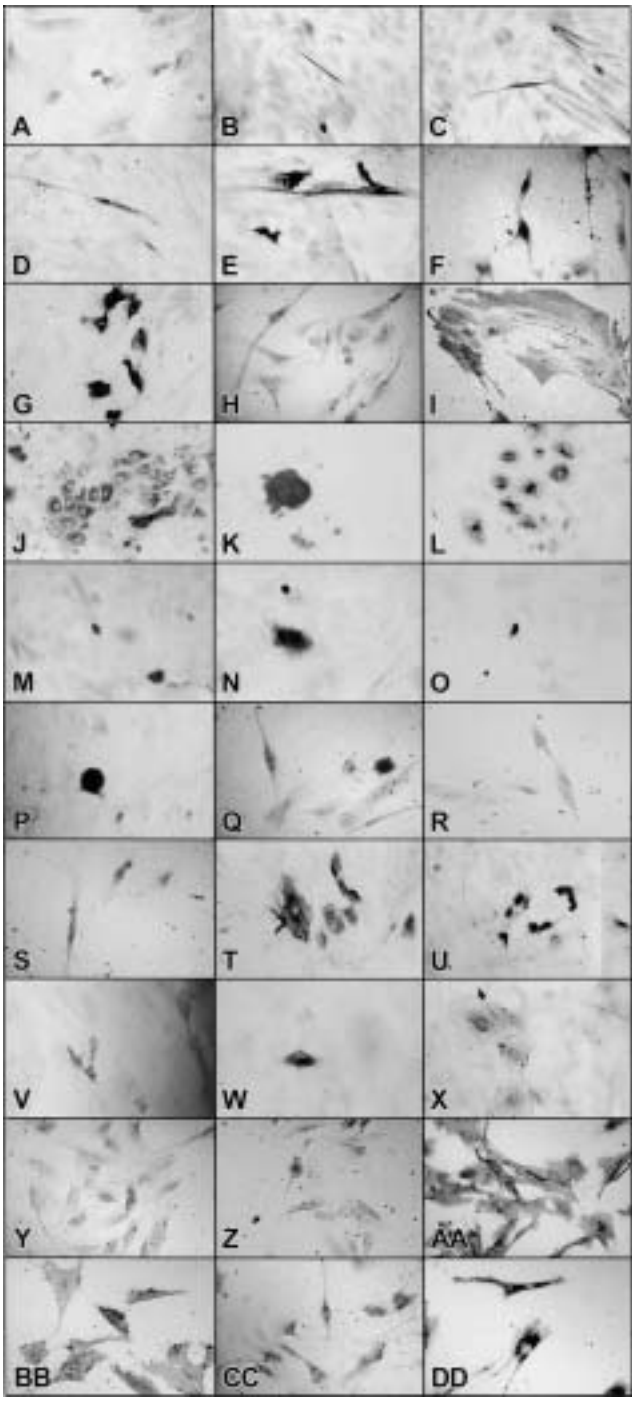
A
B
C
D
E
F
G
H
I
J
K
L
M
N
O
P
Q
R
S
T
U
V
W
X
Y
Z
AA
BB
CC
DD

Fig. 13. Adult human ($CD10^+$, $CD66e^+$) pluripotent epiblastic-like stem cell (PPELSC) lines induced to express mesodermal phenotypic expression markers. Multiple PPELSC lines were grown for 24 h to 8 wk in testing medium (TM) only; TM with 10^{-10} *M* to 10^{-6} *M* dex; TM with Sk-MMP-like, Sm-MMP-like, AMP-like, BMP-2-like, and endothelial inductive activities *(28)*; or TM with 10^{-10} *M* to 10^{-6} *M* dex and Sk-MMP-like, Sm-MMP-like, AMP-like, BMP-2-like, and endothelial inductive activities. In this particular series, PPELSCs were grown for 7 d (**A**, **B**), 1 wk (**I**, **J**, **L**), 2 wk (**C–H**), or 4 wk (**K**) in TM with 10^{-8} *M* dex (**A–L**); 2 wk (**M**, **P–S**) or 4 wk (**N**, **O**) in TM with 10^{-7} *M* dex (**M–S**); and 2 wk in TM with 10^{-6} *M* dex (**T–DD**). Morphologies and immunochemical staining as noted. Photographed with brightfield microscopy; original magnifications, ×40 (**J**, **N–P**), ×100 (**A–H**, **K–M**, **Q–S**, **U**, **V**, **Y**, **Z**, **CC**), ×200 (**I**, **T**, **W**, **X**, **AA**, **BB**, **DD**). **(A)** Mononucleated cells showing moderate intracellular staining for MyoD (OP-137). **(B)** Mononucleated cells showing moderate to heavy intracellular staining for myogenin (F5D). **(C)** Mononucleated and binucleated cells showing moderate to heavy intracellular staining for sarcomeric myosin (MF-20). **(D)** Mononucleated and binucleated cells showing moderate to heavy intracellular staining for antiskeletal muscle fast myosin (MY-32). **(E)** Mononucleated and multinucleated cells showing moderate to heavy intracellular staining for skeletal myosin heavy chain (ALD58). **(F)** Mononucleated cells showing moderate to heavy intracellular staining for skeletal myosin fast chain (A4.74). **(G)** Mononucleated cells showing heavy intracellular staining for smooth muscle α-actin (IA4). **(H)** Mononucleated cells showing moderate intracellular staining for calponin (Calp). **(I)** Mononucleated and binucleated cells showing moderate intracellular staining for cardiotin (cardiac myocytes, MAB 3252). **(J)** Mononucleated cells demonstrating heavy intracellular staining for bone sialoprotein II (WV1D1). **(K)** Nodular mass demonstrating extracellular staining for bone sialoprotein II (WV1D1). **(L)** Mononucleated cells demonstrating heavy perinuclear staining for osteopontine (MP111). **(M)** Mononucleated cells with moderate to heavy intracellular staining for cartilage-specific collagen pro-type II (CIIC1). **(N)** Nodules of cells demonstrating heavy extracellular staining for cartilage-specific collagen pro-type II (CIIC1). **(O)** Nodule of cells demonstrating heavy extracellular staining for cartilage-specific collagen type II (HC-II). **(P)** Nodule of cells demonstrating heavy extracellular staining for cartilage-specific collagen type IX (D1-9). **(Q)** Mononucleated cells demonstrating moderate to heavy intracellular staining for cartilage link protein (9/30). **(R)** Mononucleated cells demonstrating moderate intracellular staining for cartilage proteoglycan-hyaluronate binding region (12/21). **(S)** Mononucleated cells demonstrating moderate intracellular staining for versican hyaluronate binding region (12C5). **(T)** Mononucleated cells demonstrating heavy staining for human fibroblast-specific protein (IB10). **(U)** Mononucleated cells demonstrating heavy staining for CD31 (PECAM), peripheral endothelial cell adhesion molecule (P2B1). **(V)** Mononucleated cells demonstrating moderate staining for CD146, endothelial cells (H-endo). **(W)** Mononucleated cell demonstrating heavy staining for VCAM, vascular (endothelial) cell adhesion molecule (P8B1). **(X)** Mononucleated cells demonstrating moderate staining for CD62e, (endothelial) selectin-E (P2H3). **(Y)** Mononucleated cells demonstrating moderate staining for CD34, endothelial sialomucin (CD34). **(Z)** Mononucleated cells demonstrating moderate to heavy staining for CD11b, indicating granulocytes, monocytes, and/or natural killer cells (H5A4). **(AA)** Mononucleated cells demonstrating moderate to heavy staining for CD44, hyaluronate receptor (H4C4). **(BB)** Mononucleated cells demonstrating moderate to heavy staining for CD44, hyaluronate receptor (Hermes-1). **(CC)** Mononucleated cells demonstrating moderate staining for CD45, staining all hematopoietic cells except erythrocytes (H5A5). **(DD)** Mononucleated cells demonstrating heavy staining for CD63, indicating macrophages, monocytes, and/or platelets (H5C6).

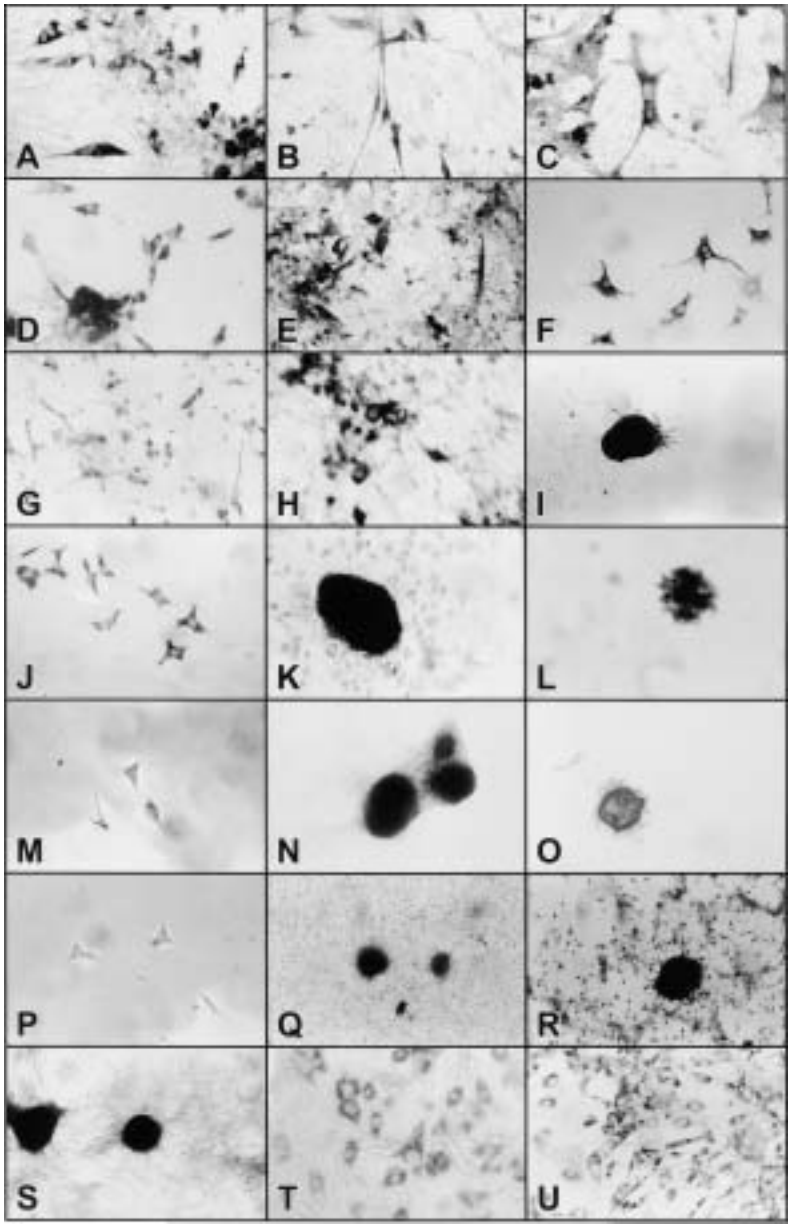

sue-specific progenitor cell clone to exhibit phenotypic expression markers for an alternate cell or tissue type. In one series of experiments, we used five separate unipotent progenitor cell clones specific for fibrogenic, myogenic, adipogenic, chondrogenic, and osteogenic tissues, respectively. Next, we incubated these clones individually for 7 d with recombinant or novel inductive factors outside their respective tissue types, removed the inductive factor, and then

Fig. 14. Adult rat pluripotent epiblastic-like stem cell clone (PPELSC) clones induced to express mesodermal lineage phenotypic expression markers *(49)*. Multiple PPELSC clonal lines were grown for 24 h to 8 wk in testing medium (TM) only; TM with 10^{-10} *M* to 10^{-6} *M* dex; TM with Sk-MMP-like, Sm-MMP-like, AMP-like, BMP-2-like, and endothelial inductive activities *(28)*; or TM with 10^{-10} *M* to 10^{-6} *M* dex and Sk-MMP-like, Sm-MMP-like, AMP-like, BMP-2-like, and endothelial inductive activities. In this particular series, cells were incubated for 1 wk (**A**, **G**, **H**, **J**), 2 wk (**B–F**, **M**, **O**, **P**, **T**, **U**), 4 wk (**N**, **Q**), 6 wk (**I**, **K**, **R**, **S**), or 8 wk (**L**) in TM and 10^{-8} *M* dex (**A–L**, **T**, **U**) or TM and 10^{-7} *M* dex (**M–S**). Photographed with brightfield microscopy; original magnifications ×200 (**A**, **C**, **F**, **H**, **J**, **M**, **P**, **T**), ×100 (**B**, **D**, **E**, **G**), or ×40 (**I**, **K**, **L**, **N**, **O**, **Q–S**, **U**). **(A)** Mononucleated cells showing heavy intracellular staining for myogenin (F5D). **(B)** Mononucleated and binucleated cells showing moderate to heavy intracellular staining for sarcomeric myosin (MF-20). **(C)** Mononucleated and binucleated cells showing moderate to heavy intracellular staining for anti-skeletal muscle fast myosin (MY-32). **(D)** Mononucleated cells showing moderate to heavy intracellular staining for skeletal myosin heavy chain (ALD58). **(E)** Mononucleated and binucleated cells showing heavy intracellular staining for skeletal myosin fast chain (A4.74). **(F)** Mononucleated cells showing heavy intracellular staining for smooth muscle α-actin (IA4). **(G)** Mononucleated cells showing moderate intracellular staining for cardiotin (cardiac myocytes, MAB 3252). **(H)** Mononucleated cells demonstrating heavy intracellular staining for bone sialoprotein II (WV1D1). **(I)** Nodule of cells demonstrating extracellular staining for bone sialoprotein II (WV1D1). **(J)** Mononucleated cells demonstrating moderate to heavy intracellular staining for osteopontine (MP111). **(K)** Nodule of cells demonstrating extracellular staining for osteopontine (MP111). **(L)** Nodule of cells demonstrating extracellular staining for calcium phosphate using the von Kossa procedure (vK). **(M)** Mononucleated cells with intracellular staining for cartilage-specific collagen pro type II (CIIC1). **(N)** Three nodules demonstrating intense extracellular staining for cartilage-specific collagen pro type II (CIIC1). **(O)** Single nodule of cells demonstrating moderate extracellular staining for cartilage-specific collagen type II (HC-II). **(P)** Mononucleated cells demonstrating moderate intracellular staining for cartilage-specific collagen type IX (D1-9). **(Q)** Three nodules demonstrating extracellular staining for sulfated glycosaminoglycan chains of proteoglycans (Perfix/Alcec Blue). **(R)** Nodule demonstrating extracellular staining for sulfated glycosaminoglycan chains of proteoglycans (Safranin-O, pH 1.0). Individual nuclei stained with antibody to β-galactosidase (Gal-19) and visualized with 3, 3′-diaminobenzidine (DAB). **(S)** Two nodules demonstrating extracellular staining for sulfated glycosaminoglycan chains of proteoglycans (Alcian Blue, pH 1.0). **(T)** Mononucleated cells with moderate to heavily stained intracellular vesicles demonstrating saturated neutral lipids (Oil Red-O), indicative of adipocytes. **(U)** Mononucleated cells with moderate to intensely stained intracellular vesicles demonstrating saturated neutral lipids (Sudan Black-B), indicative of adipocytes.

incubated the cells with insulin to accelerate phenotypic expression. For example, a unipotent myogenic progenitor cell clone was incubated separately with FMP to induce fibrogenesis, AMP to induce adipogenesis, and BMP-2 to induce chondrogenesis and osteogenesis. In all cases examined, the myogenic clone maintained its original myogenic tissue-specific programming and exhibited myogenic phenotypic expression markers, even in the presence of FMP, AMP, or BMP-2 (Table 4).

In a second series of experiments, we induced the formation of unipotent tissue-specific progenitor cells from a lineage-unrestricted mesodermal GLL stem cell clone using the same tissue-specific induction factors as above (i.e., FMP, AMP, Sk-MMP, and BMP-2). After establishment of the unipotent progeni-

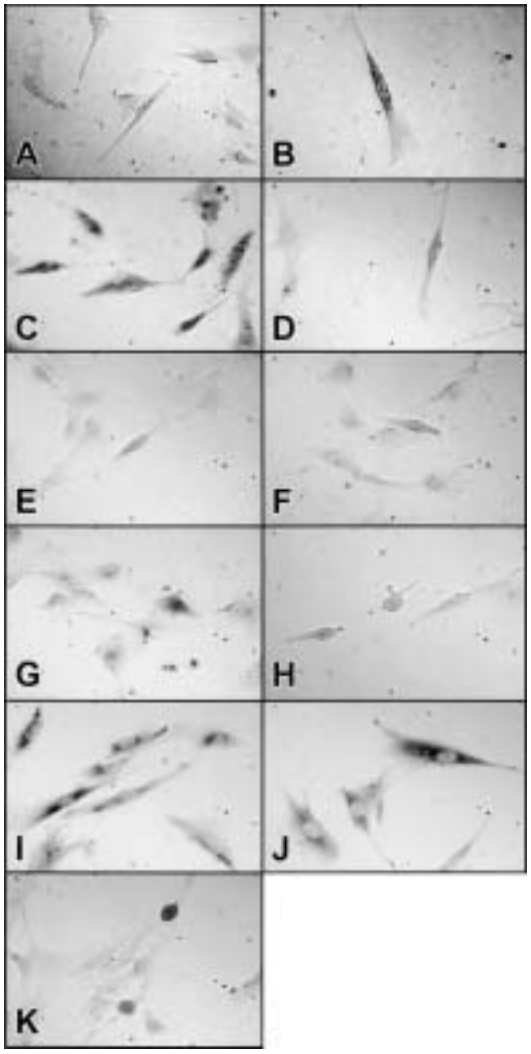

Fig. 15. Adult human ($CD10^+$, $CD66e^+$) pluripotent epiblastic-like stem cell (PPELSC) lines induced to express endodermal phenotypic markers. Multiple PPELSC lines were grown for 24 h to 8 wk in testing medium (TM) only, TM with 10^{-10} *M* to 10^{-6} *M* dex, TM with endodermal inductive activity, or TM with 10^{-10} *M* to 10^{-6} *M* dex and endodermal inductive activity. In this particular series, cells were grown for 7 d in TM, 10^{-6} *M* dex, and endodermal inductive activity. Morphologies and immunochemical staining as noted. Photographed with brightfield microscopy, original magnifications, ×100. **(A)** Mononucleated and binucleated cells showing moderate intracellular staining for human-specific α-fetoprotein (HAFP). **(B)** Mononucleated cell showing heavy intracellular staining for gastrointestinal epithelium (HESA). **(C)** Mononucleated cells showing moderate to intense intracellular staining for glucagon of endocrine pancreas (α-cells). **(D)** Mononucleated cells showing light to moderate intracellular staining for bile canalicular cells of liver (HA4c19). **(E)** Mononucleated cells showing light to moderate intracellular staining for progenitor cells and biliary epithelial cells of liver (OC3). **(F)** Mononucleated cells showing light to moderate intracellular staining for progenitor cells and biliary epithelial cells of liver (OC5). **(G)** Mononucleated cells showing moderate to heavy intracellular staining for progenitor cells and biliary epithelial cells of liver (OC10). **(H)** Mononucleated cells showing moderate intracellular staining for cytoplasm of liver hepatocytes (H.4). **(I)** Mononucleated cells showing moderate to intense staining for liver hepatocyte cell surface marker (H.1). **(J)** Mononucleated cells showing moderate to intense staining for progenitor cells, canalicular cells, and biliary epithelial cells of liver (DPP-IV). **(K)** Mononucleated cells showing light to heavy staining for biliary epithelial cells, oval cells, and hepatocyte canalicular cell (HCC) of liver (OV6).

tor cell lines, we repeated the above experiment using these same specific inductive factors with a 7-d incubation schedule, removal of the inductive factor, and then incubation of the cells with insulin to accelerate phenotypic expression. In all experiments performed, the induced unipotent progenitor cell lines maintained their originally induced tissue-specific programming (Table 4).

In a third series of experiments, we incubated a lineage-unrestricted mesodermal GLL stem cell clone with FMP followed immediately by AMP, BMP-2, or Sk-MMP; AMP followed by BMP-2 or Sk-MMP; and BMP-2 followed by Sk-MMP. The second inductive factor was then removed and the cells incubated with insulin to accelerate their phenotypic expression. These particular sequences were chosen based on the specific windows of inductive activity (*see* Windows of Inductive Activity section). In all instances, the first inductive factor was allowed its entire inductive window (i.e., d 1–3 for FMP and d 2–4 for AMP or d 3–5 for BMP-2). These results demonstrated that the first inductive factor dictated the phenotypic markers expressed by the resultant cultures (Table 4).

Throughout our 16 yr of study, we have been unable to replicate the transdifferentiation findings reported by others *(3,5,6)* using fully characterized tissue-specific progenitor cell clones, germ-layer lineage stem cell clones, pluripotent stem cell clones, or their induced progeny. However, several possibilities exist that might explain these adverse findings. The isolation and expansion procedures used to derive germ-layer lineage stem cells and pluripotent stem cells select against differentiated cells and progenitor cells. Thus, the cell populations directly affected by transdifferentiation may have been lost. Also, during extensive examinations of commercially available and novel growth factors in the stem cell–progenitor cell bioassay, only four activities were noted (i.e., proliferation, progression, induction, and inhibition). It is conceivable that a unique, as yet unrecognized, bioactive factor expressing a fifth activity is present in the tissue: transdifferentiation. This fifth activity is necessary to "dedifferentiate" tissue-specific progenitor cells or differentiated cells prior to their induction and differentiation into another tissue type (i.e., transdifferentiation).

In contrast, the previous experiments demonstrated that the first inductive factor initiated tissue induction and expression of a particular cell type. The second factor was without effect. Based on our findings, the "transdifferentiation" findings reported by others *(3,5,6)* suggested the potential for unrecognized contaminant precursor cell(s) within their tissue isolates. We therefore proposed an alternate hypothesis to transdifferentiation. We hypothesized that a tissue isolate may contain a mixture of tissue-specific progenitor cells, germ-layer lineage stem cells, and/or lineage-uncommitted pluripotent stem cells. To test this hypothesis, we first mixed clones of tissue-specific progenitor cells together and then repeated the above experiments with tissue-specific induction factors and insulin. In the initial series of experiments, we mixed two, three, four, or five unipotent clones of progenitor cells together. The results showed that a mixed population of two, three, four, or five progenitor clones would express their respective phenotypic markers, based on the inductive factors or progression factors present. However, mixed progenitor clones would not cross tissue lineages. For example, if a myogenic clone was mixed with a chondrogenic clone and incubated with FMP (to induce fibrogenesis) and insulin, only myogenic and chondrogenic phenotypic markers would be expressed (Table 4).

In the second series of experiments, we mixed a clone of mesodermal GLL stem cells with one or more clones of tissue-specific progenitor cells. We then incubated these mixed cultures with one or more tissue-specific induction factors with and without a progression factor. The results demonstrated that the progenitor cells were responsive to a progression factor and would express their tissue-specific phenotype in the presence of the progression factor or their respective tissue-specific induc-

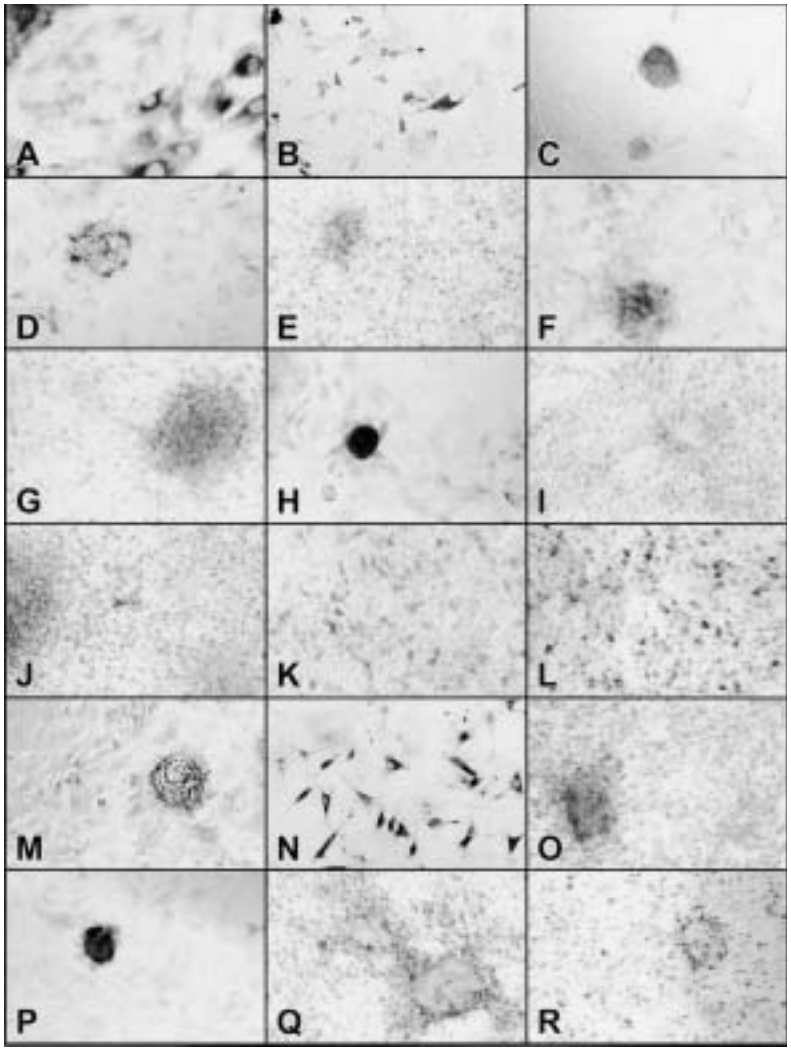

tion factor. In contrast, the mesodermal GLL stem cell clone responded to the tissue-specific induction factor but would not respond to the progression factor. For example, a myogenic clone was mixed with a chondrogenic clone and a mesodermal GLL stem cell clone. The mixed culture was then incubated with FMP (inductive factor) with and without insulin (progression factor). The mixed culture incubated with FMP and insulin demonstrated phenotypic expression markers for myogenesis, chondrogenesis, and fibrogenesis. The mixed culture incubated with FMP alone demonstrated only phenotypic expression markers for fibrogenesis (Table 4).

Transdifferentiation is proposed to occur during tissue restoration when progenitor cells derived from one organ are "reprogrammed" to form tissues of another organ *(3,5,6)*. On the basis of our studies *(28,29,43,44,48,49)* and

Fig. 16. Adult rat pluripotent epiblastic-like stem cell clone (PPELSC) clone *(49)* induced to express endodermal lineage phenotypic markers. Multiple PPELSC clonal lines were grown for 24 h to 8 wk in testing medium (TM) only, TM with 10^{-10} *M* to 10^{-6} *M* dex, TM with endodermal inductive activity, or TM with 10^{-10} *M* to 10^{-6} *M* dex and endodermal inductive activity. In this particular series, cells were incubated for 1 wk (**A**, **B**, **E**), 2 wk (**D**, **K**, **L**), 3 wk (**C**, **F**, **I**, **M**, **N**, **R**), 4 wk (**G**, **H**, **O**, **Q**), or 5 wk (**J**, **P**) in TM, 10^{-6} *M* dex, and endodermal inductive activity. Morphologies and immunochemical staining as noted. Photographed with brightfield microscopy, original magnifications, ×200 (**A**), ×100 (**B**, **D**, **H**, **K–N**, **P**), or ×40 (**C**, **E**, **I**, **J**, **Q**, **R**). **(A)** Mononucleated and binucleated cells showing intense intracellular staining for rat-specific α-fetoprotein (RAFP). **(B)** Mononucleated cells showing moderate to intense intracellular staining for rat-specific liver epithelial growth factor receptor (151-Ig). **(C)** Nodular aggregations showing moderate intracellular staining for pro-insulin of endocrine pancreas (β-cells). **(D)** Cellular aggregation showing moderate to heavy intracellular staining for glucagon of endocrine pancreas (α-cells). **(E)** Cellular aggregation and individual diffuse mononucleated cells showing moderate to intense intracellular staining for somatostatin of endocrine pancreas (δ-cells). **(F)** Cellular aggregation and individual diffuse mononucleated cells showing moderate to intense intracellular staining for ductal cells of exocrine pancreas (CK-19), ×100. **(G)** Cellular aggregation and individual diffuse mononucleated cells showing moderate to intense intracellular staining for bile canalicular cells of liver (HA4c19). **(H)** Nodule showing heavy intracellular staining for progenitor cells, biliary epithelial cells, and oval cells of liver (OC2). **(I)** Diffuse mononucleated cells showing moderate to heavy intracellular staining for progenitor cells and biliary epithelial cells of liver (OC3). **(J)** Cellular aggregation and individual diffuse mononucleated cells showing moderate to intense intracellular staining for progenitor cells and biliary epithelial cells of liver (OC4). **(K)** Diffuse mononucleated cells showing moderate to heavy intracellular staining for progenitor cells and biliary epithelial cells of liver (OC5). **(L)** Diffuse mononucleated cells showing moderate to intense intracellular staining for progenitor cells and biliary epithelial cells of liver (OC10). **(M)** Diffuse and aggregated cells showing moderate to intense intracellular staining for cytoplasm of liver hepatocytes (H.4). **(N)** Diffuse mononucleated cells showing moderate to intense intracellular staining for liver hepatocyte cell surface marker (H.1). **(O)** Diffuse and aggregated cells showing moderate to heavy intracellular staining for progenitor cells, canalicular cells, and biliary epithelial cells of liver (DPP-IV). **(P)** Nodular aggregate shows heavy to intense intracellular staining for endodermal epithelial marker of liver (DESMO). **(Q)** Nodular aggregate and diffuse cells showing moderate to heavy intracellular staining for biliary epithelial cells, oval cells, and HCC of liver (OV6). **(R)** Nodular aggregate and diffuse cells showing moderate to intense intracellular staining for canalicular cell surface protein of liver (LAP), ×100.

those of others *(103,104)*, we believe that the starting populations of tissue-specific precursor cells reported in the transdifferentiation studies may have also contained unrecognized populations of tissue-specific progenitor cells for other cell types, germ-layer lineage stem cells, and/or pluripotent stem cells that were responsible for the formation of the cells and tissues observed in their experiments. Thus, based on the proposed theory of activation of quiescent precursor cells, it is not necessary to invoke the concept of transdifferentiation to explain the results obtained by these investigators. For investigators who still maintain transdifferentiation as a valid hypothesis, we would propose a thorough characterization of the differentiation potential of their cells prior to the onset of experimentation.

TISSUE ENGINEERING

Limb regeneration in amphibians is the ultimate expression of tissue engineering, restoring both histoarchitecture and function to the limb. Young and colleagues *(24–27,31–37)* discovered that an interplay existed between tissue-resident quiescent reserve stem cells and glycosylated bioactive factors. They postulated that successful tissue engineering in humans would require knowledge of the stem cells residing in the tissues, the identity of the endogenous bioactive factors acting on these cells, and the nature of their interaction.

Young et al. discovered the existence of reserve mesodermal germ-layer lineage stem cells and pluripotent stem cells—first in adult terrestrial amphibians, next in fetal avians, and then in mammals of all ages, including humans. They discovered that proliferation agents, inductive agents, progression agents, and inhibitory agents were involved as regulatory elements in the interactions underlying tissue restoration *(24–59,106,* unpublished observations*)*.

Lucas et al. *(30,51–59,97,106–117)* discovered and engineered biocompatible controlled-release delivery vehicles for stem cells and bioactive factors, thus allowing for directed tissue repair. But probably most important of all, they identified key issues for understanding the interplay between tissue-specific progenitor cells, lineage-committed germ-layer lineage stem cells, lineage-uncommitted pluripotent stem cells, and bioactive factors during the tissue restoration process. Lucas et al. demonstrated that the majority of the granulation cell population initially present at a wound site was composed of activated uncommitted stem cells, not tissue-specific fibrogenic and myo-fibrogenic progenitor cells as previously reported. They also demonstrated that the initial inflammatory response was critical for a successful regenerative response. This inflammatory response allowed for the debridement and removal of damaged tissues, activation of quiescent stem cells, migration of the activated stem cells to the site of injury, and also migration of cells containing bioactive factors to the site of injury. They discovered that the final histoarchitecture of the tissue was not preprogrammed but rather was dictated by the action of particular growth factors at the wound site. They discovered that the introduction of any exogenous bioactive factors or cells would lead to their destruction by the inflammatory response, unless they were incorporated into protective biocompatible biomatrices. Once activated, the mesodermal GLL stem cells exhibited overlapping windows of activity with respect to inductive compounds acting on the mesodermal lineage. In sequential order, the windows of activity were as follows: fibrogenic (d 1–3), adipogenic (d 2–4), chondrogenic/osteogenic (d 3–5), and myogenic (d 4–6). This correlated with earlier data obtained after cessation of the inflammatory response in vivo or after initial plating in vitro. Under these circumstances, fibrogenic factors were active only between d 1 and 3, adipogenic factors were active only between d 2 and 4, chondrogenic/osteogenic factors were active only between d 3 and 5, and myogenic factors were active only between d 4 and 6. If fibrogenic factors were present between d 1 and 3, the mesodermal GLL stem cells would become fibrogenic and express a scar-connective tissue phenotype. If, however, the fibrogenic factors were absent or inhibited between d 1 and 3 or did not appear until d 4 and beyond, then no fibrogenic response occurred. Similarly, if myogenic factors were present only during d 1–3 or 7 and beyond, no myogenesis occurred. The mesodermal GLL stem cells would only respond to myogenic inductive factors between d 4 and 6 (Table 3).

On the basis of these observations, Young and Lucas proposed a working model (Fig. 17) for successful tissue engineering in postnatal animals, including humans. This working model is based on a three-component morphogenetic system, with each component used singly or in combination with the other component(s). The three components of this morphogenetic system are reserve stem cells, bioactive factors, and biocompatible controlled-release biomatrices.

In this model, the reserve stem cells and bioactive factors may be endogenous, being supplied by the host in vivo, or may be delivered from an exogenous source. Exogenously delivered allogeneic, syngeneic, or autologous reserve stem cells may be delivered as naive stem cells. They may also be altered ex vivo by pretreatment with bioactive factors or transfected with genes. The components, either cells and/or factors, must be incorporated into a protective biomatrix if they are to be delivered exogenously into a site that is subject to an inflammatory response. This is necessary to prevent their destruction and elimination from the area before they can influence the repair process. Failure to protect these components leads predominantly to scar tissue formation at the site of delivery.

We propose that tissue engineering can be performed using autologous, syngeneic, or allogeneic germ-layer lineage stem cells or pluripotent stem cells. This process will require that the stem cells be made to undergo lineage/tissue induction to form specific tissue types. We have begun to study the process of lineage/tissue induction of pluripotent stem cells and germ-layer lineage stem cells in several model systems. These model systems, discussed below, incorporate one or more of the components of our proposed tricomponent morphogenetic model (Fig. 17) for tissue engineering.

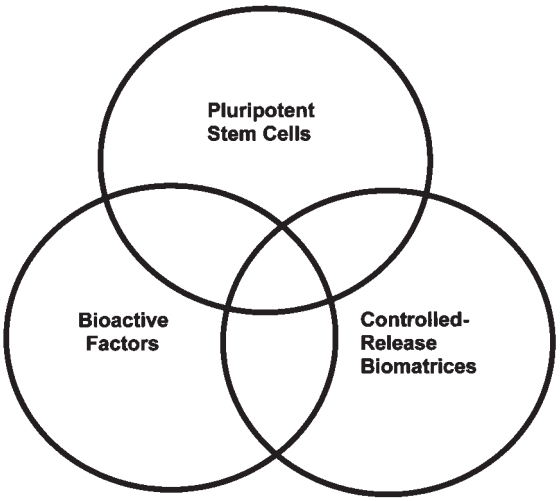

Fig. 17. Three-component morphogenetic-pharmaceutical system. The morphogenetic component to this model is the reserve stem cells. Characteristics of these reserve stem cells would include extended capabilities for self-renewal far surpassing Hayflick's limit and the ability to form any somatic cell(s) of the body using either germ-layer lineage stem cells or pluripotent epiblastic-like stem cells. The pharmaceutical component of this model encompasses both bioactive factors and biocompatible controlled-release biomatrices. Examples of bioactive factors would include agents that induce proliferation (i.e., platelet-derived growth factors -BB, -AA, -AB, etc.), agents that induce lineage commitment (i.e., BMPs, Sk-MMP, Sm-MMP, AMP, FMP, cartilage morphogenetic protein, TGF-β, FGF, nerve growth factor, keratinocyte growth factor, hepatocyte growth factor, vascular endothelial cell growth factor, etc.), progression agents that accelerate phenotypic differentiation (i.e., insulin, IGF-1, IGF-2, etc.), and agents that inhibit lineage commitment and differentiation (i.e., leukemia inhibitory factor, scar inhibitory factor, antidifferentiation factor, etc.).

Neuronal Therapy

Neurodegenerative diseases, such as Parkinson's and Huntington's diseases, and the degenerative changes observed following stroke have no known cure. Because pharmacological treatments are palliative at best, other potential treatments have been examined. One treatment strategy proposed the use of adult neuronal progenitor cells *(118,119)*. However, the location and quantity of harvested tissue, coupled with limited progenitor cell proliferation, relegated this therapy to a secondary role. Recent clinical evidence indicates that transplantation of fetal brain tissue might be a viable therapy for some neurodegenerative diseases

(120). Allogeneic embryonic stem cells have also shown promise for the production of neuronal tissues for transplant *(101,102)*. However, these experimental therapeutic approaches are limited by the restricted availability of human embryonic and fetal tissue, ethical rules, and moral issues concerning the use of human fetal tissues and embryonic stem cells in the United States and other countries, as well as the need to use toxic immunosuppressant drugs. Clearly, an alternative to the use of human tissues from fetal and/or embryonic sources would be beneficial in the treatment of neurodegenerative diseases and stroke.

Recent studies demonstrated that adult animals, including humans, contain quiescent reserve precursor cells capable of differentiating into multiple cell types. These precursor cells reside within skeletal muscle *(20,28,29,46–49,53,56,60,104,121–123)*, dermis *(28,29,47,48,124)*, and bone marrow *(8,9,13,83, 84,103,104,125–131)*. These studies demonstrate the existence of precursor cells that have capabilities for extended self-renewal. They can differentiate into cells belonging to the ectodermal lineage (e.g., neuronal progenitor cells, neurons, ganglia, oligodendrocytes, astrocytes, radial glial cells, and keratinocytes) (Figs. 11A–L, 12A–I), the mesodermal lineage (e.g., skeletal muscle, cardiac muscle, smooth muscle, white fat, brown fat, hyaline cartilage, elastic cartilage, growth plate cartilage, articular cartilage, fibrocartilage, cortical bone, trabecular bone, loose fibrous connective tissues, tendon, ligament, scar-connective tissue, endothelial cells, and erythropoietic and lymphopoietic cells) (Figs. 13A–DD, 14A–U), and the endodermal lineage (e.g., endodermal progenitor cells, gastrointestinal epithelium, liver oval cells, liver hepatocytes, liver biliary cells, liver canalicular cells, pancreatic progenitor cells, pancreatic ductal cells, and glucagon-secreting α-cells, insulin-secreting β-cells, and somatostatin-secreting δ-cells of pancreatic islets) (Figs. 15A–K, 16A–R). Autologous precursor cells can be isolated from adult animals, including humans. These cells have the capacity to form neuronal cells that could be used in the treatment of neurodegenerative diseases. Using these inducible precursor cells derived from the individual human patient rather than allogeneic fetal brain tissue or embryonic stem cells would avoid histocompatability mismatches and the need to use immunosuppressants with their attendant risk of infection.

Recent studies have shown that cells derived from bone marrow can be lineage directed to differentiate into neurons in vitro *(9,128,130)*. Similar results are obtained when the cells are transplanted into the brain *(8,125–127)*. However, the use of cells from bone marrow has its own limitations. An alternate source of stem cells that could be easily and safely harvested from the patient would be highly desirable. Young et al. *(29,48,49)* demonstrated that pluripotent stem cells can be readily derived from adult skeletal muscle and dermis by cell sorting and have the capacity to undergo extended self-renewal. These cells can form cells from all three primary germ layer lineages (i.e., ectoderm, mesoderm, and endoderm) (Figs. 11A–L, 13A–DD, 15A–K).

Recent data suggest that pluripotent stem cells derived from the skeletal muscle of adult rats can be lineage directed to express neuronal phenotypes *(60)*. These pluripotent stem cells were induced to form both floating neurospheres and adherent neuroectodermal cells located in a monolayer *(60)*. Cells were able to form neurospheres by repeated 7- to 15-d treatments with a mixture of B27, epidermal growth factor (EGF), and b-FGF. When desired, whole neurospheres could be cryopreserved. For neuronal induction, neurospheres were plated for 1–2 d in media supplemented with EGF and b-FGF, followed by either brain-derived neurotrophic factor (BDNF) or NT3 *(60,132,133)*. Directed lineage induction to form an adherent monolayer neuroectoderm was accomplished by 5 h of incubation in basal medium without serum containing dimethyl sulfoxide (DMSO), KCl, valproic acid, hydrocortisone, forskolin, butylated hydroxyanisole, and insulin followed by incubation for 2 d in Neurobasal A medium supplemented with N2, penicillin G, streptomycin, glutamine, laminin, EGF, and b-FGF *(9,60)*.

Table 6
Directed Induction of Ectodermal Germ-Layer Lineage Stem Cells into the Neurogenic Lineage

Phenotypic markers	Isolated ectodermal germ-layer lineage stem cells	Differentiated cells (from neurospheres)	Differentiated cells (monolayer conditions)
Oct-4	+	+/–	
Pax6	+	+	+
CD90	+		
CD45	–		
CD34	+/–		
Vimentin	+	+	
Myogenin	–	–	
MyoD	–	–	
Smooth muscle α-actin	–		
Nestin	–	+	+
NG2	–	+	+
b-Tubulin III (Tuj1)	–	+	+
tau protein	–		+
Neurofilament 145 kDa	–		+
Neurofilament 68 kDa	–	+	+
MOSP	–	+	+
GFAP	–	+	+ (transient, at 2 d)
MBP		+	+
CNPase	–	+	+

Oct-4, a gene directly involved in the capacity for self-renewal and totipotency of mammalian embryonic stem cells *(141)*. Pax6, a homeobox gene encoding for a transcription factor expressed from early developmental stages in embryo to adulthood in the neuroectoderm, central nervous system (CNS), and eye and also related to dopaminergic fate determination *(142, 249–251)*. CD90, a cluster of differentiation (CD) marker, also known as Thy-1, that is positive for bone marrow–derived mesenchymal progenitor cells *(84)* and skeletal muscle–derived mesodermal germ-layer lineage stem cells *(47)*. CD45, hematopoietic cell marker *(100)*. CD34, a sialoprotein present on hematopoietic stem cells, endothelial cells, and mesodermal germ-layer lineage stem cells *(47,100)* and absent on mesodermal progenitor cells derived from bone marrow stroma *(84)*. CD34 marker was absent by Fax analysis but detected on a subpopulation of ectodermal germ-layer lineage stem cells by immunocytochemistry. CD34-negative and -positive cells had similar differentiation potential (Chivatakarn and Chesselet, unpublished observations). Vimentin, a marker for early muscle cells and early glial progenitor cells *(134)*. Myogenin, marker specific of skeletal muscle *(252)*. MyoD, marker of myogenic cells *(253)*. Smooth muscle α-actin, marker of smooth muscles *(254)*. Nestin, an early marker for brain cells that is present in neuronal progenitor cells and muscle precursor cells *(135,136)*. NG2, a proteoglycan present in the membrane of progenitor cells, as well as differentiated oligodendrocytes, and in newly generated cells of the adult hippocampus *(138, 140)*. b-Tubulin III (Tuj1), an early neuronal marker *(255)*. Tau protein, a neuronal marker *(256)*. Neurofilament 145 kDa, a neuronal marker *(257)*. Neurofilament 68 kDa, a neuronal marker *(258)*. MOSP, myelin oligodendrocyte-specific protein, which is a marker of mature oligodendrocytes *(259)*. GFAP, glial fibrillary acid protein, which is a marker of astrocytes *(260)*. MBP, marker of mature oligodendrocytes *(261)*. CNPase, marker of oligodendrocytes *(262)*.

The resulting cells were characterized as being either predifferentiated pluripotent stem cells or postdifferentiated neuroectodermal cells formed by induction. The analysis was performed using morphological, immunocytochemical, and molecular procedures (Table 6) *(60)*. The cells were grown in suspension or monolayer cultures and assayed for the appropriate morphological characteristics distinguishing them as either belonging to the neurogenic or myogenic lineage (Fig. 18A–F) *(46–49,60,132)*.

Next, predifferentiated and postdifferentiated cells were stained with antibodies to cell surface

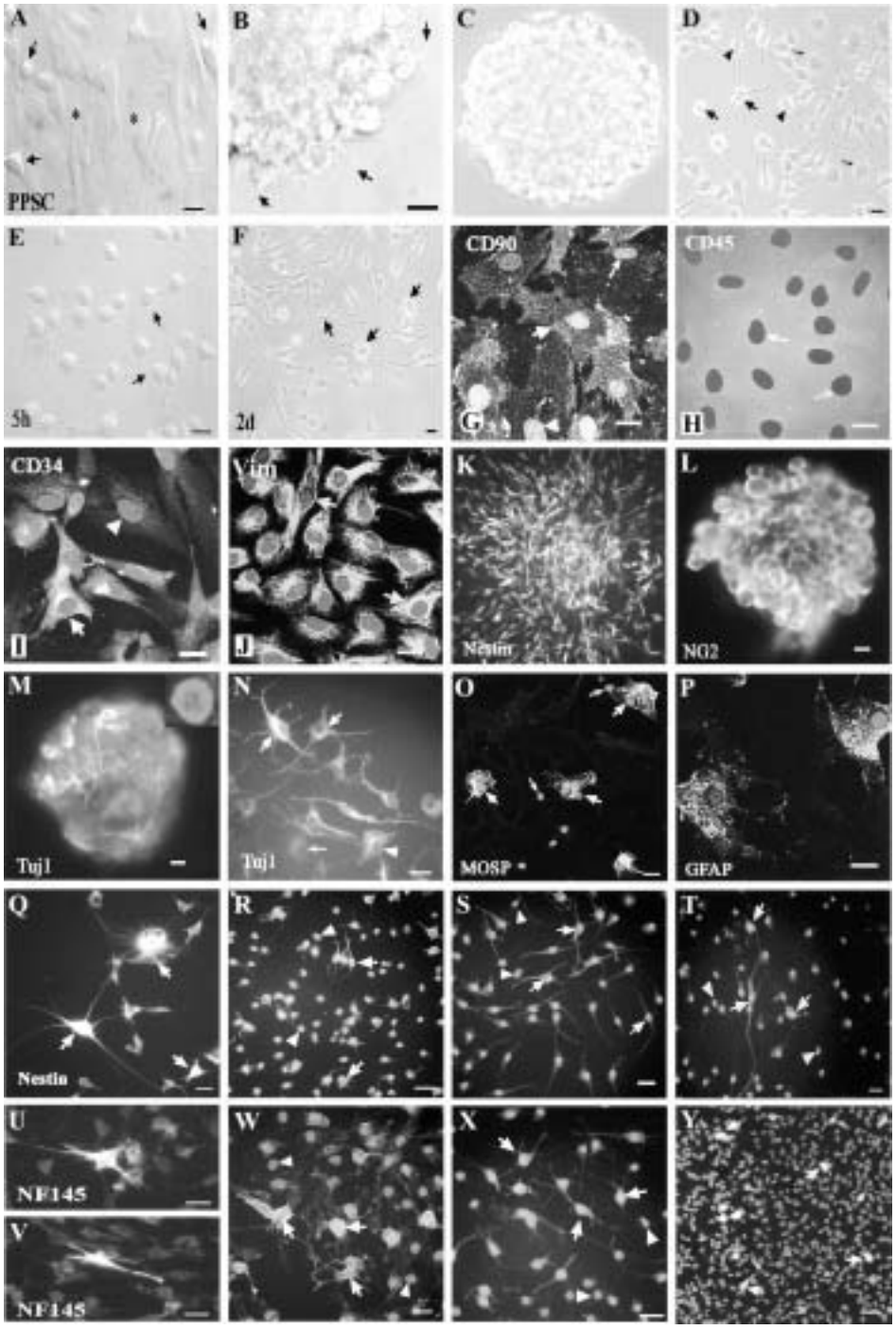
A
PPSC
B
C
D
E
5h
F
2d
CD90
G
CD45
H
CD34
I
Vim
J
K
Nestin
L
NG2
M
Tuj1
N
Tuj1
O
MOSP
P
GFAP
Q
Nestin
R
S
T
U
NF145
W
X
Y
V
NF145

Fig. 18. Pluripotent stem cells (PPSCs) induced to form neuronal lineage cells. **(A–F)** Pre- and postdifferentiation morphology of PPSCs grown in monolayer or as neurospheres. **(G–J)** Antigenic properties of undifferentiated PPSCs. **(K–M)** Intense staining of PPSC-derived neurospheres. **(N–P)** Staining of PPSCs 6 d after plating the dissociated neurospheres. **(Q–V)** Staining of PPSCs after 2 d in maturation medium in monolayer conditions. **(W–Y)** Expression of oligodendroglial markers in PPSCs after 2 d in maturation medium. Scale bar: 20 μm for **A–L** and **N–X**, 10 μm for **M**, and 40 μm for **Y**.

(A) Undifferentiated PPSCs: polygonal flat cells (*) predominated, with a few cells with round or triangular cell body (arrows). **(B)** Detail of a PPSC-derived neurosphere; note the cilia extension at the perimeter of the cluster (arrows). **(C)** PPSC-derived neurospheres observed after 10 d in the neurosphere's medium. **(D)** Morphology of cells isolated from neurospheres and plated on coverslips after 3 d. Bipolar (arrowheads), tripolar (large arrows), and large flat cells (small arrows) were observed. **(E)** Morphology of PPSCs grown as a monolayer after 5 h in the differentiation medium: most cells had round, small cell bodies and processes (arrows). **(F)** Representative field after 2 d in the maturation medium showing a majority of round cells with processes (arrows) when PPSCs are grown as a monolayer. **(G)** CD90 positive cells represent the majority of the population. Both intensely (large arrow) and moderately stained cells (arrowheads) were observed, and negative cells were very rare (top small arrow). **(H)** PPSCs showed no staining when immunocytochemistry for CD45 was carried out (arrows). **(I)** Immunolabeling for CD34: moderate-intensity (arrows) and low-intensity (arrowhead) immunostaining was found. **(J)** Immunolabeling for vimentin: the entire cell population was intensely immunoreactive for this cytoskeleton protein. Nuclei in blue were stained with 4,6-diamidino-2-phenylindole (DAPI). **(K)** Nestin. **(L)** NG2. **(M)** Tuj1, insert (upper right corner) shows cell nuclei counterstained with DAPI. **(N)** When plated, the neurospheres gave rise to round cells with numerous processes. These cells were positive for β-tubulin III (large arrows) and were surrounded by negative cells (bottom small arrow). In addition, some flat cells stained positively for β-tubulin III (arrowhead). **(O)** Cells immunostained for myelin oligodendrocyte-specific protein (MOSP) (large arrows); cells were counterstained with DAPI; small arrows point to nuclei of negative cells. **(P)** Large flat cells were positive for GFAP immunostaining. **(Q)** Cells of diverse morphology were immunostained for nestin: large flat cells (top right arrow), large round multipolar cells (left arrow), and small cells with processes (bottom right arrow). **(R)** Positive cells with round bodies and processes (arrows) immunostained for vimentin and intermingled with negative cells (arrowheads). **(S)** Cells with a neuronal-like cell process morphology were positive for β-tubulin III (Tuj1; arrows) and surrounded by negative cells whose cell nuclei were counterstained in blue with DAPI (arrowheads). **(T)** Cells with a neuronal-like cell process were positive for β-tubulin III (Tuj1; arrows) and surrounded by negative cells whose cell nuclei were counterstained in blue with DAPI (arrowheads). **(U)** Scattered cells show intense staining for NF145. **(V)** Scattered cells show intense staining for NF145. **(W)** Membrane of cells immunostained for NG2 (arrows). Cell nuclei were counterstained in blue with DAPI. Arrowheads point to negative cells for NG2. **(X)** Typical multipolar cells positive for CNPase (arrows) surrounded by negative cells (arrowheads). Counterstained with DAPI for nuclei. **(Y)** Cells immunostained for MOSP were usually round with very short processes (arrows). They were scattered among negative cells (arrowheads). Counterstained with DAPI for nuclei. (Reproduced with permission from Romero-Ramos, M., Vourc'h, P., Young, H. E., Lucas, P. A., Wu, Y., Chivatakarn, O., et al. [2002] Neuronal differentiation of stem cells isolated from adult muscle. *J. Neurosci. Res.* **69,** 894–907. Copyright 2002, Wiley-Liss.)

(CD34, CD45, CD90) markers *(47,100)* and intracellular differentiation markers for cells of the neurogenic lineage (vimentin, nestin, NG2, Tuj1, NF145, astrocyte and oligodendrocyte marker [CNPase], myelin oligodendrocyte-specific protein [MOSP], and glial fibrillary acid protein [GFAP]) *(9,48,49,60,134–140)* or the myogenic lineage (myogenin and smooth muscle α-actin) *(46–49)*. Predifferentiated cells displayed $CD34^{+/-}$, $CD45^{-}$, $CD90^{+}$, and $vimentin^{+}$ staining (Fig. 18G–J). After forming neurospheres, the cells displayed staining for nestin, NG2, and Tuj1 (Fig. 18K–M). After plating the dissociated neurospheres in conditions with NT3 or BDNF, the cells expressed Tuj1, MOSP, and GFAP (Fig. 18N–P). Postdifferentiated cells under adherent monolayer conditions displayed staining for nestin and vimentin (Fig. 18Q,R), Tuj1 and NF145 (Fig. 18S–V), and NG2, CNPase, and MOSP (Fig. 18W–Y). None of the cells assayed displayed staining for myogenin or smooth muscle α-actin (data not shown) *(60)*, indicative of induction into the mesodermal lineage.

Last, pre- and postdifferentiated cells were screened for messenger ribonucleic acids (mRNAs) characteristic of undifferentiated (*Oct-4*) *(141)*, neurogenic (*Pax6*, nestin, β-tubulin III, NF68, GFAP, and oligodendrocyte marker [MBP] *(135,136,142)*, and myogenic (myogenin and MyoD) *(46–49)* cells. Predifferentiated cells from neurospheres displayed mRNAs for *Oct-4*, *Pax6*, and nestin (Fig. 19A). Postdifferentiated cells from neurospheres and adherent neuroectoderm displayed mRNAs for *Pax6* and nestin (Fig. 19A,B), β-tubulin III, NF68, GFAP, and MBP (Fig. 19C,D). The mRNAs myogenin and MyoD specific for muscle were not detected by reverse transcriptase polymerase chain reaction (RT-PCR) in the cells at any time-points in this study *(60)*.

Previous studies by Young et al. *(28,29,41–49)* noted a plethora of pluripotent stem cells, germ-layer lineage stem cells, and progenitor cells located within the connective tissue matrices of dermis and skeletal muscle. Young and Black *(48)* proposed that a continuum of precursor cells, from the most primitive pluripotent epiblastic-like stem cells to the most differentiated unipotent progenitor cells, existed within the connective tissue compartments of organs and that these precursor cells contributed to the normal maintenance and repair of postnatal tissues. Exhaustive analyses by Young et al. using repetitive single-cell clonogenic analysis, CD marker analysis, and induced differentiation, coupled with morphological, histochemical, immunochemical, molecular, pharmacological, and physiological-functional analyses, have identified at least two discrete populations within this adult precursor stem cell continuum: mesodermal GLL stem cells and pluripotent epiblastic-like stem cells. The mesodermal GLL stem cells demonstrated the capability for extended self-renewal, contact inhibition at confluence, and the capacity to form cells restricted to the mesodermal lineage. These cells displayed a $CD34^{+}$, $CD45^{-}$, and $CD90^{+}$ marker profile (*see* Mesodermal Germ Layer Lineage Stem Cells section for complete profile). The pluripotent epiblastic-like stem cells demonstrated the capability for extended self-renewal and growth past confluence. These cells could form cells from all three primary germ-layer lineages (ectoderm, mesoderm, and endoderm). The cells displayed a $CD34^{-}$, $CD45^{-}$, and $CD90^{-}$ marker profile (*see* Pluripotent Epiblastic-Like Stem Cells section for complete profile).

In contrast, the cells isolated in the current neuronal study formed cells apparently solely of the ectodermal neurogenic lineage. These cells displayed a $CD34^{+/-}$, $CD45^{-}$, $CD90^{+}$, and $vimentin^{+}$ profile *(60)*. These results, based on both the expressed CD marker profile and the expressed differentiation potential, suggest that this cell population consists of a different population of stem cells than those previously identified by Young et al. The cells reported herein may be ectodermal GLL stem cells or neuroectodermal stem cells. However, additional studies are needed to further characterize the differentiation potential of these newly isolated stem cells.

These results confirm our ability to selectively induce reserve stem cells to undergo directed lineage induction to form cells of the neuroectodermal lineage. Although the expres-

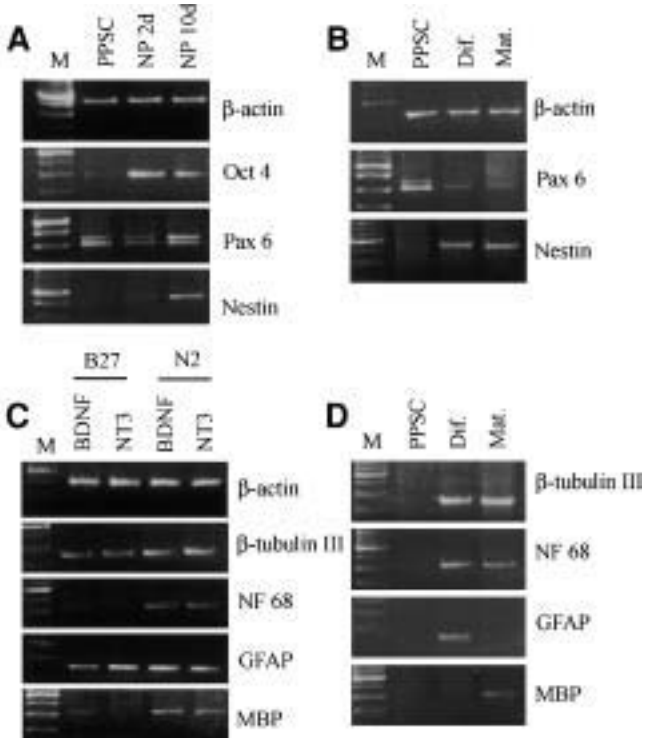

Fig. 19. RT-PCR analysis of gene expression in PPSCs and PPSC-derived neurospheres (**A**), differentiated cells from neurospheres (**C**), and PPSCs and differentiated PPSCs in monolayer conditions (**B**, **D**). Total ribonucleic acid (RNA) was extracted from undifferentiated PPSCs after the 5-h differentiation step (Dif.) and after 2 d in a maturation medium (Mat.) (**B**, **D**). M: 100-bp DNA ladder (**A–D**). The expression of the β-actin gene was used as an internal control (**A–D**).

(A) RT-PCR analysis of *Oct-4*, *Pax6*, and nestin mRNA expression in PPSCs and in neurospheres after 2 d (NP 2d) and 10 d (NP 10d). **(B)** Analysis of the expression of the genes *Pax6* and nestin. **(C)** Analysis of β-tubulin III, NF68, GFAP, and MBP mRNA expression after differentiation of neurospheres. Cells from neurospheres were plated in two different media (Nb-B27 or Nb-N2) supplemented with BDNF or NT3. Total RNA was extracted after 4 d in these differentiation media. **(D)** Analysis of the expression of the genes β-tubulin III, NF68, GFAP, and MBP. (Reproduced with permission from Romero-Ramos, M., Vourc'h, P., Young, H. E., Lucas, P. A., Wu, Y., Chivatakarn, O., et al. [2002] Neuronal differentiation of stem cells isolated from adult muscle. *J. Neurosci. Res.* **69,** 894–907. Copyright 2002, Wiley-Liss.)

sion markers observed depend on culture conditions, no stem cell population previously isolated matches these characteristics. In addition, this population can be harvested from very accessible tissues, making these cells an excellent source for autologous transplantation therapies.

Hematopoietic Therapies

Red blood cells and leukocytes or white blood cells make up the cellular elements of the peripheral blood. These cells are important for delivering oxygen to the tissues and providing host defense against infectious disease. It has been estimated that 5×10^{11} cells, including 200

billion red blood cells, must be replaced in the human body daily. To produce the needed red and white blood cells, specialized cells called bone marrow hematopoietic stem cells are induced to differentiate into the various cell types. Bone marrow hematopoietic stem cells compose approx 0.1% to 0.01% of the cells found in the human bone marrow. These stem cells have the highest proliferative potential of any hematopoietic cell type and are capable of self-renewal and differentiation *(143,144)*. To produce cells of the various lineages, cytokines are used to drive the stem cells to differentiate along the various specific pathways. Progenitor cell cytokines, such as stem cell factor, act on immature cells types, whereas end-stage cytokines act on the more differentiated cell types and induce lineage-specific differentiation *(145)*. Examples of end-stage cytokines and the cells types that are produced (in parentheses) include interleukin (IL)-3 (basophils), IL-5 (eosinophils), IL-7 (B lymphocytes), IL-2/IL-7 (prothymocytes that further differentiate into T lymphocytes in the thymus), IL-15 (natural killer cells), thrombopoietin (megakaryocytes/platelets), erythropoietin (red blood cells), granulocyte colony-stimulating factor (neutrophils), and monocyte/macrophage colony-stimulating factor (monocytes).

According to the National Blood Data Resource Center *(146)*, nearly 14 million units of whole blood are collected from donors annually in the United States. In 1999, approx 8 million volunteer donors provided whole blood that was fractionated into 26.5 million units of blood components, such as cells and plasma, to provide the needs of almost 4.5 million patients. Blood or blood components are often needed to treat patients who have suffered burns or traumatic injury or have undergone organ transplantation or heart surgery. In addition, patients who are treated for cancer may need transfusion with blood or blood components. It is anticipated that in the future, seasonal and regional shortages of blood may occur more often than they currently do as the demand for blood increases. In addition to blood, bone marrow has the potential to cure patients with numerous disorders involving blood cells *(147)*. According to the National Marrow Donor Program *(148)*, more than 12,000 bone marrow and stem cell transplants have been performed using unrelated donors since its founding in 1986. More than 4 million potential volunteer bone marrow and blood stem cell donors have been recruited to the donor registry, yet a significant number of patients cannot find an acceptable histocompatability match with those on the donor registry. In summary, there is an urgent need to have readily available blood cells and bone marrow stem cells for the increasing number of patients that need them and for those who cannot find an acceptable match with an unrelated donor for bone marrow transplantation *(149)*.

To address the deficiencies inherent in the current system for blood transfusion and bone marrow transplantation, researchers are beginning to explore the use of stem cells derived from tissues other than bone marrow *(150–152)*. Stem cells have the capability to undergo self-renewal and to differentiate to form functional tissue. Stem cells from various tissues have been shown to be able to differentiate into blood cells. Most studies to date have been performed in mice; therefore, the results are difficult to extrapolate to humans. In one study, intravenously injected stem cells derived from the skeletal muscle of mice were able to reconstitute the bone marrow compartment following whole-body irradiation *(14)*. In another study, stem cells derived from the skeletal muscle of adult mice were shown to be able to repopulate the hematopoietic compartment in mice subjected to lethal irradiation *(20)*. Stem cells derived from neural tissues of mice were found to differentiate into bone marrow stem cells, which then produced cells of the hematopoietic lineage *(15)*. These blood cells could be detected as long as 12 mo after injection of stem cells derived from neural tissue, demonstrating long-term engraftment. Interestingly, stem cells derived from the bone marrow of adult mice were also able to differentiate into cells that shared characteristics with neurons *(127)*.

Some evidence suggests that these results observed in mice can be replicated in humans. Woodbury et al. *(9)* were able to induce stem cells derived from human marrow stroma to differentiate into neuron-like cells in vitro. These investigations demonstrated that a certain amount of plasticity exists in marrow stromal stem cell populations. Another investigation showed that women who had received bone marrow transplants from male donors produced liver cells that contained the Y-chromosome *(153)*. There is a high probability that the liver cells were derived from pluripotent stem cells, endodermal GLL stem cells, and/or hepatogenic progenitor cells residing in the donor marrow. Much more work is required to begin translating the results from mouse models to the treatment of human patients.

Clinically, the advantages of using pluripotent stem cells or mesodermal GLL stem cells to produce blood components or replenish bone marrow are numerous. In vitro culture of either stem cell population may provide a virtually unlimited supply of cells for transfusion. There is obviously a need for the formation of banks of stem cells, which could serve the needs of patients whose histocompatability profiles are difficult to match. In addition, in vitro culture of pluripotent stem cells or mesodermal GLL stem cells would allow a high level of quality control to diminish the likelihood of transmission of infectious agents to the recipient of the cells. Also, it is possible that human reserve stem cells from patients with a disease originating from a single enzyme defect could be isolated and genetically manipulated in the laboratory to provide a cure *(154)*. Last, in those patients with malignant disease, such as leukemia or other cancers that have metastasized to the bone marrow, pluripotent stem cells or mesodermal GLL stem cells isolated from tissues other than bone marrow could provide a source of stem cells uncontaminated by tumor cells. These stem cells could be used to reconstitute the bone marrow after lethal irradiation or destruction of the bone marrow by chemotherapy.

Preliminary studies were performed to determine whether adult human reserve stem cells could be used in induced blood transfusion and bone marrow therapies. In the first series of experiments, sorted adult human mesodermal GLL stem cells expressing the $CD10^+$, $CD13^+$, $CD34^+$, $CD56^+$, $CD90^+$, MHC-I^+, $CD1a^-$, $CD2^-$, $CD3^-$, $CD4^-$, $CD5^-$, $CD7^-$, $CD8^-$, $CD9^-$, $CD11b^-$, $CD11c^-$, $CD14^-$, $CD15^-$, $CD16^-$, $CD18^-$, $CD19^-$, $CD20^-$, $CD22^-$, $CD23^-$, $CD24^-$, $CD25^-$, $CD31^-$, $CD33^-$, $CD36^-$, $CD38^-$, $CD41^-$, $CD42b^-$, $CD45^-$, $CD49d^-$, $CD55^-$, $CD57^-$, $CD59^-$, $CD61^-$, $CD62E^-$, $CD65^-$, $CD66e^-$, $CD68^-$, $CD69^-$, $CD71^-$, $CD79^-$, $CD83^-$, $CD95^-$, $CD105^-$, $CD117^-$, $CD123^-$, $CD135^-$, $CD166^-$, Glycophorin-A^-, HLA-$DRII^-$, FMC-7^-, Annexin-V^-, and LIN^- cell surface profile were incubated in serum-free medium only (control) or in serum-free medium containing 50 ng/mL stem cell factor, 10 ng/mL granulocyte macrophage-colony stimulating factor, 10 ng/mL granulocyte-colony stimulating factor, 10 ng/mL macrophage-colony stimulating factor, 50 ng/mL IL-3, 50 ng/mL IL-6, 2.5 U/mL erythropoietin, and 2 μg/mL insulin (experimental). The media were changed three times per week for 2 wk. The cells were released and examined for the expression of cell surface markers indicative of hematopoietic phenotypic expression using CD markers with fluorescent-activated cell surface (FACS) analysis *(47)*. Experimental treatment induced the phenotypic expression of CD4, CD36, CD38, CD45 (lymphopoietic), and Glycophorin-A (erythropoietic) cell surface markers in induced adult human mesodermal GLL stem cells (Table 7). Further experiments are needed to determine the optimum conditions for blood cell induction, especially with respect to directed induction into individual cell types. However, these results suggest the potential for induction of blood elements ex vivo using adult human mesodermal GLL stem cells.

In a second set of experiments, a clonal population of naive noninduced adult rat pluripotent epiblastic-like stem cells *(49)*, previously transfected with a gene for β-galactosidase *(29,49)*, was injected into the tail vein of adult rats. After 2–4 wk, the rats were euthanized

Table 7
Percentage of Induced Cluster of Differentiation (CD) Marker Expression in Adult Human Mesodermal Germ-Layer Lineage Stem Cells Treated with Stem Cell Factor, IL-3, IL-6, and Erythropoietin

Markers	Control	Experimental
CD4	0.17	11.36
CD34	26.10	73.20
CD36	0.24	5.60
CD38	0.17	16.12
CD45	0.35	6.21
Glycophorin-A	0.15	97.54

and the organs and tissues removed and analyzed for the presence of β-galactosidase. The results showed viable β-galactosidase-stained cells resident within the bone marrow (Fig. 20). Additional experiments are needed to determine the optimal conditions for stem cell engraftment and expression of differentiated cells in the periphery. However, although these results are very preliminary, they suggest the possibility that adult pluripotent epiblastic-like stem cells may have the potential to repopulate hematopoietic organs.

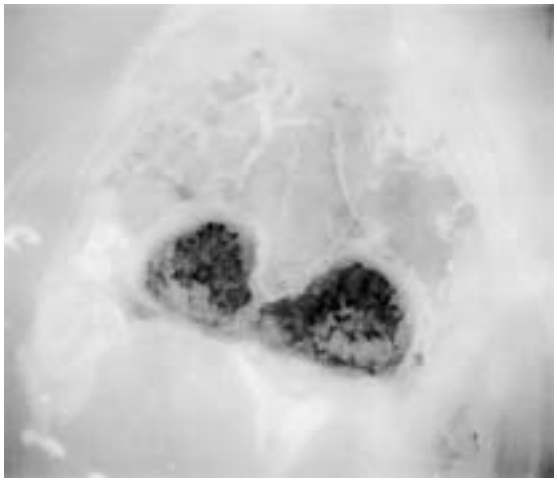

Fig. 20. Systemic injection of Lac-Z-transfected adult rat pluripotent epiblastic-like stem cell clone (PPELSC) clone with incorporation into bone marrow. Cells were expanded in medium containing PDGF-like (proliferative) and ADF-like (inhibitory) activities *(28,29)*. Cells were processed for injection as described by Asahara and colleagues *(245–248)*. Adult Sprague-Dawley rats were anesthetized and the transfected stem cells injected into the systemic circulation via the tail vein. Two weeks post injection, the animals were euthanized and the tissues processed for β-galactosidase histochemistry *(49)*. The marrow cavities of the radius and ulna demonstrate heavy staining for the Lac-Z reaction product.

Therapy for Diabetes Mellitus

Diabetes mellitus is a metabolic syndrome with a diversity of etiologies, clinical presentations, and outcomes. It is characterized by insulinopenia, fasting or postprandial hyperglycemia, and insulin resistance. Type 1 diabetes mellitus, referred to as juvenile or insulin-dependent diabetes mellitus (IDDM), is typically characterized by insulinopenia, hyperglycemia, and secondary insulin resistance *(155)*. Type 2 diabetes mellitus, referred to as adult onset or non-insulin-dependent diabetes mellitus (NIDDM), is characterized by hyperglycemia and varying degrees of primary insulin resistance with elevated plasma insulin concentrations but a decreased insulin response to challenge by a secretagogue *(156)*. Diabetes mellitus need not be overt and grossly hyperglycemic to induce detrimental metabolic changes. A growing body of evidence suggests that there are detrimental consequences to normal physical challenges such as aging, which may be inherently linked to alterations in body composition. Such challenges may result in subclinical diabetogenic changes. It is becoming increasingly clear that loss of physical strength, functional status, and immune competence are related to decreases in lean body mass observed in diabetogenic states *(157–159)*.

In 1933, Walsh and colleagues illustrated that protein wasting in type 1 diabetes mellitus could be eliminated by administration of insulin *(160)*. Later studies suggested that the degree of protein wasting might be related to the degree of pancreatic function and insulin availability *(161)*. A single mechanism of action, which describes the effect of insulin on proteolysis or proteogenesis, remains to be clearly elucidated. Decreased lean body mass in diabetes mellitus may result from the decreased number and translational efficiency of ribosomes *(162,163)*, as well as alterations in peptide chain elongation and termination *(164)*. Several studies also suggest that these effects may be modulated in part by modifications in IGF-1. Streptozotocin diabetic rats that are insulin deficient lack IGF-1. Growth retardation in diabetic infants has been ascribed to a lack of proper insulinization *(165)*. More recent studies suggest that protein nutrition, insulin, and growth may be modulated via IGF-1 *(166,167)*. Tobin et al. *(168–171)* demonstrated that transplantation with normal islets of Langerhans completely restores normal body protein levels in rats.

Islet transplantation, rather than whole-organ transplantation, has been investigated as a possible treatment for type 1 diabetes mellitus in selected patients unresponsive to exogenous insulin therapy *(172)*. Recently, the Edmonton group *(173–177)* reported that sufficient islet mass from as few as two pancreases, in combination with a new regimen of glucocorticoid-free immunosuppressive protocol, engendered sustained freedom (> 1 yr) of insulin independence in 8 of 8 *(173)* and 12 of 12 *(176,177)* patients with type 1 diabetes mellitus. Their findings indicated that islet transplantation alone was associated with minimal risk and resulted in good metabolic control *(173,174)*. However, as a result of the paucity of cadaveric organ donors, less than 0.5% of patients with type 1 diabetes mellitus could receive an islet transplant at the present time. Thus, alternative sources of insulin-secreting tissue are urgently needed *(175)*.

Recent reports *(178–180)* suggest that reversal of insulin-dependent diabetes mellitus could be accomplished using chemically induced islets generated in vitro from pancreatic ductal endodermal stem cells. In addition, Lumelsky et al. *(181)* reported the formation of 3D insulin-secreting pancreatic islets that spontaneously differentiated from embryonic stem cells. We began preliminary in vitro studies to ascertain the ability of adult pluripotent epiblastic-like stem cells to form insulin-secreting pancreatic islet-like structures. A clone of adult rat pluripotent epiblastic-like stem cells *(29,49)* was used for these studies.

One of the major differences we noted between reports of embryonic stem cells and the adult pluripotent epiblastic-like stem cells is their respective activities in serum-free defined media in the absence of an induction and/or differentiation inhibitory agent. In serum-free medium in the absence of leukemia inhibitory factor or a fibroblast feeder layer, embryonic stem cells will spontaneously differentiate into all the somatic cells present in the body *(101,102)*. Indeed, Soria et al. *(182,183)*, Assady et al. *(184)*, and Lumelsky et al. *(181)* used spontaneous differentiation directly or in combination with directed differentiation to generate pancreatic islets from embryonic stem cells. In contrast, reserve pluripotent epiblastic-like stem cells remain quiescent in serum-free defined media in the absence of either leukemia inhibitory factor or antidifferentiation factor (Figs. 8A, 9A). In other words, these adult pluripotent epiblastic-like stem cells are not preprogrammed to form any type of cell. Furthermore, pluripotent epiblastic-like stem cells remain quiescent unless a specific lineage, tissue-, or cell-inductive agent is present in the medium *(28,29,43,46–49)*. Because reserve pluripotent epiblastic-like stem cells do not exhibit spontaneous differentiation, we attempted to use direct lineage induction to generate 3D pancreatic islet-like structures (3D-ILS). The initial population of reserve stem cells consisted of a clone of pluripotent epiblastic-like stem cells. In a sequential fashion, we induced these undifferentiated stem cells to commit to form endodermal GLL stem cells and then pancreatic progenitor cells. As the

stem cells became increasingly lineage committed, there was a concomitant loss of pluripotentiality within the cell line (Table 5).

Next, we used the islet-inductive mixture of Bonner-Weir et al. *(180)* in an attempt to induce 3D-ILS in the three stem cell populations: pluripotent epiblastic-like stem cells, endodermal GLL stem cells, and pancreatic progenitor cells. For each cell line, 10^3 stem cells were plated per well ($n = 96$) and treated with serum-free defined medium containing the islet-inductive mixture *(49)*. The mean number of induced 3D-ILS formed per well (± SEM) was 0.364 ± 0.066 for the induced pluripotent epiblastic-like stem cells, 1.177 ± 0.117 for the endodermal GLL stem cells, and 10.104 ± 0.480 for the pancreatic progenitor cells. The increase in the number of constructs formed by the pancreatic progenitor cells was statistically significant compared to that induced in the pluripotent epiblastic-like stem cells or the endodermal GLL stem cells ($p < 0.05$, analysis of variance). After treatment with the islet-inductive cocktail, the cultures were stained with antibodies to insulin, glucagon, and somatostatin. Induced pluripotent epiblastic-like stem cells showed minimal intracellular staining for any of the antibodies used (Fig. 21A–C). Induced endodermal GLL stem cells showed a diffuse distribution of individual cells stained for insulin, glucagon, and somatostatin (Fig. 21D–F). Induced pancreatic progenitor cells also demonstrated 3D-ILS that exhibited staining for insulin, glucagon, and somatostatin (Fig. 21G–I).

We next examined the biological activity (i.e., insulin-secreting ability) of the 3D-ILS (Fig. 22A,B) generated from the induced-pancreatic progenitor cells in response to a glucose challenge. For comparative purposes, we isolated 200 × 150 mm native pancreatic islet equivalent units (Fig. 22C,D) from Wistar Furth rat pancreases *(168–171)* for each trial ($n = 8$ for native islets and $n = 12$ for 3D-constructs). Each well of native islets and 3D-ILS was incubated sequentially, first with testing medium (TM) only for 24 h, followed by TM + 5 m*M* glucose for 24 h, followed by TM + 5 m*M* glucose for 1 h, followed by TM + 25 m*M* glucose for 1 h. This sequence was performed in each of the respective wells examined. The media were removed and analyzed for insulin using a rat-specific insulin radioimmunoassay (RIA) (Table 8). The induced 3D-ILS secreted 22% of the amount of insulin secreted by native islets during incubation with 5 m*M* glucose for 24 h. When this was followed in each well by incubation in 5 m*M* glucose for 1 h, the 3D-ILS secreted 49% of the amount secreted by the native islets. A subsequent incubation with 25 m*M* glucose for 1 h resulted in secretion by the 3D-ILS of 42% of the amount of insulin secreted by the native islets (Table 8).

A series of positive and negative controls was performed to ensure that the RIA only measured rat insulin secreted into the media *(49)*. The positive controls consisted of a concentration range of rat insulin standards included with the kit. The negative controls consisted of serum-free defined medium with and without the insulin secretagogues in a cell-free system. Because our testing medium also contained a small amount of bovine insulin, its presence was monitored using the same concentration range as rat insulin standards in the RIA kit. No insulin was detected in any of the negative controls analyzed.

The direct lineage induction of cloned reserve pluripotent epiblastic-like stem cells to form insulin-secreting 3D-ILS proves the capabilities of these stem cells to form islet-like structures. However, use of cloned pluripotent stem cells as the starting material to generate islet-like structures for transplantation into patients is impractical at this time. First, the generation of clones by repetitive single-cell clonogenic analysis requires a minimum of 2 yr to complete. Second, use of immunosuppressants for allogeneic stem cells is mandatory as a result of potential donor-host human leukocyte antigen (HLA) mismatches. A practical alternative procedure is available. The patient's own reserve pluripotent epiblastic-like stem cells can be isolated from a small dermal or skeletal muscle biopsy and expanded in cell culture. They can then be induced to form 3D constructs that secrete insulin. These autologous constructs can then be transplanted into the

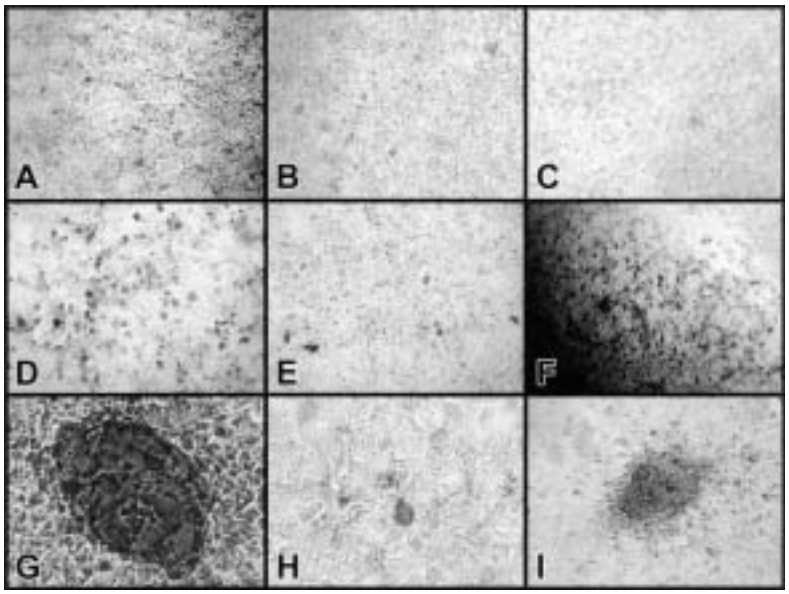

Fig. 21. Expression of insulin, glucagon, and somatostatin in adult rat pluripotent epiblastic-like stem cell clones (PPELSCs), induced endodermal GLL stem cells (EndoGLLSCs), and induced pancreatic progenitor cells (PanPCs). **(A–C)** PPELSCs *(29,49)* were expanded in medium containing PDGF-like (proliferative) and ADF-like (inhibitory) activities *(28,29)*. Twenty-four hours after plating, the cultures were switched to islet-inductive medium *(180)*, including endodermal inductive activity *(49)*. Cultures were incubated for 2 wk and processed for ELICA *(40)* using primary antibodies to insulin, glucagon, and somatostatin. Original magnifications, ×100. **(A)** Minimal intracellular staining for insulin. **(B)** Minimal intracellular staining for glucagon. **(C)** Minimal intracellular staining for somatostatin. **(D–F)** EndoGLLSCs were generated from PPELSCs by directed lineage induction. PPELSCs *(29,49)* were expanded in medium containing PDGF-like (proliferative) and ADF-like (inhibitory) activities *(28,29)*. Twenty-four hours after plating, PPELSCs were switched to medium containing endodermal inductive activity (EIM) for two passages. By the end of the second passage in EIM, the cells increased to a uniform size and shape and assumed contact inhibition, forming a single confluent layer of cells. Twenty-four hours after replating EndoGLLSCs, the cultures were switched to islet-inductive medium (IIM) *(49,180)*. Cultures were incubated for 2 wk and processed for ELICA using primary antibodies to insulin, glucagon, and somatostatin. Original magnifications, ×100. **(D)** Diffuse distribution of individual cells stained intracellularly for insulin. **(E)** Diffuse distribution of individual cells stained intracellularly for glucagon. **(F)** Diffuse distribution of individual cells stained intracellularly for somatostatin. **(G–I)** PanPCs were generated from EndoGLLSCs by directed lineage induction. EndoGLLSCs were expanded in EIM. Twenty-four hours after replating, EndoGLLSCs were switched to a pancreatic progenitor cell induction medium *(49)*. A minimum of two passages was required for the induction process. Twenty-four hours after replating, the cultures were switched to the islet-inductive medium *(49,180)*. Cultures were incubated for 2 wk and processed for ELICA using primary antibodies to insulin, glucagon, and somatostatin. Visualization of bound antibody occurred with DAB. Original magnifications, ×400 (**G**), ×300 (**H**), and ×200 (**I**). **(G)** 3D nodular islet-like structure and surrounding mononucleated cells showing moderate to heavy intracellular staining for insulin. **(H)** 3D nodular islet-like structure with a few centrally located cells showing heavy intracellular staining for glucagon. **(I)** 3D nodular islet-like structure and some surrounding mononucleated cells showing moderate to heavy intracellular staining for somatostatin. (Reproduced with permission from Young, H. E., Duplaa, C., Yost, M. J., Henson, N. L., Floyd, J. A., Detmer, K., et al. [2004] Clonogenic analysis reveals reserve stem cells in postnatal mammals: II. Pluripotent epiblastic-like stem cells. *Anat. Rec.* **276A**, in press. Copyright 2004, Wiley-Liss.)

Table 8
Glucose Challenge: Nanograms of Secreted Insulin per Well

	Testing medium only 24 h	5 m*M* for 24 h	5 m*M* for 1 h	25 m*M* for 1 h
Native islets	0 ± 0	2215 ± 282	658 ± 36	308 ± 51
3D constructs	0 ± 0	482 ± 81	325 ± 35	136 ± 26

patient. This procedure would eliminate the need for the use of immunosuppressant drugs based on donor-host HLA mismatches. As an adjunct to the above proposal, a set of experiments was performed to determine the amount of time needed to generate transplantable insulin-secreting 3D-ILS after receipt of a tissue biopsy specimen. Studies were performed with biopsy specimens from adult rats (to parallel the conditions of the rat clonal studies), adult mice, and adult humans. Depending on the species, the entire process, including receipt of the biopsy specimen, isolation of the stem cells directly from the tissue by CD marker cell sorting, stem cell expansion, and induction of transplantable islet-like structures, required 8–12 wk under nonoptimized conditions.

Articular Cartilage and Bone Repair

The existence of quiescent reserve stem cell populations involved in the repair of mesodermal tissues suggests the potential for using stem cells for the repair and/or regeneration of tissues following their loss as a result of trauma and/or disease. Indeed, use of allogeneic and autologous progenitor cells for the repair and regeneration of chondrogenic and osteogenic tissue defects is currently being investigated. For example, osteochondral allografts *(185,186)* or engraftment of cultured allogeneic chondrocytes *(187–190)* have been pursued to increase the amount of tissue available for grafting. However, these studies have encountered difficulties, including unexpected morbidity and mortality. The rejection of allogeneic cell grafts (in an environment presumed to be protected from immunologic attack), low degree of tissue union, and increased risk of disease transmission *(82,191–193)* have restricted these techniques to the treatment of individuals with large chondral or osteochondral defects *(193,194)*.

In contrast, other studies have shown that grafts of autologous perichondrium *(195,196)* or periosteum *(197–199)* can be used to repair damaged sites. These techniques depend on the presence of chondrogenic progenitor cells in the perichondrium and periosteum *(42,200)*. Because these procedures initially resulted in the formation of a material resembling hyaline cartilage, it was suggested that the chondrogenic progenitor cells underwent metaplasia to form a chondroid tissue. These procedures are limited by the lack of available tissue for grafting, as well as poor graft integration and the strong possibility that the grafted tissues will eventually undergo calcification *(201)*.

The use of differentiated autologous chondrocytes *(202–205)* or autologous osteochondral progenitor cells *(82,206)*, with subsequent expansion ex vivo prior to engraftment into the site of a chondrogenic defect, has been examined in both animals and humans with mixed results. No significant differences between experimental and controls were found in dogs *(207)*. However, successful regeneration was reported in both rabbits and humans *(206)*. Use of mature chondrocytes is particularly advantageous in treating young, healthy, active patients with clinically significant injuries (>2–3 cm^2). Unfortunately, this age group represents only a small proportion of the general population with clinically significant injuries. In addition, there are several disadvantages to using differentiated chondrocytes and chon-

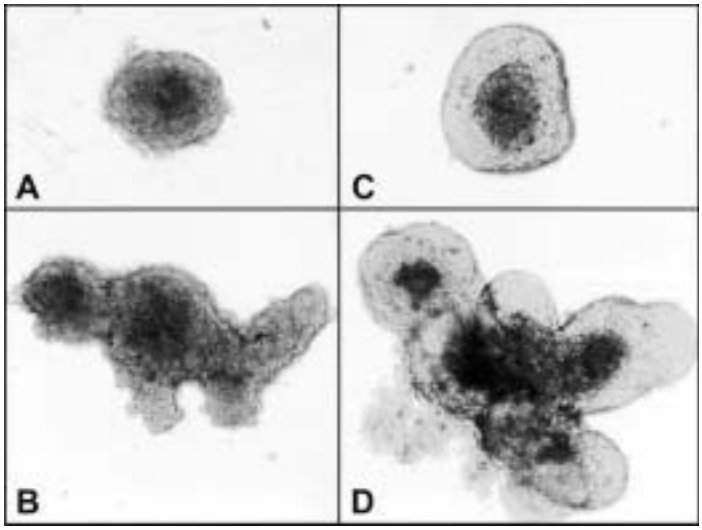

Fig. 22. 3D islet-like structures (**A**, **B**) induced from an adult rat pluripotent epiblastic-like stem cell clone (PPELSC) clone and native rat pancreatic islets (**C**, **D**) *(49)*. Cultures were photographed with phase contrast microscopy, original magnifications ×100. **(A**, **B)** 3D islet-like structures (3D-ILS) were induced from the PPELSC clone by sequential directed lineage induction (i.e., PPELSCs to EndoGLLSCs, EndoGLLSCs to PanPCs, and PanPCs to 3D-ILS) *(49)*. For an abbreviated induction protocol, see legend to Fig. 21. The induced transition from PPELSCs to EndoGLLSCs to PanPCs to 3D-ILS was monitored by changes in phenotypic lineage expression markers (*see* Table 5). Cultures were photographed with phase contrast microscopy, original magnifications ×100. **(A)** Induced single 3D islet-like structure. **(B)** Induced group of 3D islet-like structures. **(C**, **D)** Pancreatic islets from 9- to 10-wk-old male Wistar Furth rats (approx 220 g) were isolated as described *(49)*. Cultures were incubated for 24 h and photographed with phase contrast microscopy, original magnifications ×100. **(C)** Native Wistar-Furth pancreatic islet. **(D)** Native Wistar-Furth islet grouping. (Reproduced with permission from Young, H. E., Duplaa, C., Yost, M. J., Henson, N. L., Floyd, J. A., Detmer, K., et al. [2004] Clonogenic analysis reveals reserve stem cells in postnatal mammals: II. Pluripotent epiblastic-like stem cells. *Anat. Rec.* **276A**, in press. Copyright 2004, Wiley-Liss.)

drogenic progenitor cells. These disadvantages include limitation in the amount of autologous tissue that can be harvested for cell isolation and the limited capability for expansion ex vivo because these cells undergo programmed senescence and cell death as they approach Hayflick's limit (50–70 population doublings before senescence and death). Moreover, damage to the parts of the joint used for tissue harvest could have a negative impact on joint function *(82,201,208)*.

The potential for using reserve stem cells isolated from nonadjacent connective tissues to repair full-thickness cartilage defects within an articulating joint was examined in a series of studies by Lucas and colleagues *(53,209)*. Previous studies had demonstrated the potential of mesodermal GLL stem cells derived from connective tissues to form a number of different mesodermal tissues, including cartilage and bone *(41,43,56)*. Lucas et al. allowed local environmental cues (i.e., endogenous bioactive fac-

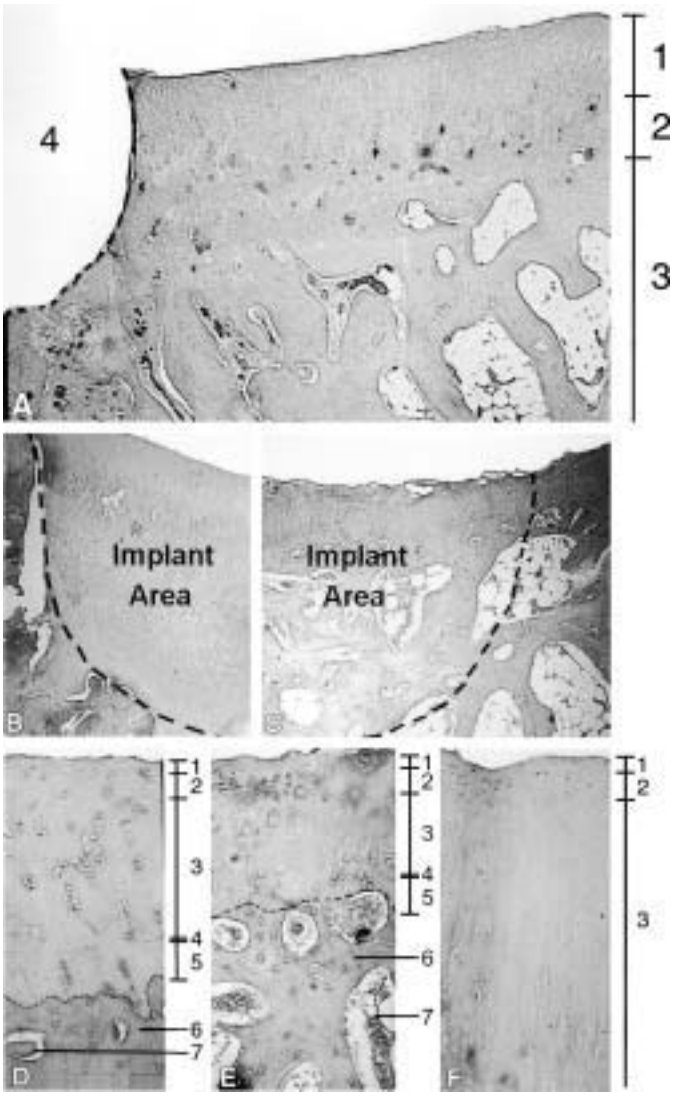

tors specific for chondrogenic and/or osteogenic tissues) to direct the differentiation of these stem cells after their placement *in situ*. Syngeneic mesodermal GLL stem cells were isolated from the connective tissues of adult rabbit skeletal muscle (including the epimysium, perimysium, and endomysium) *(38,39,53,56)*, expanded ex vivo, incorporated into a polyglycolic acid (PGA) delivery vehicle, and placed into a full-thickness cartilage defect in syngeneic rabbits. The defect was created by drilling a hole through the articular cartilage, the underlying subchondral bone, the trabecular bone, and into the marrow cavity (Fig. 23A). After 12 wk, control animals implanted with the PGA delivery vehicle alone exhibited only fibrous tissue in the

Fig. 23. **(A–F)** Use of skeletal muscle-derived mesodermal GLL stem cells to repair a full-thickness cartilage defect within the articulating joint of a rabbit knee. **(A)** Twenty-four hours after full-thickness cartilage defect created in articulating surface of knee joint. Areas: 1, articular surface; 2, subchondral bone; 3, trabecular bone with marrow-filled spaces; and 4, defect area. The defect area was created by drilling a hole through the articular cartilage, the underlying subchondral bone, and into the trabecular bone containing marrow spaces. **(B)** Twelve weeks after implantation of polyglycolic acid (PGA) delivery vehicle without cells (control). Note fibrous tissue–filling implant area and forming border along implant area. Histology of fibrous tissue does not match surrounding articular cartilage, subchondral bone, or trabecular bone with marrow-filled spaces. **(C)** Twelve weeks after implantation of PGA delivery vehicle containing connective tissue-derived syngeneic mesodermal GLL stem cells. Note regeneration of articular cartilage-like tissue covering joint surface of implant area, the regeneration of underlying subchondral bone, and the regeneration of trabecular bone with marrow-filled spaces in the lower portions of the implant area adjacent to uninjured trabecular bone. Note complete annealing of regenerated articular cartilage, subchondral bone, and trabecular bone with adjacent noninjured tissues. **(D)** Higher magnification of control region of articular cartilage overlying subchondral bone and trabecular bone with marrow-filled spaces. Note five zones of articular cartilage: (1) tangential zone, chondrocytes within lacunae between type II collagen bundles lying parallel to surface; (2) transitional zone, chondrocytes within lacunae between interwoven type II collagen bundles lying at 45-degree angles to the surface; (3) radial zone, chondrocytes in lacunae stacked in columns between type II collagen bundles lying perpendicular to surface; (4) tide water mark, acellular zone containing interlaced-interwoven type II collagen bundles and sulfated proteoglycans; and (5) zone of calcified cartilage, chondrocytes in lacunae stacked in columns between bundles of type II collagen. Carbohydrate histochemistry demonstrated chondroitin sulfate proteoglycans, keratan sulfate proteoglycans, and chondroitin sulfate/keratan sulfate proteoglycans within the extracellular matrix. The histology and histochemistry are consistent with articular cartilage. The underlying subchondral bone layer (6) shows osteocytes within lacunae between concentric lamellae surrounding marrow-filled spaces (7). Histochemistry shows type I collagen fibers and chondroitin sulfate proteoglycans within the extracellular matrices, which is consistent with subchondral compact bone. **(E)** Higher magnification of site of injury after treatment with mesodermal GLL stem cells in PGA delivery vehicle 12 wk after transplantation. Joint surface layer, composed of all five layers (1–5), although layers (3), (4), and (5) are not as thick as in control articular cartilage. Note the residual mesodermal stem cells within the transitional layer (2). Type II collagen bundles, chondroitin sulfate proteoglycans, keratan sulfate proteoglycans, and chondroitin sulfate/keratan sulfate proteoglycans within the surface layer consistent with articular cartilage. Underlying bony tissue (6) with marrow-filled spaces (7). Cells in lacunae within concentric lamellae surrounding marrow-filled spaces. Histochemistry revealed type I collagen bundles with chondroitin sulfate proteoglycans. Morphology and histochemistry consistent with subchondral compact bone. **(F)** Higher magnification of site of injury after treatment with PGA delivery vehicle only 12 wk after transplantation. Morphology shows tangential (1) and transitional (2) zones of same approximate size as control, whereas radial zone (3) is thicker than control. Histochemistry shows cells within lacunae surrounded by type I collagen bundles and chondroitin sulfate proteoglycans. Morphology and histochemistry are suggestive of an expanded articular cartilage structural framework filled with fibrocartilage. (Reproduced with permission from Young, H. E. [2000] Stem cells and tissue engineering. In: *Gene Therapy in Orthopaedic and Sports Medicine* (Huard, J. and Fu, F. H., eds., Springer-Verlag, New York, NY. Copyright 2000, Springer-Verlag.)

site of the defect (Fig. 23B). After 12 wk, experimental animals implanted with stem cells in the PGA vehicle exhibited the formation of cartilage and bone resembling that of the normal adjacent tissues (Fig. 23C). Stem cell incorporation was assessed by the surface appearance of the regenerated tissue, in combination with the histological appearance of longitudinal sections of the tissue. In addition, the collagen and glycosaminoglycan contents of the tissue were assessed by histochemistry. Good integration of the implant with the adjacent articular cartilage was observed (Fig. 23C), with restoration of the underlying osseous elements complete with trabecular bone and hematopoietic tissue (Fig. 23C,D). The regenerating surface layer displayed all five layers normally found in articular cartilage (transitional zone, tangential zone, radial zone, tidewater mark, and calcified cartilage) (cf. Fig. 23D,E). However, the inner two zones (tidewater mark and calcified cartilage) were much thinner than those observed in normal, fully formed adult articular cartilage (cf. Fig. 23D,E). The regenerating articular cartilage contained islands of apparent residual mesodermal stem cells between the tangential zone and radial zone (Fig. 23D). In some areas, there was no histologically apparent subchondral bone beneath the regenerating articular cartilage. In these areas, trabecular bone with marrow-filled spaces was found directly adjacent to calcified articular cartilage (cf. Fig. 23D,E). In other areas, subchondral bone was present (Fig. 23C). Control implant animals displayed a fibrocartilaginous tissue within the area of the defect (cf. Fig. 23E–F).

There are at least two possible explanations for the results. First, the implanted syngeneic stem cells, directed by local environmental cues, differentiated to form articular cartilage and underlying bone. A second possibility is that the implanted stem cells released a chemotactic agent that caused a directed ingrowth of stem cells from adjacent tissues. These stem cells subsequently affected the repair process that resulted in regenerating the surface articular cartilage and underlying bone.

Lucas et al. attempted to determine whether the regenerated tissue arose from implanted syngeneic stem cells or host stem cells. They killed syngeneic stem cells by freezing and thawing them prior to their incorporation into a PGA delivery vehicle. Killing the stem cells led to the development of fibrous tissue, a result comparable to that seen in the PGA controls (Fig. 23F). In another series of experiments, syngeneic smooth muscle cells were incorporated into the PGA delivery vehicle prior to implantation. Fibrous tissue was found in the implantation site in these experiments, a result comparable to that seen in the PGA controls (Fig. 23F). The donor stem cells used in the experiments of Lucas et al. were not manipulated experimentally by either biochemical or molecular techniques prior to implantation. Rather, naive stem cells responded to local environmental cues (i.e., endogenous bioactive factors) to effect regeneration. These studies suggest that viable tissue-uncommitted stem cells are required to produce the regenerative response seen here. Further studies are needed to ascertain the interplay between exogenous reserve stem cells and endogenous bioactive factors in the repair process.

Skeletal Muscle Repair

Considerable attention has focused on the isolation and characterization of endogenous bioactive factors and their importance in influencing aspects of tissue development, maturation, aging, replacement, and repair. In this regard, demineralized bone matrix has been shown to contain a number of such factors that influence proliferation, chemotaxis, angiogenesis, chondrogenesis, and osteogenesis *(90–93)*. Of particular interest has been the family of BMP in the TGF-β superfamily that induce mesodermal stem cells to differentiate into cartilage and bone *(94–96)*. As of 1990, there were no reports of efforts to determine if bone was a repository for factors that could induce mesodermal stem cells to differentiate into phenotypes other than cartilage and bone. Therefore, we examined protein extracts from demineral-

ized bone with our mixed mesodermal GLL stem cell–progenitor cell culture system *(28,29,43)*. We also implanted the protein extracts *in situ* within adult wound repair models to ascertain if additional differentiative-inductive activities were present.

Water-soluble proteins were prepared from an extract of demineralized bovine cortical bone following published protocols *(97,210,211)* (Fig. 3A). This material was then analyzed by sodium dodecyl sulfate (SDS) polyacrylamide gel electrophoresis *(212,213)*. The original extract was a crude mixture of proteins that contained at least 100 bands (Fig. 3B). Further chromatographic separation resulted in retention of both Sk-MMP and SIF activities in the fraction > 50 kDa (Fig. 3B,C; Tables 3 and 4). We next examined the effects of Sk-MMP and SIF activities on induced phenotypic expression in our mixed mesodermal GLL stem cell–progenitor cell culture system (Fig. 24). Before treatment, all cultures contained an even mixture of a stellate mesodermal GLL stem cell clone, a bipolar myoblast clone, and a spindle fibroblast clone (Fig. 24A). Both control medium (CM) and experimental medium (EM) contained FMP activity. EM-1 contained Sk-MMP, and EM-2 contained Sk-MMP and SIF. CM-1 and CM-2 contained bovine serum albumin (BSA) to control for the bovine-derived proteins. A 6-d culture with CM-1 elicited a shift of morphology toward predominantly spindle fibroblasts (Fig. 24B), and a 6-d culture of EM-1 elicited a shift in morphology toward predominantly fused bipolar cells forming multinucleated structures (Fig. 24C). A 12-d incubation in CM-2 elicited approx 98% mononucleated spindle fibroblasts (Fig. 24D), and a 12-d incubation with EM-2 elicited approx 95% of the nuclei residing within multinucleated, spontaneously contracting structures, indicative of a myogenic phenotype (Fig. 24E). The results suggest that SIF inhibited FMP induction of the cells, thus allowing Sk-MMP to induce myogenic-expressing cells within the culture.

Previous studies *(214–219)* demonstrated that insulin, IGF-1, and IGF-2 were potent stimulators of skeletal muscle cell growth and differentiation in cultured myogenic lineage-committed stem cells. Because these factors have been previously isolated from bone *(91,98)*, insulin, IGF-1, IGF-2, and isolated Sk-MMP were examined to compare their efficacy for inducing a myogenic response in our mixed mesodermal GLL stem cell–progenitor cell culture system *(28,29,43)*. Sk-MMP at 200 ng/mL elicited the highest induced myosin content at 60.2 ng myosin/μg deoxyribonucleic acid (DNA) (Fig. 25). Insulin and purified recombinant IGF-1 and IGF-2 expressed considerably less myosin-inductive activity (4.6, 9.6, and 12.8 ng myosin/μg DNA, respectively) (Fig. 25) at their maximal myogenic-inductive concentrations of 2000 ng/mL (insulin) and 200 ng/mL (IGF-1 and IGF-2). Combinations of insulin, IGF-1, and/or IGF-2 were then examined to determine if synergism between two or more of these growth factors would mimic the myogenic-inducing activity of MMP *(28,29)*. The results revealed levels of myogenic-inducing activity for insulin/IGF-1, insulin/IGF-2, IGF-1/IGF-2, and insulin/IGF-1/IGF-2 that were lower than their individual maximal myogenic-inductive values (data not shown). These results suggest that Sk-MMP activity within the preparation of water-soluble proteins and independent of, or synergistic with, insulin, IGF-1, and IGF-2 is responsible for the increased level of induced myogenic response in the cultured mesodermal stem cells.

Previous studies *(220–223)* have shown that although mammalian skeletal muscle will undergo a repair process after trauma, restoration of physiological function is compromised because of the increased proliferation of the surrounding connective tissues, eventually forming a nonfunctional fibrous scar. One method proposed to increase skeletal muscle function was to sever the neurovascular connections of homologous or autologous grafted muscles. The reported maximal values for restoration of function were greater than operated controls but significantly less than nonoperated controls *(224–226)*. We were intrigued with the possibility that selective inhibitory factors such as SIF could prevent the differentiation of

Fig. 24. **(A–E)** The myogenic-inductive potential of skeletal muscle morphogenetic protein (Sk-MMP) and fibrogenic-inhibitory potential of scar inhibitory factor (SIF) in the presence of fibroblast morphogenetic protein (FMP). **(A)** A mixed culture containing equal quantities of three clonal cell populations—that is, a mesodermal GLL stem cell clone (St), a unipotent myoblast progenitor cell clone (Bp), and a unipotent fibroblast progenitor cell clone (Sp) *(41)* were used. Cells were plated and expanded in medium containing 'PDGF-like (proliferative) and ADF-like (inhibitory) activities *(28,29)*. Cultures were grown for 48 h and photographed with phase contrast microscopy, original magnification ×200. **(B)** After the initial 48 h, experimental cultures were switched to basal medium containing Sk-MMP, SIF, and FMP *(28,43)*. Cultures were incubated for an additional 6 d and photographed with phase contrast microscopy. Note the large branched multinucleated structure (MT) surrounded by a majority of stellate and bipolar cells. Original magnification ×200. **(C)** After the initial 48 h, control cultures were switched to basal medium containing BSA and FMP *(28,43)*. The BSA was added to the medium to control for the bovine-derived proteins Sk-MMP and SIF. Cultures were incubated for an additional 6 d and photographed with phase contrast microscopy. Note a majority of spindle-shaped cells (Sp), a few stellate cells (St), and an absence of bipolar cells. Original magnification ×200. **(D)** Experimental cultures from **B** were incubated for an additional 6 d with Sk-MMP, SIF, and FMP. Cultures were halted and processed for staining with toluidine blue. The nuclei in ten ×40 fields were counted. Approximately 95% of the nuclei resided in multinucleated structures (MT). Parallel experimental cultures generated similar structures and demonstrated positive staining for sarcomeric myosin, skeletal muscle fast myosin, myosin heavy chain, and myosin fast chain, all indicative of a multinucleated skeletal muscle phenotype. **(E)** Control cultures from **C** were incubated an additional 6 d with BSA and FMP. Cultures were halted and processed for staining with toluidine blue. The nuclei in ten ×40 fields were counted. Approximately 98% of the nuclei resided in mononucleated spindle-shaped cells (Sp).

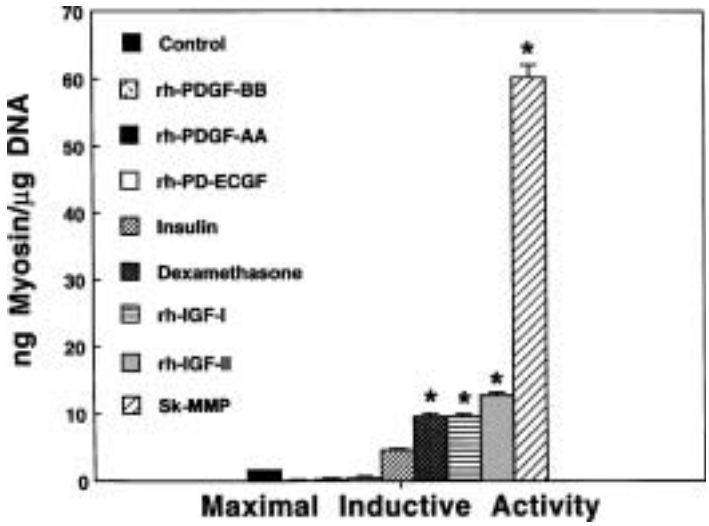

Fig. 25. Ability of various bioactive factors to induce sarcomeric myosin expression in a clone of mesodermal GLL stem cells. A mesodermal GLL stem cell clone *(41)* was used. Cells were plated in medium containing PDGF-like (proliferative) and ADF-like (inhibitory) activities *(28,29)*. Cultures were grown for 24 h and then switched to basal medium containing 0.00 ng/mL control, 100 ng/mL rh-PDGF-BB, 200 ng/mL rh-PDGF-AA, 5 ng/mL rh-PD-ECGF, 2 µg/mL insulin, 10^{-8} *M* dexamethasone, 200 ng/mL IGF-1, 200 ng/mL IGF-2, and 200 ng/mL Sk-MMP. Cultures were incubated for an additional 5 d, halted, and processed for quantitative ELICA using the MF-20 antibody to quantify sarcomeric myosin per microgram DNA *(40,43)*. Data points represent means ± SD, n = 18 for for each bioactive factor, n = 144 for control. Asterisk (*) denotes statistically significant differences from control. $p < 0.05$.

reserve stem cells into fibroblasts, whereas factors such as Sk-MMP could induce the reserve stem cells to form skeletal muscle.

This combined pharmacological approach could potentially minimize scar tissue formation while stimulating skeletal muscle regeneration, thus resulting in a much stronger muscle than trauma-induced regeneration.

Therefore, we next examined the ability of SIF to inhibit fibrogenesis and Sk-MMP to induce a myogenic response within an adult in vivo mammalian skeletal muscle repair model. Sk-MMP with and without SIF was incorporated into either a collagen-based controlled-release delivery vehicle (CDV) or a polyanhydride-based controlled-release delivery vehicle (PDV) *(99)* and implanted into the posterior thigh musculature of adult mice. Harvested implants were processed for light microscopy and assayed morphologically *(35,36,72)*.

Control implants, containing either no additional material or an equivalent amount of BSA, demonstrated the appearance of small regenerating myotubes at the interface between the scar and transected tissues (Fig. 26A), whereas the remaining operational field area consisted of a dense interwoven connective tissue scar (Fig. 26B). In contrast, experimental implants revealed the presence of small regenerating myoblasts (Fig. 26C) and linear multinucleated myotubes embedded within the confines of a connective tissue scar (Fig. 26D).

The results from these in vivo studies suggested that although Sk-MMP was acting on

the reserve stem cells, additional factors were active as well, inducing a fibrogenic response in the majority of these reserve stem cells. This necessitated a potential regimen to decrease or inhibit abnormal fibrogenesis leading to scar tissue formation while allowing induced myogenesis to occur. In the next series of experiments, we included SIF with Sk-MMP in both the collagen-(CDV + Sk-MMP + SIF)- and polyanhydride-(PDV + Sk-MMP + SIF)-based delivery vehicles. The addition of SIF to Sk-MMP induced intact regenerating muscle fascicles in both delivery vehicle implantations. Myofibers with centrally located nuclei located within the regenerating muscle fascicles were surrounded by a thin layer of endomysial-like connective tissue; each fascicle was surrounded by a perimysial-like connective tissue covering, and the collection of muscle fascicles were surrounded by a thin epimysial-like sheet of connective tissue (Fig. 26E,F). In the PDV + Sk-MMP + SIF implantation (Fig. 26F), a neurovascular triad (nerve, artery, and vein) was also embedded within the perimysial connective tissue compartment of the regenerating muscle. The presence of the neurovascular triad suggests the potential for restoration of physiological function.

Relative measurements were performed to compare myofiber size between BSA-treated control implants and Sk-MMP/SIF-treated experimental implants. As shown (Fig. 27), myofiber size was considerably smaller in the Sk-MMP/SIF-treated animals than in the BSA-treated animals. These results suggest that a greater number of myofibers were undergoing a regenerative process in the Sk-MMP/SIF-treated experimentals than in the BSA-treated controls.

These in vitro and in vivo observations suggest that SIF inhibits scar tissue formation, whereas Sk-MMP induces the differentiation of reserve stem cells to commit to a myogenic phenotype. These observations also encourage further experiments aimed at examining additional factors that may induce or inhibit stem cell differentiation.

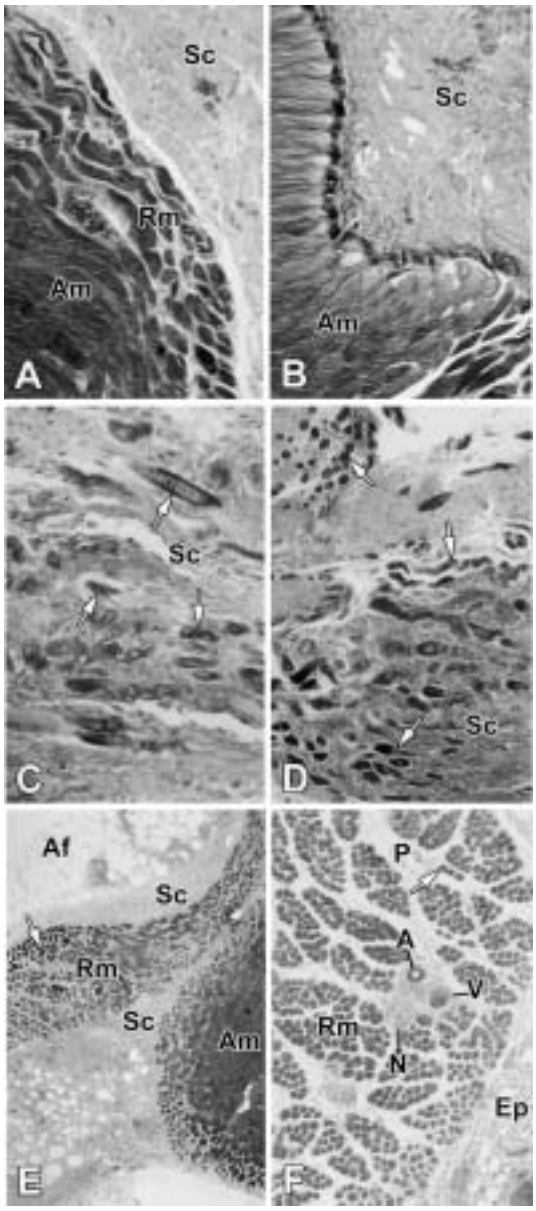

Therapy for Myocardial Repair

Death and disability from cardiac dysfunction cost the United States nearly 750,000 lives per year. The annual cost of ischemic heart disease is approx $100 billion *(227)*. In most cases

Fig. 26. Implantation of novel inductive compounds to induce skeletal muscle restoration in the muscle gap model in the adult mouse. Adult male mice were anesthetized, shaved along their dorsal surface, and a small skin incision made on their lower extremities. The hamstring musculature was dissected free and incised to create a muscle flap. A 1-mm^3 piece of skeletal muscle was removed from the hamstring musculature, deep to the muscle flap, creating a muscle pouch. This was performed bilaterally. The removed piece of skeletal muscle was replaced with the following: (1) either nothing (operation control) or delivery vehicle only (DV control) on one side and (2) delivery vehicle incorporated with either Sk-MMP (DV + Sk-MMP experimental) or Sk-MMP and SIF (DV + Sk-MMP + SIF experimental) on the contralateral side. The particular bioerodible, biocompatible delivery vehicles used were composed of either type I collagen or polycarboyxphenoxypropane (PCPP). After placement of the implant material, the muscle flap was sutured shut to maintain the implant material *in situ*, and the skin was closed with staples. Mice were allowed to recover in a warmed heating area and then fed and watered ad libitum until termination of experiments. At termination, mice were euthanized, shaved, the skin incised, and the lower extremity removed by disarticulation at the hip. The hindlimbs were skinned, washed with DPBS, and fixed with either 10% formalin containing 10% cetylpyridinium chloride for retention of glycosylated compounds for glycoconjugate histochemistry *(36)* or Zenker's formol solution for collagen histochemistry *(74)*. Am, adult muscle myofibers; Rm, regenerating muscle myofibers; Sc, scar tissue; arrow, regenerating myofibers; Af, adult fat; Rf, regenerating fat; P, perimysium; Ep, epimysium. Original magnifications, ×100 (**A–D**, **F**) and ×50 (**E**). **(A)** Collagen-DV only. Transected adult musculature with relatively large-diameter adult myofibers (lower left), connective scar composed of type I collagen, and regenerating myofibers interposed between adult muscle and connective tissue scar. Absence of regenerating myofibers within scar tissue. **(B)** PCPP-DV only. Transected adult musculature appears adjacent to connective tissue scar. However, note the absence of myofibers interposed between the two tissues and absence of myofibers within scar tissue. **(C)** Collagen-DV + Sk-MMP. Regenerating myotubes within connective tissue scar at some distance from transected adult musculature. **(D)** PCPP-DV + Sk-MMP. Note regenerating myotubes within connective tissue scar at some distance from transected adult musculature. **(E)** Collagen-DV + Sk-MMP + SIF. Note scar tissue intervening between adult fat and regenerating muscle fascicle and between regenerating muscle fascicle, regenerating fat, and adult muscle. **(F)** PCPP-DV + Sk-MMP + SIF. Portion of regenerating muscle displaying normal skeletal muscle histoarchitecture (i.e., regenerating myofibers surrounded by endomysium, fascicles surrounded by perimysium, and entire muscle surrounded by epimysium). Note the presence of an intact neurovascular triad consisting of nerve, artery, and vein within regenerating muscle perimysium. The restoration of skeletal muscle histoarchitecture and the presence of a neurovascular triad suggest the potential for restoration of the physiological function of the muscle.

of myocardial infarction, an area of the heart muscle becomes ischemic and proceeds toward dysfunctional scar tissue. Technology leading to repair of damaged myocardium *in situ* would enable the medical community to change the current treatment modality of medical management to one of regeneration *(228)*.

Tremendous advances in stem cell technology indicate that it might be possible to effect repair of damaged myocardium via injection of autologous cells. Numerous cell sources have been tried in the effort to repair injured myocardium, including skeletal myoblasts *(229,230)*, fetal and neonatal cardiomyocytes *(231,232)*, and embryonic stem cells *(233)*. The current strategy is to inject live naive pluripotent stem cells into and around the area of infarction. It is anticipated that the microenvi-

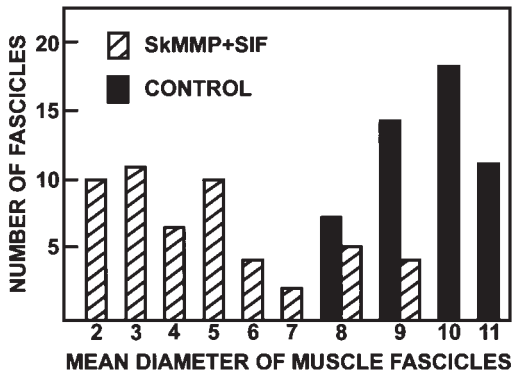

Fig. 27. Histogram of mean diameter of muscle fascicles in control implants vs implants containing Sk-MMP and SIF. Controls consisted of operational controls and delivery vehicle controls (DV-controls) (*see* Fig. 26). Experimentals consisted of implants of type I collagen-delivery vehicle containing Sk-MMP and SIF (collagen-DV + Sk-MMP + SIF) and polycarboxyphenoxypropane-delivery vehicle containing Sk-MMP and SIF (PCPP-DV + Sk-MMP + SIF) (*see* Fig. 26). Microscopic fields were photographed per implant, printed at the same magnification, and measured. Results demonstrate that muscle fascicles (solid) from control implants are of larger overall mean diameter than muscle fascicles (diagonals) from Sk-MMP and SIF implants.

ronment of the healing myocardium will direct the naive pluripotent stem cells to integrate with the existing tissue and to differentiate to form the appropriate phenotype. Studies have shown that injection of cardiomyocytes leads to improvements in systolic performance, compliance, peri-infarct perfusion, and global ventricular function *(234–236)*. Injected cardiomyocytes have been shown to form gap junctions with the existing tissue *(237)*. These results indicate that this is a promising area for further investigation. The focus of this study was to investigate the possibility of injecting adult-derived pluripotent epiblastic-like stem cells to repair the damage produced by myocardial infarction.

A Lac-Z-transfected adult rat pluripotent epiblastic-like stem cell clone was injected into normal and myocardial infarcted hearts of 200- to 300-g rats. Myocardial infarction was induced by cryoinjury along the course of the left coronary artery. Injection of the stem cells occurred directly into the left ventricle through a subxiphoid window or systemically via tail vein injection *(49, 238)*. There were five different groups of rats: (1) sham-operated heart control (n = 3), (2) ischemic heart control (n = 3), (3) pluripotent stem cell–implanted normal heart (n = 12), (4) pluripotent stem cell–implanted ischemic heart (n = 7), and (5) pluripotent cells injected in the tail vein of a rat that underwent myocardial infarction (n = 7). Normal hearts implanted with pluripotent stem cells were harvested from 1 d to 4 wk later. Ischemic hearts implanted with pluripotent stem cells were injected from immediately to 1 wk postinjury. These hearts were harvested from 1 d to 4 wk later and processed for immunocytochemistry and confocal microscopy (*239*).

Stem cells readily attach and grow on the gelatin-coated tissue culture plastic. The anti-β-galactosidase antibody reacted with the Lac-Z protein both within the nucleus and, to a lesser extent, within the cell cytoplasm (Fig. 28A). This demonstrates that all of the cells that were injected were positive for β-galactosidase and could be readily detected following injection into the animals. One week after injection of the cells into the normal heart, β-galactosidase-positive cells could be located in the myocardium (Fig. 28B). Cryogenic infarction caused the cardiac tissue to become whitish gray in color in contrast to the normal deep red of the heart tissue under gross inspection. Tissue obtained from animals into which pluripotent stem cells had been injected into ischemic myocardium demonstrated groups of living cells positive for β-galactosidase incorporated into the myocardium (Fig. 28C). Many of the β-galactosidase-positive cells may be seen in cross-section in Fig. 28C. These cells are smaller in diameter than the endogenous myocytes but similar in appearance. Inspection of normal myocardium immediately adjacent

to infarcted tissue demonstrated the ability of the cells to home in on the damaged myocardium after tail vein injection (Fig. 28D). A thorough inspection of the infarcted area revealed few, if any, β-galactosidase-positive cells in the surrounding noninjured tissues (data not shown).

Our study reports that pluripotent stem cells derived from adults survived in normal and infarcted hearts following direct injection. Following injection of the tail vein, the cells were able to home in on the damaged heart after ischemic injury. The cell line used in this study was derived from adults and therefore different from other cell lines reported to date in the literature. In previous reports, fetal stem cells and autologous myoblasts have been shown to engraft in the heart, but these cell lines have limited therapeutic application in humans. This work raises the possibility that adult pluripotent stem cells could be isolated from a patient, expanded in culture, and reinfused back into the patient. Such autologous transplantation would have the potential for wide application, as the cells are readily available. Moreover, this approach would obviate the need for immunosuppression with its attendant dangers.

Gene Therapy

We have proposed the use of pluripotent stem cells as HLA-matched delivery vehicles for gene therapy *(45)*. This proposal is predicated on the hypothesis that the insertion of an exogenous gene will not alter the developmental potential of the pluripotent stem cells. As an initial test of this proposal, a pluripotent epiblastic-like stem cell clone was transfected with Lac-Z and then analyzed both in vitro and in vivo for retention of pluripotent capabilities *(49)*.

LacZ expression was evaluated by histochemical and immunochemical procedures *(240)*.

The transfected stem cell clone was examined in our standard insulin/dexamethasone bioassay. Incubation with insulin did not alter the phenotypic expression of the cells compared to untreated controls. This suggested that the stem cells had not converted to progenitor cells as a result of either the transfection procedure itself or incorporation of Lac-Z into its genome. In contrast, dexamethasone incubation induced the expression of morphological phenotypes consistent with >30 cell types from all three germ-layer lineages. Immunochemical and histochemical analyses confirmed these cell lineages (Figs. 4B, 10, 12, 14, 16, 21, 22). In addition, these same morphologies coexpressed the reaction product for β-galactosidase (Fig. 29). These results suggest that gene-transfected pluripotent epiblastic-like stem cells retain pluripotent capabilities without loss of the expression of the transfected gene.

In vivo transplantation studies were performed to examine incorporation of transfected stem cells into various mesodermal tissues in the body with subsequent coexpression of the gene product. As shown, naive pluripotent epiblastic-like stem cells previously transfected with Lac-Z were found incorporated into both bone marrow (Fig. 20) and myocardial infarcted tissues (Fig. 28). These results suggest that transfection of these pluripotent epiblastic-like stem cells did not alter their subsequent differentiation capabilities. These results also suggest the potential use of autologous pluripotent epiblastic-like stem cells as delivery vehicles for gene therapy.

CONCLUSIONS

The development of an individual proceeds from the totipotent zygote. The zygote begins dividing, and the resultant blastomeres differentiate and segregate by lineage commitment into two pluripotent layers—the trophoblast, which eventually forms the extra-embryonic membranes of the placenta, and the inner cell mass, which will eventually form the embryo. The inner cell mass continues its development by segregating into the hypoblast and epiblast. These layers further segregate into the pluripo-

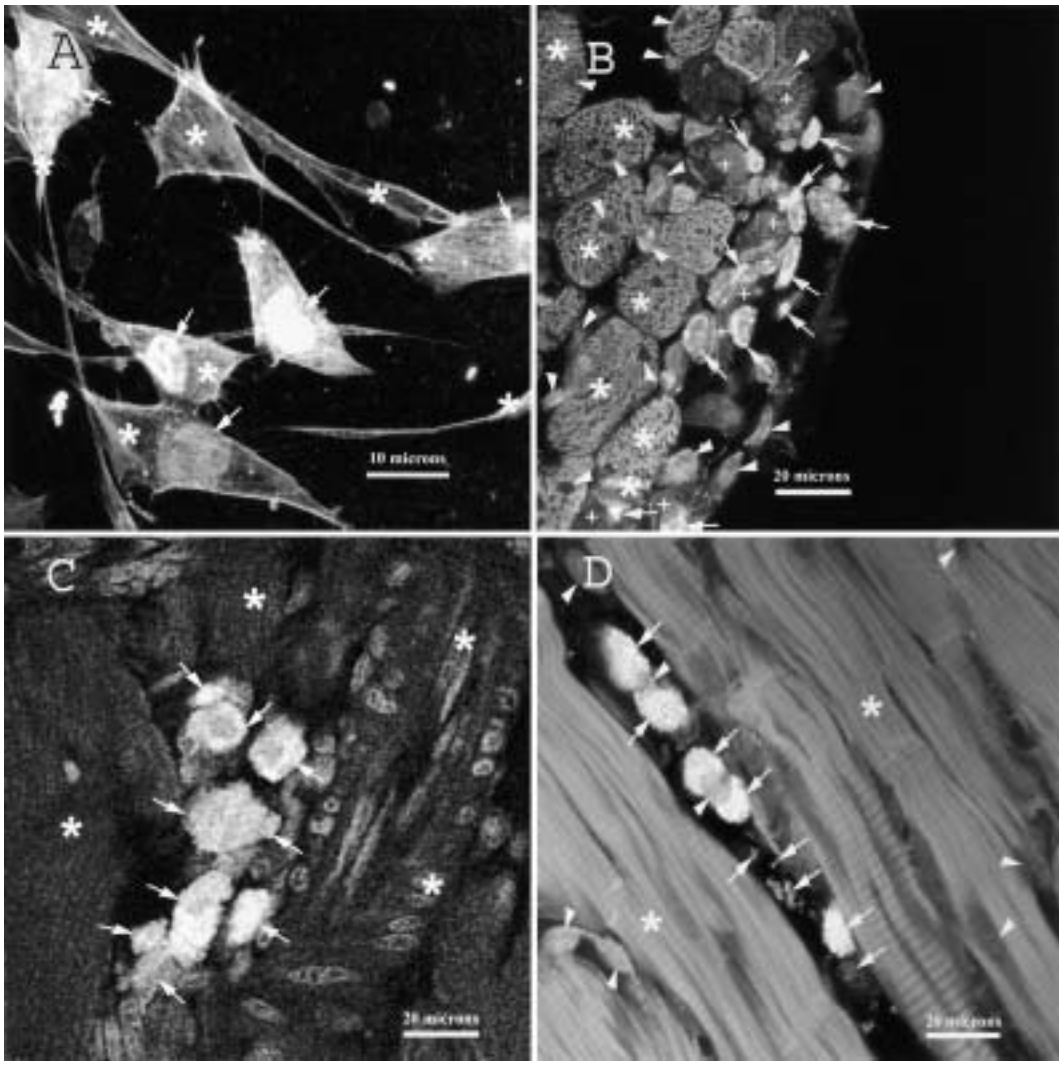

Fig. 28. Laser confocal microscopy of Lac-Z-transfected pluripotent epiblastic-like stem cell (PPELSC) clone. **(A)** Laser-scanning confocal micrograph of PPELSC in culture on gelatin-coated tissue culture plastic. The f-actin in the cytoskeleton has been stained using rhodamine phalloidin (arrowhead). The β-galactosidase has been immunohistochemically labeled green (arrow) using an fluoresceine isothiocyanate (FITC) fluorophore. **(B)** β-galactosidase-positive (β-gal +) cells localized in normal heart tissue 1 wk after direct injection of cells into the left ventricle (arrows). End views of myofibril bundles stained with rhodamine phalloidin can be seen (asterisk, *). Cell nuclei (arrowhead) are stained with topro-3 (a DNA intercalating dye). **(C)** The β-gal + cells localized in ischemic heart tissue 1 wk after direct injection of cells into the left ventricle (arrow). The cells were injected through a subxiphoid window 3 d after cryoinjury. **(D)** The β-gal + cells (arrow) localized in normal heart tissue immediately adjacent to the site of cryoinjury. Cell nuclei are stained with topro-3 (arrowhead). These cells were injected systemically into the tail vein of the rat following injury. (Reproduced with permission from Young, H. E., Duplaa, C., Yost, M. J., Henson, N. L., Floyd, J. A., Detmer, K. [2004] Clonogenic analysis reveals reserve stem cells in postnatal mammals: II. Pluripotent epiblastic-like stem cells. *Anat. Rec.* **276A**, in press. Copyright 2004, Wiley-Liss.)

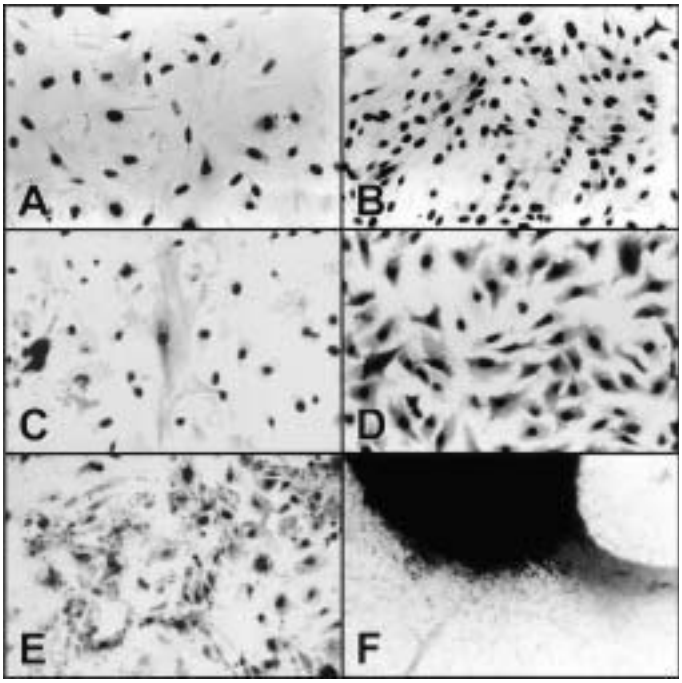

Fig. 29. Induced phenotypic expression in Lac-Z-transfected PPELSCs. A β-galactosidase-transfected adult rat PPELSC clone *(29,49)* was used. Cells were plated in medium containing PDGF-like (proliferative) and ADF-like (inhibitory) activities *(28,29,49)*. **(A)** Cultures were expanded for 2 d and processed for β-galactosidase immunocytochemistry *(49)*, original magnification ×200. **(B)** Cultures were expanded for 4 d and processed for β-galactosidase immunocytochemistry *(49)*, original magnification ×100. **(C)** After expansion for 2 d, the cultures were switched to serum-free medium containing Sm-MMP *(28)*. Cultures were incubated for an additional 3 d and processed for both β-galactosidase and smooth muscle α-actin (IA4) immunocytochemistry *(49)*, original magnification ×100. **(D)** After expansion for 2 d, the cultures were switched to serum-free medium containing Sm-MMP *(28)*. Cultures were incubated for an additional 14 d and processed for both β-galactosidase and smooth muscle α-actin (IA4) immunocytochemistry *(49)*, original magnification ×200. The nuclei in ten ×40 fields were counted. Approximately 90% of the nuclei resided in cells demonstrating intracellular staining for the IA4 antibody. **(E)** After expansion for 2 d, the cultures were switched to serum-free medium containing AMP *(28)*. Cultures were incubated for an additional 14 d, processed for β-galactosidase immunocytochemistry followed by counterstaining in Sudan Black-B to demonstrate intracellular vesicles containing saturated neutral lipids, indicative of adipocytes, original magnification ×100. **(F)** After expansion for 2 d, the cultures were switched to serum-free medium containing BMP-2 and 10^{-7} *M* dexamethasone to induce chondrogenesis *(28)*. Cultures were incubated for an additional 14 d and processed for β-galactosidase immunocytochemistry, followed by counterstaining in Alcian Blue at pH 1.0 to identify cartilage-specific sulfated proteoglycans *(41,42,44,46,47)*. A large nodule costains for nuclear β-gal and pericellular chondroitin sulfate/keratan sulfate glycosaminoglycans, indicative of a cartilage nodule, original magnification ×40.

tent primary germ layers of the ectoderm, mesoderm, and endoderm. Segregation through lineage commitment into multipotent, tripotent, bipotent, and eventually unipotent progenitor cells further defines the differentiation pathways of the cells and their ultimate function.

We propose that although most cells progress through this sequence in forming the intact individual, a few cells leave this pathway to become sequestered as quiescent reserve precursor cells. On the basis of previous and current studies *(9,17,24–47,49–60, 103–105,123,200,241–243)*, Young and Black *(48)* proposed a model of quiescent precursor cells within postnatal animals, including humans. The model encompasses precursor cells from the most primitive pluripotent epiblastic-like stem cell to the most differentiated unipotent progenitor cell. Tissue-committed progenitor cells, lineage-restricted germ-layer stem cells, and lineage-uncommitted pluripotent stem cells are present throughout the postnatal individual as reserve populations of precursor cells. Results from our isolation, cloning, and cell-sorting studies confirm the presence of these precursor cells within adult tissues. Similarly, results from our neuronal, hematopoietic, diabetic, chondrogenic, osteogenic, myogenic, and cardiogenic studies confirm our ability to selectively induce adult pluripotent stem cells to undergo directed lineage induction. Thus, our studies support the hypothesis that the activation of quiescent precursor cells is a potential component of tissue restoration. During tissue replacement, quiescent stem cells also may become activated, proliferate, differentiate, and assist the tissue-committed progenitor cells in forming the missing tissues.

There are potential advantages for using adult reserve stem cells for autologous transplantation. Reserve stem cells can be directly isolated from newborn to geriatric individuals, including patients awaiting treatment. Adult reserve stem cells can be derived from a small biopsy of skeletal muscle or dermis. Reserve stem cells are telomerase positive, indicating that vast quantities of cells can be produced from a few harvested cells. Reserve stem cells can be stored for long periods with minimal loss of cell viability, pluripotentiality and/or function. Adult pluripotent stem cells can be induced to form cells from the three primary germ-layer lineages (i.e., ectoderm, mesoderm, and endoderm). Adult germ-layer lineage stem cells can subsequently form all somatic cell types within their respective germ-layer lineages. These results suggest that reserve stem cells derived from skeletal muscle and/or dermis comprise a potential source for the production of neurons and glia, hematopoietic cells, pancreatic islets, cartilage, bone, skeletal muscle, blood vessels, heart tissue, and other somatic cells of the body. Additional studies are planned or currently under way to determine whether adult reserve stem cell transplants can be used in the treatment of Parkinson's disease, blood transfusions, bone marrow transplants, diabetes, resurfacing articular cartilage, bone repair, muscular dystrophy, ischemia, and myocardial infarctions.

ACKNOWLEDGMENTS

I would like to thank Dr. P. M. Johnston, Emeritus Professor and Chairman, Department of Zoology, University of Arkansas, Fayetteville, AR. Without his three tenets for research (i.e., "don't always believe negative consensus opinion, even if it is in the scientific literature"; "know your model system"; and "tissue never lies"), I would not have progressed as far with the adult stem cell research. I would especially like to thank Paul A. Lucas for the generous exchange of ideas, reagents, and unpublished observations. I would like to thank my collaborators, coauthors, and technical assistants for their insight and work ethic. I would like to thank Cindy Frisbie, Anthony G. Frisbie, Jane Moore-Schwartz, Faye Frazer, John Reichert, and John Knight for photographic assistance. The MyoD1 clone, maintained in the expression vector pVZCII-α3 scribe, and the myogenin cDNA probe, subcloned into Bluescribe pEMSV-α2

M13, were generous gifts from Dr. W. E. Wright. Bovine nasal septum A1D1 proteoglycan and the 5D4 antikeratan sulfate antibody were the kind gifts of Dr. J. H. Kimura, Department of Biochemistry, Rush Presbyterian–St. Luke's Medical Center, Chicago, IL.

We thank I. K. Moutsatsos, Genetics Institute, Inc., Cambridge, MA for the gifts of rhBMP-2 and rhBMP-4. The PD-ECGF, IGF-2, IGF-1, PDGF-AA, and PDGF-BB were generous gifts from G. F. Pierce, Amgen, Thousand Oaks, CA. Sk-MMP, SIF, and ADF were the generous gifts of L. Rifkin, MorphoGen Pharmaceuticals, Inc., New York, NY. The following antibodies were obtained from the Developmental Studies Hybridoma Bank, developed under the auspices of the NICHD and maintained by the University of Iowa, Department of Biological Sciences, Iowa City, IA 52242: MC480, MC631, and MC813-70, developed by D. Solter; FORSE-1, developed by P. Patterson; RAT-401 and Rip, developed by S. Hockfield; RT-97, developed by J. Wood; 8A2, developed by V. Lemmon; SV2, developed by K. M. Buckley; VM-1, developed by V.,B. Morhenn; 151-Ig, developed by A. Hubbard; 40E-C, developed by A. Alvarez-Buylla; F5D, developed by W. E. Wright; MF-20 and ALD-58, developed by D. A. Fischman; A4.74, developed by H. M. Blau; CIIC1, developed by R. Holmdahl and K. Rubin; D1-9, developed by X.-J. Ye and K. Terato; 9/30/8A4 and 12/21/1C6, developed by B. Caterson; 12C5, developed by R. A. Asher; WV1D1 (9C5) and MP111B10$_1$, developed by M. Solursh and A. Frazen; P2B1 and P2H3, developed by E. A. Wayner and G. Vercellotti; P8B1, developed by E. A. Wayner and T. LeBien; HA4c19, developed by A. Hubbard; Hermes-1, developed by E. C. Butcher; and H4C4, H5A5, H5C5, H5C6, and H5A4, developed by J. T. August and J. E. K. Hildreth.

We would like to thank Robert L. Price, PhD, director of Instrumentation Resource Facility at the University of South Carolina School of Medicine, for the use of his facility for the confocal microscopy images.

This research was supported by grants from Rubye Ryle Smith Charitable Trust (HEY), Lucille M. and Henry O. Young Estate Trust (HEY), MedCen Community Health Foundation (HEY, TAS, JH, FPB, T-JL, ACB), MorphoGen Pharmaceuticals, Inc. (HEY, M-FC), Biostar (M-FC), Pasarow Foundation (M-FC), UCLA Morris K. Udall Parkinson's Disease Research Center of Excellence (M-FC), P50NS38367 (M-FC), NIH grants K25-HL67097 and HL072096 (MJY), NASA Cooperative Agreement NCC5-575 (MJY), and the University of South Carolina Research and Productive Scholarship Program (MJY).

REFERENCES

1. Toole, B. P. and Gross, J. (1971) The extracellular matrix of the regenerating newt limb: synthesis and removal of hyaluronate prior to differentiation. *Dev. Biol.* **25,** 57–77.
2. Stocum, D. L. (1998) Regenerative biology and engineering: strategies for tissue restoration. *Wound Rep. Reg.* **6,** 276–290.
3. Tsai, R. Y., Kittappa, R., and McKay, R. G. D. (2002) Plasticity, niches, and the use of stem cells. *Dev. Cell* **2,** 707–712.
4. Donovan, P. J. and Gearhart, J. (2001) The end of the beginning for pluripotent stem cells. *Nature* **414,** 92–97.
5. Forbes, S. J., Vig, P., Poulsom, R., Wright, N. A., and Alison, M. R. (2002) Adult stem cell plasticity: new pathways of tissue regeneration become visible. *Clin. Sci. (Lond.)* **103,** 355–369.
6. Poulsom, R., Alison, M. R., Forbes, S. J., and Wright, N. A. (2002) Adult stem cell plasticity. *J. Pathol.* **197,** 441–456.
7. Eglitis, M. A. and Mezey, E. (1997) Hematopoietic cells differentiate into both microglia and macroglia in the brains of adult mice. *Proc. Natl. Acad. Sci. USA* **94,** 4080–4085.
8. Brazelton, T. R., Rossi, F. M., Keshet, G. I., and Blau, H. M. (2000) From marrow to brain: expression of neuronal phenotypes in adult mice. *Science* **290,** 1775–1779.
9. Woodbury, D., Schwarz, E. J., Prockop, D. J., and Black, I. B. (2000) Adult rat and human bone marrow stromal cells differentiate into neurons. *J. Neurosci. Res.* **61,** 364–370.
10. Petersen, B. E., Bowen, W. C., Patrene, K. D., Mars, W. M., Sullivan, A. K., Murase, N., et al. (1999) Bone marrow as a potential source of hepatic oval cells. *Science* **284,** 1168–1170.

11. Lagasse, E., Connors, H., Al-Dhalimy, M., Reitsma, M., Dohse, M., Osborne, L., et al. (2000) Purified hematopoietic stem cells can differentiate into hepatocytes in vivo. *Nat. Med.* **6,** 1229–1234.
12. Theise, N. D., Badger, S., Serena, R., Henegariu, O., Sell, S., Crawford, J. M., et al. (2000) Derivation of hepatocytes from bone marrow cells in mice after radiation-induced myeloablation. *Hepatology* **31,** 235–240.
13. Ferrari, G., Cusella-De Angelis, G., Coletta, M., Paolucci, E., Stornaiuolo, A., Cossu, G., et al. (1998) Muscle regeneration by bone marrow-derived myogenic progenitors. *Science* **279,** 1528–1530.
14. Gussoni, E., Soneoka, Y., Strickland, C. D., Buzney, E. A., Khan, M. K., Flint, A. F., et al. (1999) Dystrophin expression in the mdx mouse restored by stem cell transplantation. *Nature* **401,** 390–394.
15. Bjornson, C. R., Rietze, R. L., Reynolds, B. A., Magli, M. C., and Vescovi, A. L. (1999) Turning brain into blood: a hematopoietic fate adopted by adult neural stem cells in vivo. *Science* **283,** 534–537.
16. Vescovi, A. L., Galli, R., and Gritti, A. (2001) The neural stem cells and their transdifferentiation capacity. *Biomed. Pharmacother.* **55,** 201–205.
17. Clarke, D. L., Johansson, C. B., Wilbertz J., Veress, B., Nilsson, E., Karlstrom, H., et al. (2000) Generalized potential of adult neural stem cells. *Science* **288,** 1660–1663.
18. Galli, R., Borello, U., Gritti, A., Minasi, M. G., Bjornson, C., Coletta, M., et al. (2000) Skeletal myogenic potential of human and mouse neural stem cells. *Nat. Neurosci.* **3,** 986–991.
19. Tsai, R. Y. and McKay, R. D. (2000) Cell contact regulates fate choice by cortical stem cells. *J. Neurosci.* **20,** 3725–3735.
20. Jackson, K. A., Mi, T., and Goodell, M. A. (1999) Hematopoietic potential of stem cells isolated from murine skeletal muscle. *Proc. Natl. Acad. Sci. USA* **96,** 14482–14486.
21. Bjerknes, M. and Cheng, H. (2002) Multipotential stem cells in adult mouse gastric epithelium. *Am. J. Physiol. Gastrointest. Liver Physiol.* **283,** G767–G777.
22. Grounds, M. D., Garrett, K. L., Lai, M. C., Wright, W. E., and Beilharz, M. W. (1992) Identification of muscle precursor cells in vivo by use of MyoD1 and myogenin probes. *Cell. Tiss. Res.* **267,** 99–104.
23. Beauchamp, J. R., Heslop, L., Yu, D. S. W., Tajbakhsh, S., Kelly, R. G., Wernig, A., et al. (2000) Expression of CD34 and Myf5 defines the majority of quiescent adult skeletal muscle satellite cells. *J. Cell. Biol.* **151,** 1221–1233.
24. Young, H. E. (1977) Epidermal ridge formation during limb regeneration in the adult salamander, *Ambystoma annulatum. Proc. Ark. Acad. Sci.* **31,** 107–109.
25. Young, H. E. (1977) Limb regeneration in the adult salamander, Ambystoma annulatum Cope 1889 (Amphibia: Ambystomatidae). Fayetteville: University of Arkansas Library Press.
26. Young, H. E. (1977) Anomalies during limb regeneration in the adult salamander, *Ambystoma annulatum. Proc. Ark. Acad. Sci.* **31,** 110–111.
27. Young, H. E. (1983) *A Temporal Examination of Glycoconjugates During the Initiation Phase of Limb Regeneration in Adult Ambystoma.* Texas Tech University Library Press, Lubbock, TX.
28. Young, H. E. (2000) Stem cells and tissue engineering. In *Gene Therapy in Orthopaedic and Sports Medicine* (Huard, J., Fu, F. H., eds.). Springer-Verlag, New York, pp. 143–173.
29. Young, H. E. (2004) Existence of reserve quiescent stem cells in adults, from amphibians to humans. *Curr. Top. Microbiol. Immunol.* **280**, 71–109.
30. Young, H. E. and Lucas, P. A. (1998) Pluripotent mesenchymal stem cells and methods of use thereof. US Patent No. 5,827,735.
31. Young, H. E., Bailey, C. F., and Dalley, B. K. (1983) Environmental conditions prerequisite for complete limb regeneration in the post-metamorphic adult land-phase salamander, Ambystoma. *Anat. Rec.* **206,** 289–294.
32. Young, H. E., Bailey, C. F., and Dalley, B. K. (1983) Gross morphological analysis of limb regeneration in postmetamorphic adult Ambystoma. *Anat. Rec.* **206,** 295–306.
33. Young, H. E., Dalley, B. K., and Markwald, R. R. (1983) Identification of hyaluronate within peripheral nervous tissue matrices during limb regeneration. In *Developing and Regenerating Vertebrate Nervous Systems, Neurology and Neurobiology* (Coates, P. W., Markwald, R. R., Kenny, A.D., eds.). Alan R. Liss, New York, vol. 6, pp. 175–183.
34. Young, H. E., Dalley, B. K., and Markwald, R. R. (1983) The interaction of glycosaminoglycans (GAG) and nervous tissue regeneration in adult Ambystoma. *Anat. Rec.* **205,** 202.

35. Young, H. E., Bailey, C. F., Markwald, R. R., and Dalley, B. K. (1985) Histological analysis of limb regeneration in postmetamorphic adult Ambystoma. *Anat. Rec.* **212,** 183–194.
36. Young, H. E., Dalley, B. K., and Markwald, R. R. (1989) Glycoconjugates in normal wound tissue matrices during the initiation phase of limb regeneration in adult Ambystoma. *Anat. Rec.* **223,** 231–241.
37. Young, H. E., Young, V. E., and Caplan, A. I. (1989) Comparison of fixatives for maximal retention of radiolabeled glycoconjugates for autoradiography, including use of sodium sulfate to release unincorporated [35S]sulfate. *J. Histochem. Cytochem.* **37,** 223–228.
38. Young, H. E., Morrison, D. C., Martin, J. D., and Lucas, P. A. (1991) Cryopreservation of embryonic chick myogenic lineage-committed stem cells. *J. Tiss. Cult. Meth.* **13,** 275–284.
39. Young, H. E., Ceballos, E. M., Smith, J. C., Lucas, P. A., and Morrison, D. C. (1992) Isolation of embryonic chick myosatellite and pluripotent mesenchymal stem cells. *J. Tiss. Cult. Meth.* **14,** 85–92.
40. Young, H. E., Sippel, J., Putnam, L. S., Lucas, P. A., and Morrison, D. C. (1992) Enzyme-linked immuno-culture assay. *J. Tiss. Cult. Meth.* **14,** 31–36.
41. Young, H. E., Ceballos, E. M., Smith, J. C., Mancini, M. L., Wright, R. P., Ragan, B. L., et al. (1993) Pluripotent mesenchymal stem cells reside within avian connective tissue matrices. *In Vitro Cell. Dev. Biol. Anim.* **29A,** 723–736.
42. Young, H. E., Mancini, M. L., Wright, R. P., Smith, J. C., Black, A. C., Jr., Reagan, C. R., et al. (1995) Mesenchymal stem cells reside within the connective tissues of many organs. *Dev. Dynam.* **202,** 137–144.
43. Young, H. E., Wright, R. P., Mancini, M. L., Lucas, P. A., Reagan, C. R., and Black, A. C., Jr. (1998) Bioactive factors affect proliferation and phenotypic expression in pluripotent and progenitor mesenchymal stem cells. *Wound Rep. Reg.* **6,** 65–75.
44. Young, H. E., Rogers, J. J., Adkison, L. R., Lucas, P. A., and Black, A. C., Jr. (1998) Muscle morphogenetic protein induces myogenic gene expression in Swiss-3T3 cells. *Wound Rep. Reg.* **6,** 530–541.
45. Young, H. E., Steele, T. A., Bray, R. A., Detmer, K., Blake, L. W., Lucas, P. A., et al. (1999) Human pluripotent and progenitor cells display cell surface cluster differentiation markers CD10, CD13, CD56, and MHC Class-I. *Proc. Soc. Exp. Biol. Med.* **221,** 63–71.
46. Young, H. E., Duplaa, C., Young, T. M., Floyd, J. A., Reeves, M. L., Davis, K. H., et al. (2001) Clonogenic analysis reveals reserve stem cells in postnatal mammals: I. Pluripotent mesenchymal stem cells. *Anat. Rec.* **263,** 350–360.
47. Young, H. E., Steele, T., Bray, R. A., Hudson, J., Floyd, J. A., Hawkins, K. C., et al. (2001) Human reserve pluripotent mesenchymal stem cells are present in the connective tissues of skeletal muscle and dermis derived from fetal, adult, and geriatric donors. *Anat. Rec.* **264,** 51–62.
48. Young, H. E. and Black, A. C., Jr. (2004) Adult stem cells. *Anat. Rec.*, **276A**, 75–102.
49. Young, H. E., Duplaa, C., Yost, M. J., Henson, N. L., Floyd, J. A., Detmer, K., et al. (2004) Clonogenic analysis reveals reserve stem cells in postnatal mammals: II. Pluripotent epiblastic-like stem cells. *Anat. Rec.* **276A**, in press.
50. Lucas, P. A., Calcutt, A. F., Ossi, P., Young, H. E., and Southerland, S. S. (1993) Mesenchymal stem cells from granulation tissue. *J. Cell. Biochem.* **17E,** 122.
51. Lucas, P. A., Young, H. E., and Laurencin, C. T. (1994) Muscle morphogenetic protein and use thereof. US Patent No. 5,328,695.
52. Lucas, P. A., Calcutt, A. F., Ossi, P., Young, H. E., and Southerland, S. S. (1994) Granulation tissue contains cells capable of differentiating into multiple mesenchymal phenotypes. *J. Cell. Biochem.* **18C,** 276.
53. Lucas, P. A., Calcutt, A. F., Southerland, S. S., Wilson, J. A., Harvey, R. L., Warejcka, D. J., et al. (1995) A population of cells resident within embryonic and newborn rat skeletal muscle is capable of differentiating into multiple mesodermal phenotypes. *Wound Rep. Reg.* **3,** 457–468.
54. Lucas, P. A., Warejcka, D. J., Zhang, L. -M., Newman, W. H., and Young, H. E. (1996) Effect of rat mesenchymal stem cells on the development of abdominal adhesions after surgery. *J. Surg. Res.* **62,** 229–232.
55. Lucas, P. A., Warejcka, D. J., Young, H. E., and Lee, B. Y. (1996) Formation of abdominal adhesions is inhibited by antibodies to transforming growth factor-beta1. *J. Surg. Res.* **65,** 135–138.
56. Pate, D. W., Southerland, S. S., Grande, D. A., Young, H. E., and Lucas, P. A. (1993) Isolation and differentiation of mesenchymal stem cells from rabbit muscle. *Surg. Forum* **44,** 587–589.

57. Rogers, J. J., Young, H. E., Adkison, L. R., Lucas, P. A., and Black, A. C., Jr. (1995) Differentiation factors induce expression of muscle, fat, cartilage, and bone in a clone of mouse pluripotent mesenchymal stem cells. *Am. Surg* **61,** 231–236.
58. Dixon, K., Murphy, R. W., Southerland, S. S., Young, H. E., Dalton, M. L., and Lucas, P. A. (1996) Recombinant human bone morphogenetic proteins-2 and 4 (rhBMP-2 and rhBMP-4) induce several mesenchymal phenotypes in culture. *Wound Rep. Reg.* **4,** 374–380.
59. Warejcka, D. J., Harvey, R., Taylor, B. J., Young, H. E., and Lucas, P. A. (1996) A population of cells isolated from rat heart capable of differentiating into several mesodermal phenotypes. *J. Surg. Res.* **62,** 233–242.
60. Romero-Ramos, M., Vourc'h, P., Young, H. E., Lucas, P. A., Wu, Y., Chivatakarn, O., et al. (2002) Neuronal differentiation of stem cells isolated from adult muscle. *J. Neurosci. Res.* **69,** 894–907.
61. Thornton, C. S. (1968) Amphibian limb regeneration. In *Advances in Morphogenesis* (Brachet, J., King, T. J. V., eds.). Academic Press, New York, vol. 7, pp. 205–249.
62. Singer, M. (1978) On the nature of the neurotrophic phenomenon in urodele regeneration. *Am. Zool.* **18,** 829–841.
63. Tank, P. W. and Holder, N. (1981) Pattern regulation in the regenerating limbs of urodele amphibians. *Quart Rev Biol* **56,** 113–142.
64. Brockes, J. P. (1997) Amphibian limb regeneration: rebuilding a complex structure. *Science* **276,** 81–87.
65. Iten, L. E. and Bryant, S. V. (1973) Forelimb regeneration from different levels of amputation in the newt, *Notophthalamus viridescens*: length, rate, stage. *Wilhelm Roux Arch.* **173,** 77–89.
66. Farber, J. (1959) An experimental analysis of regional organization in the regenerating forelimb of the axolotl (*Ambystoma mexicanum*). *Arch. Biol.* **71,** 1–72.
67. Tank, P. W., Carlson, B. M., and Connelly, T. G. (1976) A staging system for forelimb regeneration in the axolotl, *Ambystoma mexicanum. J. Morph.* **150,** 117–128.
68. Stocum, D. L. (1979) Stages of forelimb regeneration in *Ambystoma maculatum. J. Exp. Zool.* **209,** 395–416.
69. Scadding, S. R. (1977) Phylogenetic distribution of limb regeneration capacity in adult amphibia. *J. Exp. Zool.* **202,** 57–68.
70. Singer, M. (1951) Induction of regeneration of the forelimb of the frog by augmentation of the nerve supply. *Proc. Soc. Exp. Biol. Med.* **76,** 413–416.
71. Pritchette, W. H. and Dent, J. N. (1972) The role of size in the rate of limb regeneration in the adult newt. *Growth* **36,** 275–289.
72. Young, H. E., Dalley, B. K., and Markwald, R. R. (1989) Effect of selected denervations on glycoconjugate composition and tissue morphology during the initiation phase of limb regeneration in adult Ambystoma. *Anat. Rec.* **223,** 231–241.
73. Brockes, J. P. (1997) Amphibian limb regeneration: rebuilding a complex structure. *Science* **276,** 81–87.
74. Young, H. E., Carrino, D. A., and Caplan, A. I. (1989) Histochemical analysis of newly synthesized and resident sulfated glycosaminoglycans during musculogenesis in the embryonic chick leg. *J. Morphol.* **201,** 85–103.
75. Mauro, A. (1961) Satellite cell of skeletal muscle fibers. *J. Biophys. Biochem. Cytol.* **9,** 493–498.
76. Campion, D. R. (1984) The musce satellite cell: a review. *Int. Rev. Cytol.* **87,** 225–251.
77. Ailhaud, G., Grimaldi, P., and Negrel, R. (1992) Cellular and molecular aspects of adipose tissue development. *Annu. Rev. Nutr.* **12,** 207–233.
78. Cruess, R. L. (1982) *The Musculoskeletal System: Embryology, Biochemistry, and Physiology.* Churchill Livingston, New York.
79. Vierck, J. L., McNamara, J. P., and Dodson, M. V. (1996) Proliferation and differentiation of progeny of ovine unilocular fat cells (adipofibroblasts). *In Vitro Cell. Dev. Biol. Anim.* **32,** 564–572.
80. Owen, M. (1988) Marrow stromal cells. *J. Cell. Sci. Suppl.* **10,** 63–76.
81. Beresford, J. N. (1989) Osteogenic stem cells and the stromal system of bone and marrow. *Clin. Orthop.* **240,** 270–280.
82. Caplan, A. I., Elyaderani, M., Mochizuki, Y., Wakitani, S., and Goldberg, V. (1997) Principles of cartilage repair and regeneration. *Clin. Orthop. Rel. Res.* **342,** 254–269.
83. Prockop, D. J. (1997) Marrow stromal cells as stem cells for nonhematopoietic tissues. *Science* **276,** 71–74.
84. Pittenger, M. F., Mackay, A. M., Beck, S. C., Jaiswal, R. K., Douglas, R., Mosca, J. D., et al. (1999) Multilineage potential of adult human mesenchymal stem cells. *Science* **148,** 143–147.

85. Palis, J. and Segel, G. B. (1998) Developmental biology of erythropoiesis. *Blood Rev.* **12,** 1061–1064.
86. McGuire, W. P. (1998) High-dose chemotherapy and autologous bone marrow or stem cell reconstitution for solid tumors. *Curr. Probl. Cancer* **22,** 135–137.
87. Ratajczak, M. Z., Pletcher, C. H., Marlicz, W., Machlinski, B., Moore, J., Wasik, M., et al. (1998) CD34+, kit+, rhodamine 123 (low) phenotype identifies a marrow cell population highly enriched for human hematopoietic stem cells. *Leukemia* **12,** 942–950.
88. Hayflick, L. (1965) The limited *in vitro* lifetime of human diploid cell strains. *Exp. Cell. Res.* **37,** 614–636.
89. Young, H. E., Carrino, D. A., and Caplan, A. I. (1990) Changes in synthesis of sulfated glycoconjugates during muscle development, maturation, and aging in embryonic to senescent CBF-1 mouse. *Mech. Ageing Dev.* **53,** 179–193.
90. Urist, M. R. (1965) Bone: formation by autoinduction. *Science* **150,** 893–899.
91. Hauschka, P. V., Mavrakos, A. E., Iafrati, M. D., Doleman, S. E., and Klagsbrun, M. (1986) Growth factors in bone matrix: isolation of multiple types by affinity chromatography on heparin-Sepharose. *J. Biol. Chem.* **261,** 12665–12674.
92. Linkhart, T. A., Jennings, J. C., Mohan, S., Wakley, G. K., and Baylink, D. J. (1986) Characterization of mitogenic activities extracted from bovine bone matrix. *Bone* **7(6),** 479–487.
93. Canalis, E., McCarthy, T., and Centrella, M. (1988) Growth factors and the regulation of bone remodeling. *J. Clin. Invest.* **81,** 277–281.
94. Wozney, J. M., Rosen, V., Celeste, A. J., Mitsock, L. M., Whitters, M. J., Kriz, R. W., et al. (1988) Novel regulators of bone formation: molecular clones and activities. *Science* **242,** 1528–1534.
95. Urist, M. R. (1989) Bone morphogenetic protein, bone regeneration, heterotopic ossification, and the bone-bone marrow consortium. In *Bone and Mineral Research* (Peck, W. A., ed.). Elsevier, New York, vol. 6, pp. 57–112.
96. Wang, E. A., Rozen, V., D'Alessandro, J. S., Bauduy, M., Cordes, P., Harada, T., et al. (1990) Recombinant human bone morphogenetic protein induces bone formation (cartilage induction). *Proc. Natl. Acad. Sci. USA* **87,** 2220–2224.
97. Syftestad, G. T., Lucas, P. A., and Caplan, A. I. (1985) The in vitro chondrogenic response of limb-bud mesenchyme to a water-soluble fraction prepared from demineralized bone matrix. *Differentiation* **29,** 230–237.
98. Frolik, C. A., Ellis, F., and Williams, C. (1988) Isolation and characterization of insulin-like growth factor-II from human bone. *Biochem. Biophys. Res. Commun.* **151,** 1011–1018.
99. Lucas, P. A., Young, H. E., and Putnam, L. S. (1991) Quantitation of chondrogenesis in culture using Alcec blue staining. *FASEB J.* **5,** A390.
100. Kishimoto, T., Kikutani, H., Borne, A. E. G. K.r.v.d., Goyert, S. M., Mason, D., Miyasaka, M., et al. (1997) *Leucocyte Typing VI: White Cell Differentiation Antigens.* Garland, Hamden, CT.
101. Thomson, J. A., Itskovitz-Eldor, J., Shapiro, S. S., Waknitz, M. A., Swiergiel, J. J., Marshall, V. S., et al. (1998) Embryonic stem cell lines derived from human blastocysts. *Science* **282,** 1145–1147.
102. Shamblott, M. J., Axelman, J., Wang, S., Bugg, E. M., Littlefield, J. W., Donovan, P. J., et al. (1998) Derivation of pluripotent stem cells from cultured human primordial germ cells. *Proc. Natl. Acad. Sci. USA* **95,** 13726–13731.
103. Reyes, M. and Verfaillie, C. M. (2001) Characterization of multipotent adult progenitor cells, a subpopulation of mesenchymal stem cells. *Ann. N Y Acad. Sci.* **938,** 231–233; discussion 233–235.
104. Jiang, Y., Vaessen, B., Lenvik, T., Blackstad, M., Reyes, M., and Verfaillie, C. M. (2002) Multipotent progenitor cells can be isolated from bone marrow, muscle and brain. *Exp. Hematol.* **30,** 896–904.
105. McKinney-Freeman, S. L., Jackson, K. A., Camargo, F. D., Ferrari, G., Mavillio, F., and Goodell, M. A. (2002) Muscle-derived hematopoietic stem cells are hematopoietic in origin. *Proc. Natl. Acad. Sci. USA* **99,** 1341–1346.
106. Lucas, P. A., Calcutt, A. F., Mulvaney, D. J., Young, H. E., and Southerland, S. S. (1992) Isolation of putative mesenchymal stem cells from rat embryonic and adult skeletal muscle. *In Vitro Cell. Dev. Biol.* **28,** 154A.
107. Lucas, P. A., Syftestad, G. T., and Caplan, A. I. (1986) Partial isolation and characterization of a chemotactic factor from adult bovine bone for mesenchymal cells. *Bone* **7,** 365–371.
108. Lucas, P. A., Price, P. A., and Caplan, A. I. (1988) Chemotactic response of mesenchymal cells, fibroblasts and osteoblast-like cells to bone Gla protein. *Bone* **5,** 19–23.

109. Lucas, P. A., Syftestad, G. T., and Caplan, A. I. (1988) A water-soluble fraction from adult bone stimulates the differentiation of cartilage explants of embryonic muscle. *Differentiation* **37,** 47–52.
110. Lucas, P. A., Syftestad, G. T., Goldberg, V. M., and Caplan, A. I. (1989) Ectopic induction of cartilage and bone by water-soluble proteins from bovine bone using a collagenous delivery vehicle. *Biomed. Mater. Res.* **23(A, Suppl. 1),** 23–39.
111. Lucas, P. A., Laurencin, C., Syftestad, G. T., Domb, A., Goldberg, V. M., Caplan, A. I., et al. (1990) Ectopic induction of cartilage and bone by water-soluble proteins from bovine bone using a polyanhydride delivery vehicle. *J. Biomed. Mater. Res.* **24,** 901–911.
112. Lucas, P. A. and Dziewiatkowski, D. D. (1987) Feedback control of selected biosynthetic activities of chondrocytes in culture. *Connec. Tiss. Res.* **16,** 323–341.
113. Lucas, P. A. and Caplan, A. I. (1988) Chemotactic response of embryonic limb bud mesenchymal cells and muscle-derived fibroblasts to transforming growth factor-beta. *Connec. Tiss. Res.* **18,** 1–7.
114. Lucas, P. A. (1989) Chemotactic response of osteoblast-like cells to transforming growth factor-beta. *Bone* **10,** 459–463.
115. Bowerman, S. G., Taylor, S. S., Putnam, L., Young, H. E., and Lucas, P. A. (1991) Transforming growth factor-β (TGF-β) stimulates chondrogenesis in cultured embryonic mesenchymal cells. *Surg. Forum* **42,** 535–536.
116. Shoptaw, J. H., Bowerman, S., Young, H. E., and Lucas, P. A. (1991) Use of gelfoam as a substrate for osteogenic cells of marrow. *Surg. Forum* **42,** 537–538.
117. Hinton, J. L., Jr., Warejcka, D. J., Mei, Y., McLendon, R. E., Laurencin, C., Lucas, P. A., et al. (1995) Inhibition of epidural scar formation after lumbar laminectomy in the rat. *Spine* **20,** 564–570; discussion 579–580.
118. Reynolds, B. A. and Weiss, S. (1992). Generation of neurons and astrocytes from isolated cells of the adult mammalian central nervous system. *Science* **255,** 1707–1710.
119. Gage, F. H., Coates, P. W., Palmer, T. D., Kuhn, H. G., Fisher, L. J., Suhonen, J. O., et al. (1995) Survival and differentiation of adult neuronal progenitor cells transplanted to the adult brain. *Proc. Natl. Acad. Sci. USA* **92,** 11879–11883.
120. Bjorklund, A. and Lindvall, O. (2000) Cell replacement therapies for central nervous system disorders. *Nat. Neurosci.* **3,** 537–544.
121. Cornelison, D. D. and Wold, B. J. (1997) Single-cell analysis of regulatory gene expression in quiescent and activated mouse skeletal muscle satellite cells. *Dev. Biol.* **191,** 270–283.
122. Bosch, P., Musgrave, D. S., Lee, J. Y., Cummins, J., Shuler, T., Ghivizzani, T. C., et al. (2000) Osteoprogenitor cells within skeletal muscle. *J. Orthop. Res.* **18,** 933–944.
123. Lee, J. Y., Qu-Petersen, Z., Cao, B., Kimura, S., Jankowski, R., Cummins, J., et al. (2000) Clonal isolation of muscle-derived cells capable of enhancing muscle regeneration and bone healing. *J. Cell. Biol.* **150,** 1085–1100.
124. Toma, J. G., Akhavan, M., Fernandes, K. J., Barnabe-Heider, F., Sadikot, A., Kaplan, D. R., et al. (2001) Isolation of multipotent stem cells from the dermis of mammalian skin. *Nat. Cell. Biol.* **3,** 778–784.
125. Azizi, S. A., Stokes, D., Augelli, B. J., DiGirolamo, C., and Prockop, D. J. (1998) Engraftment and migration of human bone marrow stromal cells implanted in the brains of albino rats-similarities to astrocyte grafts. *Proc. Natl. Acad. Sci. USA* **95,** 3908–3913.
126. Kopen, G. C., Prockop, D. J., and Phinney, D. G. (1999) Marrow stromal cells migrate throughout forebrain and cerebellum, and they differentiate into astrocytes after injection into neonatal mouse brains. *Proc. Natl. Acad. Sci. USA* **96,** 10711–10716.
127. Mezey, E., Chandross, K. J., Harta, G., Maki, R. A., and McKercher, S. R. (2000) Turning blood into brain: cells bearing neuronal antigens generated in vivo from bone marrow. *Science* **290,** 1779–1782.
128. Sanchez-Ramos, J., Song, S., Cardozo-Pelaez, F., Hazzi, C., Stedeford, T., Willing, A., et al. (2000). Adult bone marrow stromal cells differentiate into neural cells in vitro. *Exp. Neurol.* **164,** 247–256.
129. Colter, D. C., Sekiya, I., and Prockop, D. J. (2001) Identification of a subpopulation of rapidly self-renewing and multipotential adult stem cells in colonies of human marrow stromal cells. *Proc. Natl. Acad. Sci. USA* **98,** 7841–7845.
130. Deng, W., Obrocka, M., Fischer, I., and Prockop, D. J. (2001) In vitro differentiation of human marrow stromal cells into early progenitors of neural cells by conditions that

increase intracellular cyclic AMP. *Biochem. Biophys. Res. Commun.* **282,** 148–152.
131. Reyes, M., Lund, T., Lenvik, T., Aguiar, D., Koodie, L., and Verfaillie, C. M. (2001) Purification and ex vivo expansion of postnatal human marrow mesodermal progenitor cells. *Blood* **98,** 2615–2625.
132. Reynolds, B. A., Tetzlaff, W., and Weiss, S. (1992). A multipotent EGF-responsive striatal embryonic progenitor cell produces neurons and astrocytes. *J. Neurosci.* **12,** 4565–4574.
133. Svendsen, C. N., ter Borg, M. G., Armstrong, R. J., Rosser, A. E., Chandran, S., Ostenfeld, T., et al. (1998) A new method for the rapid and long term growth of human neural precursor cells. *J. Neurosci. Methods* **85,** 141–152.
134. Cochard, P. and Paulin, D. (1984) Initial expression of neurofilaments and vimentin in the central and peripheral nervous system of the mouse embryo in vivo. *J. Neurosci.* **4,** 2080–2094.
135. Lendahl, U., Zimmerman, L. B., and McKay, R. D. (1990) CNS stem cells express a new class of intermediate filament protein. *Cell* **60,** 585–595.
136. Zimmerman, L., Parr, B., Lendahl, U., Cunningham, M., McKay, R., Gavin, B., et al. (1994) Independent regulatory elements in the nestin gene direct transgene expression to neural stem cells or muscle precursors. *Neuron* **12,** 11–24.
137. Feldman, D. H., Thinschmidt, J. S., Peel, A. L., Papke, R. L., and Reier, P. J. (1996) Differentiation of ionic currents in CNS progenitor cells: dependence upon substrate attachment and epidermal growth factor. *Exp. Neurol.* **140,** 206–217.
138. Dawson, M. R., Levine, J. M., and Reynolds, R. (2000) NG2-expressing cells in the central nervous system: are they oligodendroglial progenitors? *J. Neurosci. Res.* **61,** 471–479.
139. Gritti, A., Galli, R., and Vescovi, A. L. (2001) Cultures of stem cells of the central nervous system. In *Protocols for Neural Cell Culture* (Fedoroff, S., Richardson, A., eds.). Totowa, NJ, Humana Press, pp. 173–198.
140. van Praag, H., Schinder, A. F., Christie, B. R., Toni, N., Palmer, T. D., and Gage, F. H. (2002) Functional neurogenesis in the adult hippocampus. *Nature* **415,** 1030–1034.
141. Pesce, M. and Scholer, H. R. (2001). *Oct-4*: gatekeeper in the beginnings of mammalian development. *Stem Cells* **19,** 271–278.
142. Mansouri, A., Hallonet, M., and Gruss, P. (1996) Pax genes and their roles in cell differentiation and development. *Curr. Opin. Cell. Biol.* **8,** 851–857.
143. Orkin, S. H. and Zon, L. I. (2002) Hematopoiesis and stem cells: plasticity versus developmental heterogeneity. *Nat. Immunol.* **3,** 323–328.
144. Mertelsmann, R. (2000) Plasticity of bone marrow-derived stem cells. *J. Hematother. Stem Cell Res.* **9,** 957–960.
145. Alexander, W. S. (1998) Cytokines in hematopoiesis. *Int. Rev. Immunol.* **16,** 651–682.
146. National Blood Data Resource Center (www.nbdrc.org).
147. Slavin, S. (2000) New strategies for bone marrow transplantation. *Curr. Opin. Immunol.* **12,** 542–551.
148. National Marrow Donor Program (www.marrow.org).
149. Confer, D. L. (1997) Unrelated marrow donor registries. *Curr. Opin. Hematol.* **4,** 408–412.
150. van der Kooy, D. and Weiss, S. (2000) Why stem cells? *Science* **287,** 1439–1441.
151. Weissman, I. L. (2000) Translating stem and progenitor cell biology to the clinic: barriers and opportunities. *Science* **287,** 1442–1446.
152. Vogel, G. (2000) Cell biology: stem cells: new excitement, persistent questions. *Science* **290,** 1672–1674.
153. Alison, M. R., Poulsom, R., Jeffery, R., Dhillon, A. P., Quaglia, A., Jacob, J., et al. (2000) Hepatocytes from non-hepatic adult stem cells. *Nature* **406,** 257.
154. Li, F., Linton, G. F., Sekhsaria, S., Whiting-Theobald, N., Katkin, J. P., Gallin, J. I., et al. (1994) CD34+ peripheral blood progenitors as a target for genetic correction of the two flavocytochrome b558 defective forms of chronic granulomatous disease. *Blood* **84,** 53–58.
155. Eisenbarth, G. S., Connelly, J., and Soeldner, J. S. (1987) The "natural" history of Type I diabetes. *Diabetes/Metabolism Rev.* **3,** 873–891.
156. Ward, W. K., Beard, J. C., and Porte, D., Jr. (1986) Clinical aspects of islet b-cell function in non-insulin dependent diabetes mellitus. *Diabetes/Metabolism Rev.* **2,** 297–313.
157. Chandra, R. K. (1989) Nutritional regulation of immunity and risk of infection in old age. *Immunology* **67,** 141–147.
158. Fiatarone, M. A., Marks, E. C., Ryan, N. D., Meridith, C. N., Lipsitz, L. A., and Evans, W. J. (1990) High-intensity strength training in nonagenarians: effects on skeletal muscle. *JAMA* **263,** 3029–3034.

159. Frontera, W. R., Hughes, V. A., Lutz, K. J., and Evans, W. J. (1991) A cross-sectional study of muscle strength and mass in 45- to 78 yr-old men and women. *J. Appl. Physiol* **71,** 644–650.
160. Walsh, C. H., Soler, N. G., James, H., Harvey, T. C., Thomas, B. J., Fremlin, J. H., et al. (1976) Studies in whole body potassium and whole body nitrogen in newly diagnosed diabetics. *Q. J. Med.* **45(178),** 295–301.
161. Nair, K. S., Garrow, J. S., Ford, C., Mahler, R. F., and Halliday, D. (1983) Effect of poor diabetic control and obesity on whole body protein metabolism in man. *Diabetologia* **25,** 400–403.
162. Morgan, H. E., Jefferson, L. S., Wolpert, E. B., and Rannels, D. E. (1971) Regulation of protein synthesis in heart muscle: II. Effect of amino acid levels and insulin on ribosomal aggregation. *J. Biol. Chem.* **246,** 2163–2170.
163. Jefferson, L. S., Li, J. B., and Rannels, S. R. (1977) Regulation by insulin of amino acid release and protein turnover in the perfused rat hemicorpus. *J. Biol. Chem.* **252,** 1476–1483.
164. Peavy, D. E., Taylor, J. M., and Jefferson, L. S. (1978) Correlation of albumin production rates and mRNA levels in livers of normal, diabetic and insulin-treated diabetic rats. *Proc. Natl. Acad. Sci. USA* **75,** 5879–5883.
165. Froesch, E. R., Guler, H. P., Schmid, C., Ernst, M., and Zapf, J. (1990) Insulin-like growth factors. In *Ellenberg and Rifkin's Diabetes Mellitus: Theory and Practice* (Rifkin, H., Porte, D., eds.). Elsevier, New York, pp. 154–169.
166. Lemozy, S., Pucilowska, L. B., and Underwood, L. E. (1994) Reduction of insulin-like growth factor-1 (IGF-1) in protein-restricted rats is associated with differential regulation of IGF-binding protein messenger ribonucleic acids in liver and kidney, and peptides in liver and serum. *Endocrinology* **135,** 617–623.
167. Straus, D. S. (1994) Nutritional regulation of hormones and growth factors that control mammalian growth. *FASEB J.* **8,** 6–12.
168. Tobin, B. W., Lewis, J. T., Chen, Z., Tobin, B. L., and Finegood, D. T. (1995) Insulin action in a model of graded insulin secretion using islet transplanted rats. *Transplantation* **59,** 1–6.
169. Tobin, B. W., Lewis, J. T., Tobin, B. L., and Finegood, D. T. (1995) Insulin action in previously diabetic rats receiving graded numbers of islets of Langerhans. *Transplantation* **59,** 1464–1470.
170. Tobin, B. W. and Marchello, M. J. (1995) Islet transplantation reverses carcass protein loss in diabetic rats without inducing disproportionate fat accumulation. *Diabetologia* **38,** 881–888.
171. Tobin, B. W., Welch-Holland, K. R., and Marchello, M. J. (1997) Pancreatic islet transplantation improves body composition, decreases food intake and normalizes feed efficiency in previously diabetic female rats. *J. Nutr.* **127,** 1191–1197.
172. Weir, G. C. and Bonner-Weir, S. (1998) Islet transplantation as a treatment for diabetes. *J. Am. Optom. Assoc.* **69,** 727–732.
173. Shapiro, A. M. J., Lakey, J. R. T., Ryan, E. A., Korbutt, G. S., Toth, E., Warnock, G. L., et al. (2000) Islet transplantation in seven patients with type 1 diabetes mellitus using a glucocorticoid-free immunosuppressive regimen. *N. Engl. J. Med.* **343,** 230–237.
174. Shapiro, A. M. J., Ryan, E. A., and Lakey, J. R. T. (2001) Pancreatic islet transplantation in the treatment of diabetes mellitus. *Best Practice Res. Clin. Endocrin. Metab.* **15,** 241–264.
175. Shapiro, A. M. J. and Lakey, J. R. T. (2000) Future trends in islet transplantation. *Diabetes Tech. Ther.* **2,** 449–452.
176. Ryan, E. A., Lakey, J. R. T., and Shapiro, A. M. J. (2001) Clinical results after islet transplantation. *J. Invest. Med.* **49,** 559–562.
177. Ryan, E. A., Lakey, J. R. T., Rajotte, R. V., Korbutt, G. S., Kin, T., Imes, S., et al. (2001) Clinical outcomes and insulin secretion after islet transplantation with the Edmonton protocol. *Diabetes* **50,** 710–719.
178. Cornelius, J. G., Tchernev, V., Kao, K. J., and Peck, A. B. (1997) In vitro-generation of islets in long-term cultures of pluripotent stem cells from adult mouse pancreas. *Horm. Metab. Res.* **29(6),** 271–277.
179. Ramiya, V. K., Maraist, M., Arfos, K. E., Schatz, D. A., Peck, A. B., and Cornelius, J. G. (2000) Reversal of insulin-dependent diabetes using islets generated in vitro from pancreatic stem cells. *Nat. Med.* **6(3),** 278–282.
180. Bonner-Weir, S., Taneja, M., Weir, G. C., Tatarkiewicz, K., Song, K.-H., Sharma, A., et al. (2000) In vitro cultivation of human islets from expanded ductal tissue. *Proc. Natl. Acad. Sci. USA* **97,** 7999–8004.
181. Lumelsky, N., Blondel, O., Laeng, P., Velasco, I., Ravin, R., and McKay, R. (2001) Differentiation of embryonic stem cells to insulin-secreting structures similar to pancreatic islets. *Science* **292,** 1389–1393.

182. Soria, B., Roche, E., Berna, G., Leon-Quinto, T., Reig, J. A., and Martin, F. (2000) Insulin-secreting cells derived from embryonic stem cells normalize glycemia in streptozotocin-induced diabetic mice. *Diabetes* **49,** 157–162.
183. Soria, B., Skoudy, A., and Martin, F. (2001) From stem cells to beta cells: new strategies in cell therapy of diabetes mellitus. *Diabetologia* **4,** 407–415.
184. Assady, S., Maor, G., Amit, M., Itskovitz-Eldor, J., Skorecki, K. L., and Tzukerman, M. (2001) Insulin production by human embryonic stem cells. *Diabetes* **50,** 1691–1697.
185. Mankin, H. J. (1982) The response of articular cartilage to mechanical injury. *J. Bone Joint Surg. Am.* **64,** 460–466.
186. McDermott, A. G., Langer, F., Pritzker, K. P., and Gross, A. E. (1985) Fresh small-fragment osteochondral allografts: long-term follow-up study on first 100 cases. *Clin. Orthop.* **197,** 96–102.
187. Chesterman, P. J. and Smith, A. U. (1968) Homotransplantation of articular cartilage and isolated chondrocytes: an experimental study in rabbits. *J. Bone Joint Surg. Br.* **50,** 184–197.
188. Bentley, G. and Greer, R. B., III. (1971) Homotransplantation of isolated epiphyseal and articular cartilage chondrocytes into joint surfaces of rabbits. *Nature* **230,** 385–388.
189. Green, W. T. (1977) Articular cartilage repair: behavior of rabbit chondrocytes during tissue culture and subsequent allografting. *Clin. Orthop.* **124,** 237–250.
190. Moskalewski, S. (1991) Transplantation of isolated chondrocytes. *Clin. Orthop.* **272,** 16–20.
191. Wakitani, S., Kimura, T., Hirooka, A., Ochi, T., Yoneda, M., Yasui, N., et al. (1989) Repair of rabbit articular surfaces with allograft chondrocytes embedded in collagen gel. *J. Bone Joint Surg. Br.* **71,** 74–80.
192. Kawabe, N. and Yoshinato, M. (1991) The repair of full thickness articular cartilage defects: immune responses to reparative tissue formed by allogeneic growth plate chondrocytes. *Clin. Orthop.* **268,** 279–293.
193. Matsusue, Y., Yamamuro, T., and Hama, H. (1993) Arthroscopic multiple osteochondral transplantation to the chondral defect in the knee associated with anterior cruciate ligament disruption. *Arthroscopy* **9,** 318–321.
194. Garret, J. C. (1986) Treatment of osteochondral defects of the distal femur with fresh osteochondral allografts: a preliminary report. *Arthroscopy* **2,** 222–226.
195. Skoog, T. and Johansson, S. H. (1976) The formation of articular cartilage from free perichondrial grafts. *Plast. Reconstr. Surg.* **57(1),** 1–6.
196. Homminga, G. N., Bulstra, S. K., Bouwmeester, P. S., and van der Linden, A. J. (1990) Perichondral grafting for cartilage lesions of the knee. *J. Bone Joint Surg. Br.* **72,** 1003–1007.
197. Rubak, J. M. (1982) Reconstruction of articular cartilage defects with free periosteal grafts: an experimental study. *Acta Orthop. Scand.* **53,** 175–80.
198. O'Driscoll, S. W., Keeley, F. W., and Salter, R. B. (1988) Durability of regenerated articular cartilage produced by free autogenous periosteal grafts in major full-thickness defects in joint surfaces under the influence of continuous passive motion: a follow-up report at one year. *J. Bone Joint Surg. Am.* **70,** 595–606.
199. Ritsila, V. A., Santavirta, S., Alhopuro, S., Poussa, M., Jaroma, H., Rubak, J. M., et al. (1994) Periosteal and perichondral grafting in reconstructive surgery. *Clin. Orthop.* **302,** 259–265.
200. Caplan, A. I. (1991) Mesenchymal stem cells. *J. Orthop. Res.* **9,** 641–650.
201. Minas, T. and Neher, S. (1997) Current concepts in the treatment of articular cartilage defects. *Orthopedics* **20,** 525–538.
202. Grande, D. A., Pitman, M. I., Peterson, L., Menche, D., and Klein, M. (1989) The repair of experimentally produced defects in rabbit articular cartilage by autologous chondrocyte transplantation. *J. Orthop. Res.* **7,** 208–218.
203. Brittberg, M., Lindahl, A., Nilsson, A., Ohlsson, C., Isaksson, O., and Peterson, L. (1994) Treatment of deep cartilage defects in the knee with autologous chondrocyte transplantation. *N. Engl. J. Med.* **331,** 889–895.
204. Brittberg, M., Nilsson, A., Lindahl, A., Ohlsson, C., and Peterson, L. (1996) Rabbit articular cartilage defects treated with autologous cultured chondrocytes. *Clin. Orthop.* **326,** 270–283.
205. Frenkel, S. R., Toolan, B., Menche, D., Pitman, M. I., and Pachence, J. M. (1997) Chondrocyte transplantation using a collagen bilayer matrix for cartilage repair. *J. Bone Joint Surg. Br.* **79,** 831–836.
206. Wakitani, S., Goto, T., Pineda, S. J., Young, R. G., Mansour, J. M., Caplan, A. I., et al. (1994) Mesenchymal cell-based repair of large, full-thickness defects of articular cartilage. *J. Bone Joint Surg. Am.* **76,** 579–592.

207. Breinan, H. A., Minas, T., Hsu, H.-P., Nehrer, S., Sledge, C. B., and Spector, M. (1997) Effect of cultured autologous chondrocytes on repair of chondral defects in a canine model. *J. Bone Joint Surg. Am.* **79,** 1439–1451.
208. Kolettas, E., Buluwela, L., Bayliss, M. T., and Muir, H. I. (1995) Expression of cartilage-specific molecules is retained on long-term culture of human articular chondrocytes. *J. Cell. Sci.* **108,** 1991–1999.
209. Grande, D. A., Southerland, S. S., Manji, R., Pate, D. W., Schwartz, R. E., and Lucas, P. A. (1995) Repair of articular cartilage defect using mesenchymal stem cells. *Tiss. Eng.* **1,** 345–353.
210. Syftestad, G. T. and Caplan, A. I. (1984) A fraction from extracts of demineralized adult bone stimulates the conversion of mesenchymal cells into chondrocytes. *Dev. Biol.* **104,** 348–356.
211. Sato, S., Rahemtulla, F., Prince, C. W., Tomana, M., and Butler, W. T. (1985) Acidic glycoproteins from bovine compact bone. *Connect. Tiss. Res.* **14(1),** 51–64.
212. Laemmli, U. K. (1970) Cleavage of structural proteins during the assembly of the head of bacteriophage T4. *Nature* **227(259),** 680–685.
213. Roberts, R. M., Baumbach, G. A., Buhi, W. C., Denny, J. B., Fitzgerald, L. A., Babelyn, S. F., and Horst, M. N. (1984) Analysis of membrane polypeptides by two-dimensional polyacrylamide gel electrophoresis. In: *Molecular and Chemical Characterization of Membrane Receptors* (Venter, J., ed.). Alan R. Liss, New York, pp. 61–113.
214. Ewton, D. Z. and Florini, J. R. (1981) Effects of somatomedins and insulin on myoblast differentiation in vitro. *Dev. Biol.* **86,** 31–39.
215. Florini, J. R., Roberts, A. B., Ewton, D. Z., Falen, S. L., Flanders, K. C., and Sporn, M. B. (1986) Transforming growth factor-beta: a very potent inhibitor of myoblast differentiation, identical to the differentiation inhibitor secreted by Buffalo rat liver cells. *J. Biol. Chem.* **261,** 16509–16513.
216. Florini, J. R., Ewton, D. Z., Falen, S. L., and Van Wyck, J. J. (1986) Biphasic concentration dependency of stimulation of myoblast differentiation by somatomedins. *Am. J. Physiol.* **250,** C771–C778.
217. Florini, J. R. and Magri, K. A. (1989) Effects of growth factors on myogenic differentiation. *Am. J. Physiol.* **256,** C701–C711.
218. Sejersen, T., Betscholtz, C., Sjolund, M., Heldin, C. H., Estermark, B., and Thyberg, J. (1986) Rat skeletal myoblasts and arterial smooth muscle cells express the gene for the A chain but not the gene for the B chain (c-sis) of platelet-derived growth factor (PDGF) and produce a PDGF-like protein. *Proc. Natl. Acad. Sci. USA* **83,** 6844–6848.
219. Ewton, D. Z., Falen, S. L., and Florini, J. R. (1987) The type-II insulin-like growth factor (IGF) receptor has low affinity for IGF-I analogs: pleiotypic actions of the IGFs on myoblasts are apparently mediated by the type-I receptor. *Endocrinology* **120,** 115–123.
220. Allbrook, D. (1981) Skeletal muscle regeneration. *Muscle Nerve* **4,** 234–245.
221. Carlson, B. M. (1973) The regeneration of skeletal muscle: a review. *Am. J. Anat.* **137,** 119–149.
222. Carlson, B. M. (1979) Relationship between tissue and epimorphic regeneration of skeletal muscle. In: *Muscle Regeneration* (Mauro, A., ed.). Raven, New York, p. 57.
223. Carlson, B. M. (1986) Regeneration of entire skeletal muscles. *Fed. Proc.* **45,** 1456–1460.
224. Carlson, B. M. and Faulkner, J. A. (1983) The regeneration of skeletal muscle fibers following injury: a review. *Med. Sci. Sports Exerc.* **15,** 187–198.
225. Faulkner, J. A. and Carlson, B. M. (1986) Skeletal muscle regeneration: a historical perspective. *Fed. Proc.* **45,** 1454–1455.
226. Donovan, C. M. and Faulkner, J. A. (1987) Plasticity of skeletal muscle: regenerating fibers adapt more rapidly than surviving fibers. *J. Appl. Physiol.* **62,** 2507–2511.
227. Schoen, F. J. (1999) The heart. In: *Pathological Basis of Disease*, 6th ed. (Cotran, R., Kumar, V., and Collins, T., eds.), W. B. Saunders, Philadelphia, pp. 543–599.
228. Chiu, R. C.-J. (2001) Theraputic cardiac angiogenesis and myogenesis: the promises and challenges on a new frontier. *J. Thorac. Cardiovasc. Surg.* **122(5),** 851–852.
229. Marelli, D., Desrosiers, C., El-Alfy, M., Kao, R. L., and Chiu, R. C. (1992) Cell transplantation for myocardial repair: an experimental approach. *Cell. Transplant.* **1,** 383–390.
230. Taylor, D. A., Atkins, B. Z., Hungspreugs, P., Jones, T. R., Reedy, M. C., Hutchenson, K. A., et al. (1997) Delivery of primary autologous skeletal myoblasts into rabbit heart by coronary infusion: a potential approach to myocardial repair. *Proc. Assoc. Am. Physicians* **109,** 245–253.

231. Koh, G. Y., Soonpaa, M. H., Klug, M. G., and Field, L. (1993) Long-term survival of AT-1 cardiomyocyte grafts in syngenic myocardium. *Am. J. Physiol.* **264** (*Heart Circ. Physiol.* **33**), H1727–H1733.
232. Soonpaa, M. H., Koh, G. Y., Klug, M. G., and Field, L. G. (1994) Formation of nascent intercalated disks between grafted cardiomyocytes and host myocardium. *Science* **264,** 98–101.
233. Klung, M., Soonpaa, M., Koh, G., and Field, L. (1996) Genetically selected cardiomyocytes from differentiating embryonic stem cells form stable intracardiac grafts. *J. Clin. Invest.* **98,** 216–224.
234. Taylor, D. A., Atkins, B. Z., Hungspreugs, P., Jones, T. R., Reddy, M. C., Hutcheson, K. A., et al. (1998) Regenerating functional myocardium: improved performance after skeletal myoblast transplantation. *Nat. Med.* **4(8),** 929–933.
235. Sakai, T., Li, R.-K., Weisel, R. D., Mickle, D. A., Kim, E.-J., Tomita, S., et al. (1999) Autologous heart cell transplantation improves function after myocardial injury. *Ann. Thorac. Surg.* **68,** 2074–2081.
236. Li, R.-K., Weisel, R. D., Mickle, D. A., Jia, Z.-Q., Kim, E. J., Sakai, T., et al. (2000) Autologous porcine heart cell transplantation improved heart function after a myocardial infarction. *J. Thorac. Cardiovasc. Surg.* **119,** 62–68.
237. Reincke, H., Zhang, M., Bartosek, T., and Murry, C. E. (1999) Survival, integration, and differentiation of cardiomyocyte grafts: a study in normal and injured rat hearts. *Circulation* **100,** 193–202.
238. Weksler, B., Ng, B., Lenert, J., and Burt, M. (1994) A simplified method for endotracheal intubation in the rat. *J. Appl. Physiol.* **76(4),** 1823–1825.
239. Price, R. L., Chintanowonges, C., Shiraishi, I., Borg, T. K., and Terracio, L. (1996) Local and regional variations in myofibrillar patterns in looping rat hearts. *Anat. Rec.* **245,** 83.
240. Couffinhal, T., Kearney, M., Sullivan, A., Silver, M., Tsurumi, Y., and Isner, J. M. (1997) Histochemical staining following LacZ gene transfert underestimates transfection efficiency. *Hum. Gene Ther.* **8,** 929–934.
241. Saito, T., Dennis, J. E., Lennon, D. P., Young, R. G., and Caplan, A. I. (1995) Myogenic expression of mesenchymal stem cells within myotubes of *mdx* mice in vitro and in vivo. *Tiss. Eng.* **1,** 327–343.
242. Deasy, B. M., Jankowski, R. J., and Huard, J. (2001) Muscle-derived stem cells: characterization and potential for cell-mediated therapy. *Blood Cells Mol. Dis.* **27,** 924–933.
243. Jankowski, R. J., Haluszczak, C., Trucco, M., and Kuard, J. (2001) Flow cytometric characterization of myogenic cell populations obtained via the preplate technique: potential for rapid isolation of muscle-derived stem cells. *Hum. Gene Ther.* **12,** 619–628.
244. Dent, C. L. and Latchman, D. S. (1993) DNA mobility shift assays. In: *Transcription Factors: A Practical Approach* (Latchman, D.S., ed.). Oxford University Press, New York, pp. 1–26.
245. Callaerts, P., Halder, G., and Gehring, W. J. (1997) *PAX-6* in development and evolution. *Annu. Rev. Neurosci.* **20,** 483–532.
246. Vitalis, T., Cases, O., Engelkamp, D., Verney, C., and Price, D. J. (2000) Defect of tyrosine hydroxylase-immunoreactive neurons in the brains of mice lacking the transcription factor *Pax6*. *J. Neurosci.* **20,** 6501–6516.
247. Mastick, G. S. and Andrews, G. L. (2001) *Pax6* regulates the identity of embryonic diencephalic neurons. *Mol. Cell. Neurosci.* **17,** 190–207.
248. Wright, W. E., Binder, M., and Funk, W. (1991) Cyclic Amplification Selection of Targets (CASTing) for the myogenin consensus binding site. *Mol. Cell. Biol* **11,** 4104–4110.
249. Kraus, B. and Pette, D. (1997) Quantification of MyoD, myogenin, MRF4 and Id-1 by reverse transcriptase polymerase chain reaction in rat muscles: effects of hypothyroidism and chronic low-frequency stimulation. *Eur. J. Biochem.* **247,** 98–106.
250. Skalli, O., Ropraz, P., Trzeciak, A., Benzonana, G., Gillessen, D., and Gabbiani, G. (1986) A monoclonal antibody against α-smooth muscle actin: a new probe for smooth muscle differentiation. *J. Cell. Biol.* **103,** 2787–2796.
251. Alexander, J. E., Hunt, D. F., Lee, M. K., Shabanowitz, J., Michel, H., Berlin, S. C., et al. (1991) Characterization of posttranslational modifications in neuron-specific class III β-tubulin by mass spectrometry. *PNAS* **88,** 4685–4689.
252. Dotti, C. G., Banker, G. A., and Binder, L. I. (1987) The expression and distribution of the microtubule-associated proteins tau and microtubule-associated protein 2 in hippocampal neurons in the rat in situ and in cell culture. *Neuroscience* **1,** 121–130.
253. Debus, E., Weber, K., and Osborn, M. (1983) Monoclonal antibodies specific for glial fibrillary acidic (GFA) protein and for each of the

neurofilament triplet polypeptides. *Differentiation* **25,** 193–203.
254. Shaw, G., Osborn, M., and Weber, K. (1986) Reactivity of a panel of neurofilament antibodies on phosphorylated and dephosphorylated neurofilaments. *Eur. J. Cell. Biol.* **42,** 1–9.
255. Beck, K. D., Powell-Braxton, L., Widmer, H.-R., Valverde, J., and Hefti, F. (1995) *Igf*1 Gene disruption results in reduced brain size, CNS, hypomyleination and loss of hippocampal granule and striatal parvalbumin-containing neurons. *Neuron* **14,** 717–730.
256. Justicia, C., Gabriel, C., and Planas, A. M. (2000) Activation of the JAK/STAT pathway following transient focal cerebral ischemia: signaling through Jak 1 and Stat 3 in astrocytes. *Glia* **30,** 253–270.
257. Zhang, S. C. (2001) Defining glial cells during CNS development. *Nat. Rev. Neurosci.* **2,** 840–843.
258. Spinkle, T. J., Agee, J. F., Tippins, R. B., Chamberlain, C. R., Faguet, G. B., and DeVries, G. H. (1987) Monoclonal antibody production to human and bovine 2′:3′-cyclic nucleotide 3′-phosphodiesterase (CNPase): high-specificity recognition in whole brain acetone powder and conservation of sequence between CNP1 and CNP2. *Brain Res.* **426,** 349–357.
259. Asahara, T., Kalka, C., and Isner, J. M. (2000) Stem cell therapy and gene transfer for regeneration. *Gene Ther.* **7,** 451–457.
260. Kalka, C., Masuda, H., Takahashi, T., Kalka-Moll, W. M., Silver, M., Kearney, M., et al. (2000) Transplantation of ex vivo expanded endothelial progenitor cells for therapeutic neovascularization. *Proc. Natl. Acad. Sci. USA* **97,** 3422–3427.
261. Masuda, H., Kalka, C., and Asahara, T. (2000) Endothelial progenitor cells for regeneration. *Hum. Cell.* **13,** 153–160.
262. Murayama, T., Tepper, O. M., Silver, M., Ma, H., Losordo, D. W., Isner, J. M., et al. (2002) Determination of bone marrow-derived endothelial progenitor cell significance in angiogenic growth factor-induced neovascularization in vivo. *Exp. Hematol.* **8,** 967–972.